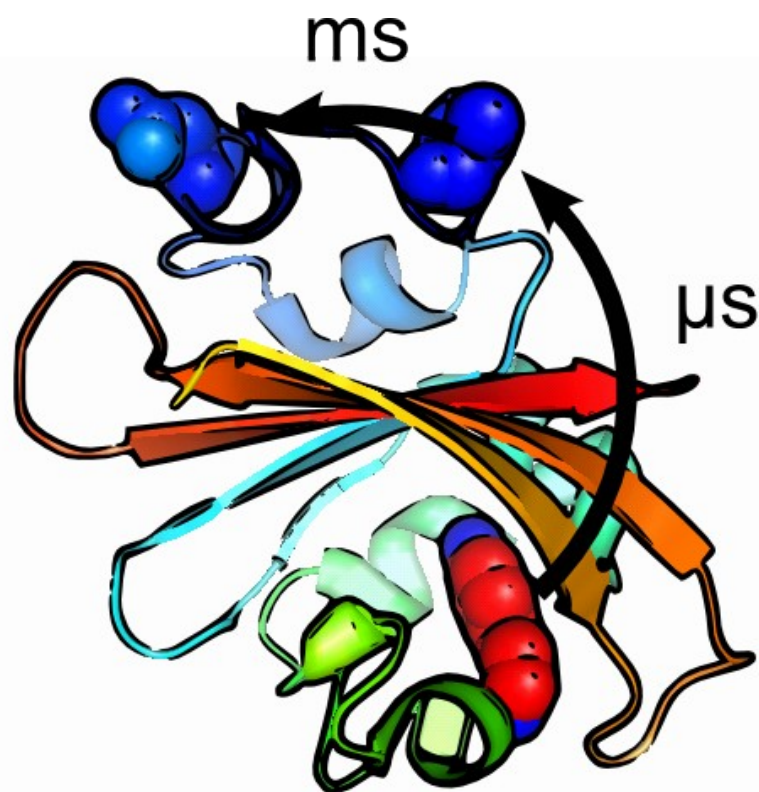


Monitoring
light induced conformational changes
in photoreceptors
by time resolved spectroscopy



Daniel Hörsch

im Fachbereich Physik der Freien Universität Berlin eingereichte
Dissertation

2009

Freie Universität  Berlin

First referee
Second referee
Date of Disputation

Prof. Dr. Maarten P. Heyn
Prof. Dr. Holger Dau
13th May 2009

Abstract

Photoreceptors are important model systems for the investigation of protein signal transduction and protein kinetics in general. Because they are activated by light it is possible to resolve their activation kinetics with high time resolution by optical methods. In this thesis I methodically focus on time resolved fluorescence spectroscopy as a tool to characterize the light-induced conformational changes associated with the activation of several photoreceptors. Furthermore I introduce the method of transient fluorescence spectroscopy as a valuable tool to study the kinetics of the activation processes. Transient absorption spectroscopy is used as a complementary technique. This study's emphasis is on measurements on Photoactive Yellow Protein (PYP) which is the structural prototype of the ubiquitous PAS domain family. Additionally the photoreceptors rhodopsin and the LOV2 domain from phototropin 1 are investigated to show the general applicability of the introduced methods.

Chapter 1 provides a general introduction to the investigated biological systems Photoactive Yellow Protein, rhodopsin and LOV2. Moreover the applied methods are explained.

Chapter 2 (Otto et al. (2005) *Biochemistry* 44, 16804-16816) is about time resolved fluorescence intensity and depolarization experiments on the unique tryptophan W119 of PYP from *Halorhodospira halophila* whose fluorescence is quenched by energy transfer to the 4-hydroxycinnamoyl chromophore of the protein. The different fluorescence lifetimes of several photointermediates could be explained by dramatic changes of the κ^2 factor due to changes in the orientation of the chromophore transition dipole moment. The κ^2 factors were calculated from high resolution X-ray structures. The results of this chapter were already part of my diploma thesis and are shown here because they provide the background of some of the work described in the following chapters.

Chapter 3 (Hoersch et al. (2008) *J. Phys. Chem. B* 112, 9118-9125) introduces the technique of transient fluorescence spectroscopy to study the photocycle kinetics of PYP at alkaline pH. In this way the tryptophan fluorescence lifetime of the short living intermediate I_1 could be determined. In a next step it was compared with calculated lifetimes, based on two different I_1 high resolution X-ray structures. As only one of the calculated lifetimes was in agreement with the experiment, we could exclude one of the structures, which is presumably not present in solution at alkaline pH. Additionally we determined the tryptophan fluorescence lifetime of the alkaline intermediate I_1' from measurements of the tryptophan fluorescence decay in a photostationary equilibrium under background illumination. We predicted the chromophore conformation of this intermediate for which the crystal structure is not yet known to be similar to that of the I_2 intermediate.

Abstract

Chapter 4 (Hoersch et al. (2007) *Biophysical Journal* 93, 1687-1699) is about the role of a conserved salt bridge between the PAS core and the N-terminal domain in the activation of PYP. Therefore the effect of ionic strength on the conformational equilibrium between the I_2 intermediate and the signaling state I_2' and on the recovery rate was investigated by time resolved absorption and fluorescence spectroscopy. The salt dependency of the equilibrium constant and the recovery rate could be explained quantitatively by the screening of a monovalent ion pair. Furthermore the salt effect was eliminated in the mutant K110A below 600 mM KCl. Thus we concluded that the salt linkage K110/E12 between the β -sheet of the PAS core and the N-terminal domain stabilizes the photoreceptor in the inactive state in the dark and is broken in the light-induced formation of the signaling state.

In Chapter 5 (Hoersch et al. (2009) *Physical Chemistry Chemical Physics*, DOI: 10.1039/b821345c) the kinetics of the structural change in the N-terminal domain of PYP is investigated by transient absorption spectroscopy of the dye labeled mutants A5C and N13C. The transient red-shift of the absorption band of the attached dye iodoacetamidofluorescein (IAF) suggested conformational changes near the labeling sites. As the transient dye signal is correlated with the intermediate I_2 in A5C-AF and with I_2' in N13C-AF we concluded that the light-induced structural signal propagates from the chromophore binding pocket via A5 to N13 where it causes major changes in the protein conformation.

Chapter 6 (Hoersch et al. (2008) *Biochemistry* 47, 11518-11527) applies the technique of transient fluorescence spectroscopy to bovine rhodopsin. The transient tryptophan fluorescence of this photoreceptor decreases with the same kinetics as the rise of the M_{II} state as measured by the transient absorption increase at 360 nm. This could be explained by an increase in energy transfer to the retinylidene chromophore caused by the increased spectral overlap in the signaling state M_{II} . Furthermore the kinetics of the Alexa594 fluorescence increase in ROS membranes selectively labeled at cysteine 316 was measured and compared with the kinetics of the M_{II} formation and the kinetics of the proton uptake from the solvent. As the fluorescence change lags behind the Schiff base deprotonation but precedes the proton uptake the sequence Schiff base deprotonation, structural change, proton uptake seems to be a good model for the molecular events of rhodopsin activation. So far this sequence of events has only been established with the less relevant rhodopsin/micelle systems and with different results.

Chapter 7 deals with the transient tryptophan fluorescence of the light sensing LOV2-J α domain of the photoreceptor phototropin1 from *Avena sativa*. The transient fluorescence signal of this domain increases biexponentially with time constants of 450 μ s and 3.8 ms at 20 °C. As these transitions are invisible in the transient absorption data in the UV-VIS range we expanded the LOV2-J α photocycle scheme by two more intermediates. These have the same absorption spectra but different tryptophan fluorescence quantum yields and are associated with previously undetected conformational changes of the protein. Furthermore we determined the activation energy of the mean transient fluorescence kinetics to be 18.2 kcal/mol. We compared this value with the activation energy of 18.5 kcal/mol for the I_2/I_2' transition in the photoreceptor PYP which we measured also by transient tryptophan fluorescence spectroscopy. The similar kinetics of the conformational change in both photoreceptor systems may be related to their shared PAS domain fold.

In Chapter 8 the results and conclusions of the experiments described in this thesis are summarized and future experiments are proposed.

Table of Contents

Abstract.....	1
Abbreviations.....	4
Chapter 1.....	7
General Introduction.....	8
Photoreceptors.....	8
Methods.....	26
Motivation and goals of this work.....	37
References.....	39
Chapter 2.....	49
Time-resolved single tryptophan fluorescence in photoactive yellow protein monitors changes in the chromophore structure during the photocycle via energy transfer.....	50
Chapter 3.....	51
Distinguishing chromophore structures of photocycle intermediates of the photoreceptor PYP by transient fluorescence and energy transfer.....	52
Chapter 4.....	53
Role of a conserved salt bridge between the PAS core and the N-terminal domain in the activation of the photoreceptor Photoactive Yellow Protein.....	54
Chapter 5.....	55
Time-resolved spectroscopy of dye-labeled PYP suggests a pathway of light-induced structural changes in the N-terminal cap.....	56
Chapter 6.....	57
Monitoring the conformational changes of photoactivated rhodopsin from μ s to seconds by transient fluorescence spectroscopy.....	58
Chapter 7.....	59
The kinetics of light induced conformational change in phot1 LOV2-J α probed by transient tryptophan fluorescence.....	60
Abstract.....	61
Introduction.....	62
Materials and Methods.....	64
Results and Discussion.....	65
Conclusions.....	71
References.....	72
Chapter 8.....	75
Conclusions and Outlook.....	76
PYP.....	76
Rhodopsin.....	79
LOV2.....	81
BLUF.....	82
Transient Fluorescence Anisotropy.....	84
Summary.....	86
References.....	87
Acknowledgments.....	90
List of Publications.....	91
Publications in Scientific Journals.....	91
Contributions to Scientific Conferences.....	92
Zusammenfassung.....	93

Abbreviations

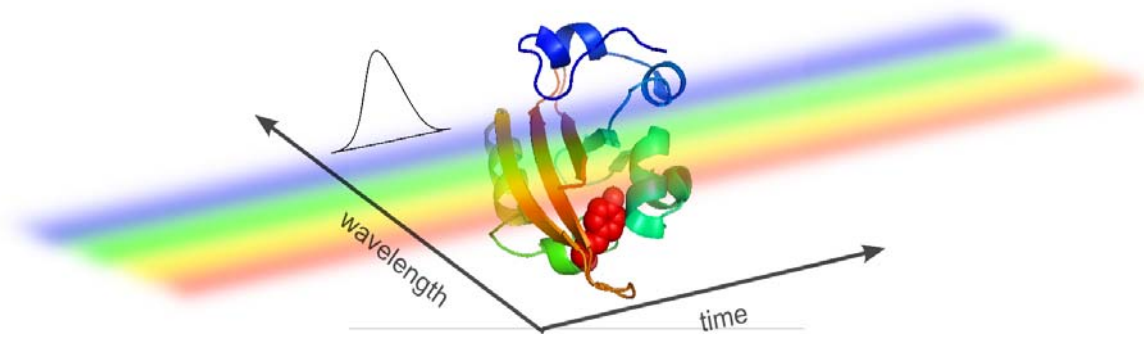
PYP	Photoactive Yellow Protein
PAS	PER- period clock protein/ ARNT- aryl hydrocarbon receptor nuclear translocator/ SIM-single minded
LOV	Light/Oxygen/Voltage
BLUF	Blue Light Using FAD
Ppr	PYP phytochrome-related
Ppd	PYP/bacteriophytochrome/diguanylate cyclase
D	Aspartic acid
E	Glutamic acid
H	Histidine
K	Lysine
R	Arginine
N	Asparagine
Q	Glutamine
S	Serine
T	Threonine
I	Isoleucine
L	Leucine
V	Valine
M	Methionine
W	Tryptophan
F	Phenylalanine
Y	Tyrosine
A	Alanine
G	Glycine

Abbreviations

C	Cysteine
P	Proline
Lys	Lysine
Trp	Tryptophan
Cys	Cysteine
GDP	Guanosinediphosphate
GMP	Guanosinemonophosphate
cGMP	cyclic Guanosinemonophosphate
ESR	Electron Spin Resonance
FTIR	Fourier Transform Infrared Spectroscopy
NMR	Nuclear Magnetic Resonance
CD	Circular Dichroism
ORD	Optical Rotatory Dichroism
DMPC	Dimyristoylphosphatidylcholine
SPC	Single Photon Counting
FMN	Flavinmononucleotide
FAD	Flavin Adenine Dinucleotide

Abbreviations

Chapter 1



General Introduction

Photoreceptors

General

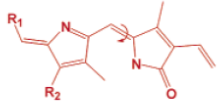
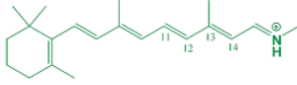
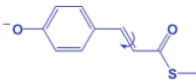
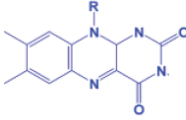
classes	CHROMOPHORES example	key structural element	PHOTOSENSOR FAMILY	PHOTOCHEMISTRY
tetrapyrroles	phytochromobilin		Phytochromes	<i>trans</i> ↔ <i>cis</i>
polyenes	retinal		Rhodopsins	<i>trans</i> ↔ <i>cis</i>
	coumaric acid		Xanthopsins	<i>trans</i> ↔ <i>cis</i>
'aromatics'	flavin		Cryptochromes	electron transfer?
			Phototropin	cysteinyll adduct formation
			BLUF proteins	proton transfer?

Figure 1 Classification of the family of photoreceptors by their different chromophores. Figure taken from (1)

Organisms have to adapt to their environment in order to survive. Thus they developed several protein sensors which probe their surrounding. As light is necessary for the survival of many organisms (especially the photosynthetic ones) they developed a variety of light sensing proteins. These molecular light sensors are called photoreceptors.

In addition to their biological importance photoreceptors are excellent model systems for biological signal transduction and protein kinetics. As they can be activated by short light pulses it is possible to resolve their reaction kinetics with high time resolution with optical methods.

In general photoreceptors consist of a protein (called apo protein) and a cofactor (called chromophore). When light is absorbed by the chromophore it changes its configuration. This leads to conformational changes of the protein and the formation of the signaling state of the receptor. In this way light is translated into a signal which is recognizable for the cell and triggers the signal transduction pathway.

To classify the many different photoreceptors it is useful to distinguish them by their different cofactors. In this way Van der Horst et al. (1) divided the photoreceptors into four families: Rhodopsins which bind retinal as a chromophore, phytochromes which bind linear tetrapyrroles, the xantopsins which bind coumaric acid and the flavin binding photoreceptors. The big family of flavin binding photoreceptors is further divided into the sub classes of cryptochromes, phototropins and BLUF proteins according to amino acid sequence similarities.

The families of photoreceptors are shown in Figure 1 together with the chemical

Chapter 1

structure of their chromophores and their photochemistry.

For the first three families the light induced configuration change is an E/Z isomerization of the chromophore. For the flavin binding photoreceptors the primary photochemistry is not clear yet with the exception of the phototropins. Here the absorption of light leads to a transient cysteinyl adduct formation in the LOV1 and LOV2 domains (2).

PYP

Biology/sequence

Photoactive Yellow Protein is the only member of the photoreceptor family of xantopsins. So far 14 Photoactive Yellow Proteins in 12 different organisms are identified, which are presumed to bind p-coumaric acid as a chromophore via thiol-ester linkage to a conserved cysteine residue (see Figure 1) (3). They are single domain proteins or parts of multidomain fusion proteins. Ppr from the organism *Rhodothalassium salexigens* for example consists of a PYP- and a phytochrome-domain. It is furthermore the only xantopsin for which the biological function is known. It regulates the chalcone synthase gene expression in response to blue light (4). The sequence of the Photoactive Yellow Proteins and the PYP-domains of the fusion proteins Ppr and Ppd from *Thermochromatium tepidum* are shown in Figure 2A. Highly conserved and functionally critical residues are indicated by an asterisk respective an At sign. The sequence identity of the PYPs varies between 19 to 78% and there are 6 absolutely conserved amino acids (G29, G59, F62, F63, A67 and C69) (3). The degree of sequence identity in dependency of the sequence position is shown in Figure 2B.

In this study we investigated the PYP from *Halorhodospira halophila*, the first PYP discovered. It is a small (14-kDa, 125 amino acids) soluble cytoplasmic protein and has an absorption maximum at 446 nm. Its amino acid sequence is shown in the line 3 of Figure 2A. The colored bars in Figure 2 highlight the secondary structure elements of PYP which are derived from the crystal structure of PYP from *H. halophila* which is discussed in the following paragraph.

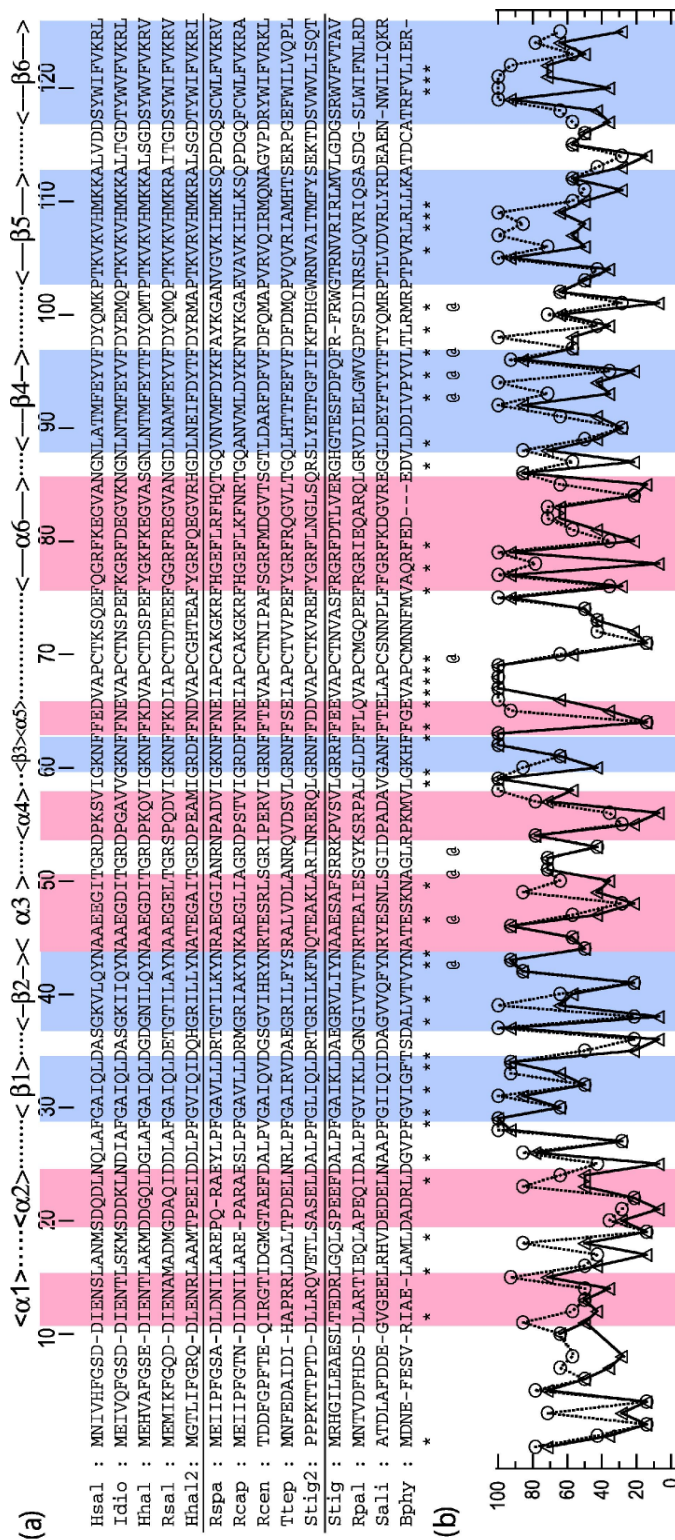


Figure 2 a Sequence alignment of Photoactive Yellow Proteins respective PYP-domains of proteins from the organisms *Halo* (*Hhal*, *Hhal2*), *Halo* (*Hsal*), *Idio* (*Idio*), *Thermo* (*Ttep*), *Rhodo* (*Rspa*, *Rcap*, *Rsal*, *Rcen*), *Rhodo* (*Rpal*), *Stigma* (*Stig*, *Stig2*), *Burkholderia* (*Bphy*) and *Salinibacter* (*Sali*). Secondary structure elements are indicated by colored bars (α -helices red, β -sheet blue), residues indicated with * are highly conserved, residues indicated by @ are functional critical. **b** Degree of sequence identity (Δ) and similarity (\circ) for the residues in the PYP domains (groups of similar amino acids are (D, E), (H, K, R), (N, Q, S, T) (I, L, V, M, W, F, Y) and (A, G)). The figure is taken from (3).

Structure

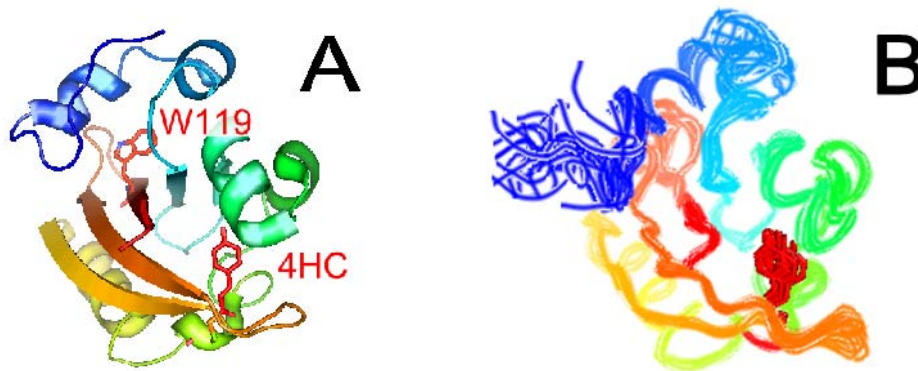


Figure 3 **A** Backbone crystal structure of PYP based on Protein Data Bank file 1NWZ.pdb (5). The chromophore, C69 and W119 are shown as sticks. **B** overlay of 26 possible PYP structures derived from NMR experiments based on Protein Data Bank file 3PHY.pdb (6). The chromophore is shown as sticks.

The crystal structure of the PYP ground state has been solved to a resolution of 0.85 Å and is shown in Figure 3A. It is composed of several α -helices and a central β -sheet which divides the protein into 2 parts both forming a hydrophobic core. On one side is the chromophore binding domain on the other the N-terminal cap.

Chromophore binding domain and central β -sheet form the PAS-domain of the protein. PYP is the structural prototype of this large and diverse family of sensory proteins, as it was the first member for which the X-ray structure has been solved (7, 8). Note that PAS is an acronym for **PER/ARNT/SIM** which were the first three identified members of the family. PER stands for the *Drosophila* Period clock protein, ARNT for the vertebrate Aryl hydrocarbon receptor nuclear translocator and SIM for the *Drosophila* Single-minded. Over 2000 proteins, which mainly are involved in signal transduction, have been identified to contain one or more PAS domains (9). In contrast to PYP, which is a single PAS domain protein with a ~30 amino acid N-terminal extension, most proteins containing PAS domains have a multidomain architecture (10).

The ground state structure of PYP was also determined with atomic resolution by NMR-spectroscopy (6). An ensemble of the 26 most probable atomic structures are shown in Figure 3B. They resemble the crystal structure to a high degree, with the exception of parts of the N-terminal cap which are poorly resolved in the NMR-structures and are therefore thought to be highly flexible in solution.

Recently the crystal structure of PYP was solved by neutron diffraction experiments (11, 12). In this way the positions of the protons in the protein crystal could be resolved. Figure 4 shows the structure of the binding pocket with the unusually short H-bonds between the chromophore and neighboring amino acids E46 and Y42 which stabilize the ground state structure, and have a big influence on the dark state absorption spectrum and the photocycle kinetics (13, 14).

PYP contains a highly conserved single tryptophan at the position 119 in the amino acid sequence. It is part of the central β -sheet at the interface to the N-terminal cap as shown in Figure 3A. The distance W119-chromophore is ~16 Å.

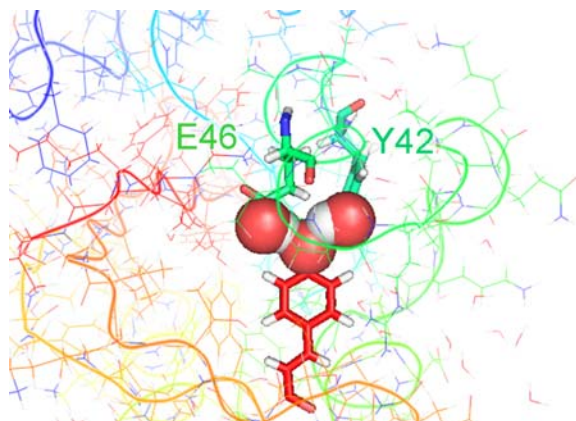


Figure 4 Crystal structure of the chromophore binding pocket of PYP in the ground state P based on the protein data bank file 2QWS.pdb derived from neutron scattering experiments (11). The chromophore (red) and the amino acids E46 and Y42 are shown as sticks. The O and H atoms involved in the H-bonds between the chromophore and E46 and Y42 are shown as red and grey spheres.

Photocycle

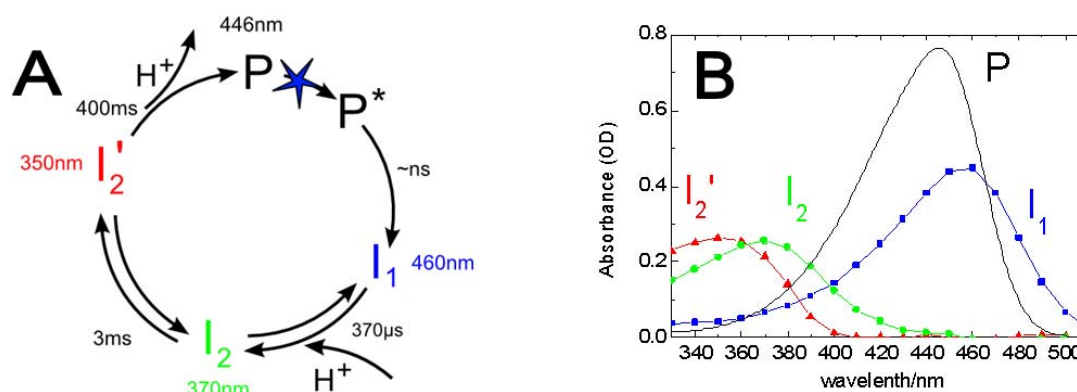


Figure 5 **A** Photocycle of PYP at pH 7 in the time window from μs to seconds together with the apparent time constants of the transitions and the absorption maxima of the intermediates. **B** Absorption spectra of PYP ground state and photointermediates from (15) calculated from transient absorption data.

The absorption of light by PYP leads to a fast isomerization of the chromophore around its C7=C8 double bond (shown in Figure 1) and triggers a sequence of thermal relaxations which end in a recovery to the ground state in less than one second. The current photocycle model at pH 7 in the time window from μs to seconds is shown in Figure 5A (the earlier photointermediates I_0 and I_0^\ddagger with lifetimes in the range of ps to ns are not shown because they are not relevant for this study). The corresponding UV-VIS absorption spectra of the photointermediates are shown in Figure 5B and are derived from transient absorption spectroscopy measurements (15). The existence of equilibria between the photocycle intermediates, which is pH (15, 16) dependent, has been proven by double flash experiments (17).

The structure of the photocycle intermediates have been investigated by various biophysical techniques. In I_1 , which absorbs at 460 nm, the thioester group of the chromophore is flipped over (18). It decays with a time constant of several hundred μs to the blue shifted intermediate I_2 with an absorption maximum at 370 nm and a protonated chromophore (15). Major structural changes occur in the transition from I_2 to I_2' which absorbs at 350 nm with a time constant around 2 ms (19-22).

Chapter 1

These conformational changes include the exposure of a hydrophobic patch, which was shown by transient dye binding experiments (20, 22). This is a hint to the putative signaling mechanism of the photoreceptor as the hydrophobic patch might act as an interface for a binding partner. Therefore I_2' is believed to be the signaling state of PYP.

Crystal structures of several photointermediates have been solved by time resolved and low temperature X-ray crystallography (23-25). For the intermediate I_1 two possible structures exist, one with a broken H-bond between E46 and the chromophore. For I_2 the crystal structures show a flip of the aromatic ring out of the binding pocket, breaking the hydrogen bonds of the O⁻ group to the residues E46 and Y42 and forming of a new one to R52. The crystal structures of the binding pocket in P and I_2 are shown in Figure 6. For the signaling state I_2' no X-ray structure exists because the major structural changes associated with the formation of this intermediate are blocked in PYP crystals, probably due to crystal lattice constraints (18). On the other hand a NMR-spectroscopy study on a PYP construct called Δ PYP lacking the N-terminal cap resolved the protein structures of the ground state and a photoactivated state. The backbone of the 20 most probable Δ PYP ground state structures is shown in Figure 7A. It resembles the NMR-structure of the PAS-domain in the wild type protein to a high degree. The determination of the structure of the photoactivated state was possible, as the recovery rate of the protein construct is reduced by a factor of 1000 in comparison to wild type. The 20 most probable light activated Δ PYP structures are shown in Figure 7B, which all show a nearly complete light-induced unfolding of the α -helices of the construct. However whether the photoactivated Δ PYP structures resemble the ones for the PAS domain of photoactivated wild type is doubtful, as the photocycle kinetics of both proteins are very different (26).

This highlights the importance of the N-terminal cap, whose amino acids are at least 15 Å away from the chromophore binding pocket, for the proper functioning of the protein. Furthermore there are several studies which suggest that the big light-induced conformational changes in PYP are concentrated in this domain (27-29). It is therefore an important and still unresolved question how the light signal is transduced from the chromophore binding pocket across the central β -sheet to the N-terminal cap. The dependency of the recovery kinetics on the salt concentration of the solution is abolished in PYP constructs lacking the N-terminal cap, suggesting ionic interactions between this domain and the PAS-core being responsible for this effect in wild type (30). In the crystal structure of ground state PYP there is a salt bridge between K110 in the central β -sheet and E12 in one of the N-terminal cap α -helices (5), which was hypothesized to mediate the interaction between both domains (31).

As mentioned in the previous paragraph the single tryptophan W119 of PYP is located at the interface between the β -sheet and the N-terminal cap, which is a prominent position to monitor the light-induced changes in interaction between both domains. A study investigating the tryptophan fluorescence spectra of PYP in the dark state and a steady-state photo equilibrium under background illumination showed that there are light-induced changes in the tryptophan emission quantum yield, the maximum emission wavelength and the accessibility to fluorescence quencher molecules (32).

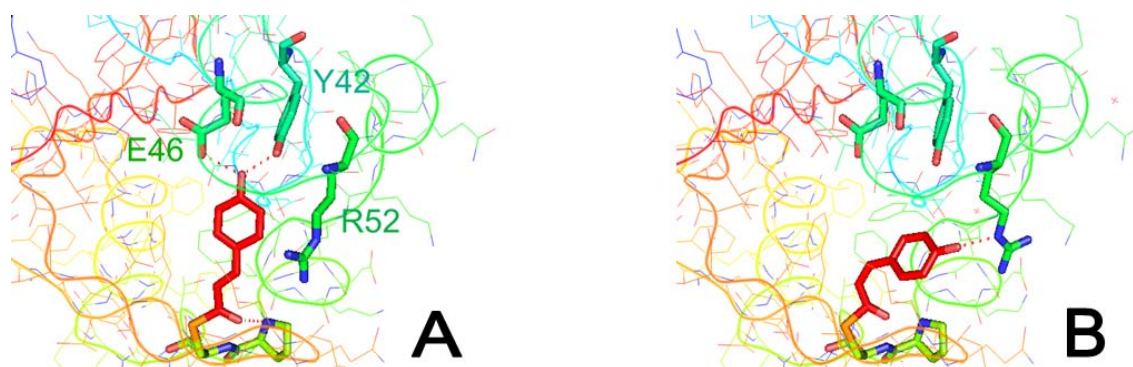


Figure 6 Crystal structure of the chromophore binding pocket of PYP in the ground state P (**A**) and the photointermediate I₂ (**B**) based on the protein data bank file 1TS0.pdb (24). The chromophore (red) and the amino acids E46, Y42, P68 and C69 are shown as sticks. H-bonds between the chromophore and neighboring amino acids are indicated by red dotted lines.

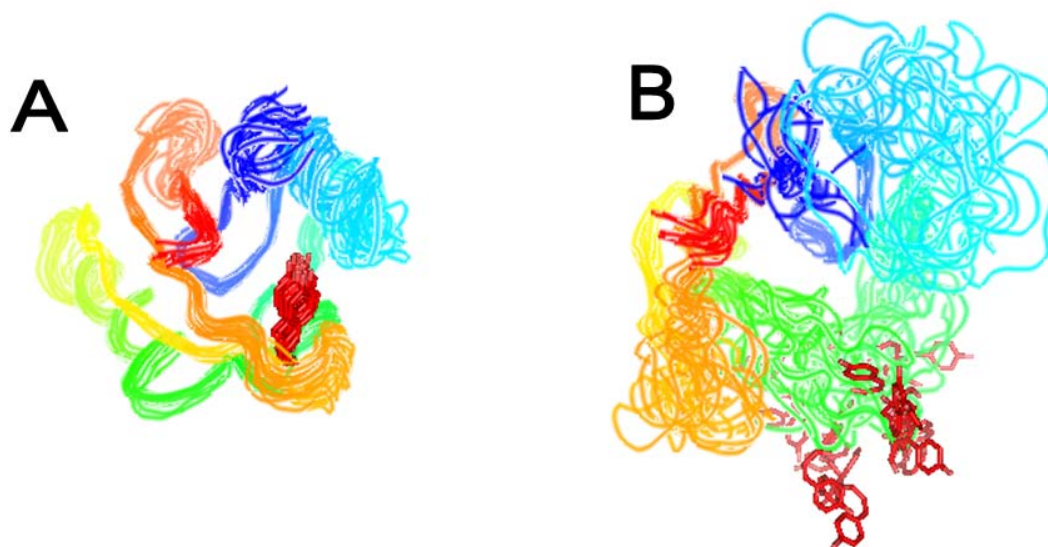


Figure 7 Overlay of 20 possible Δ PYP structures in the dark state P (**A**) and under blue light illumination (**B**) derived from NMR experiments based on Protein Data Bank files 1XFN.pdb and 1XFQ.pdb (33). The chromophore is shown as sticks.

Rhodopsin

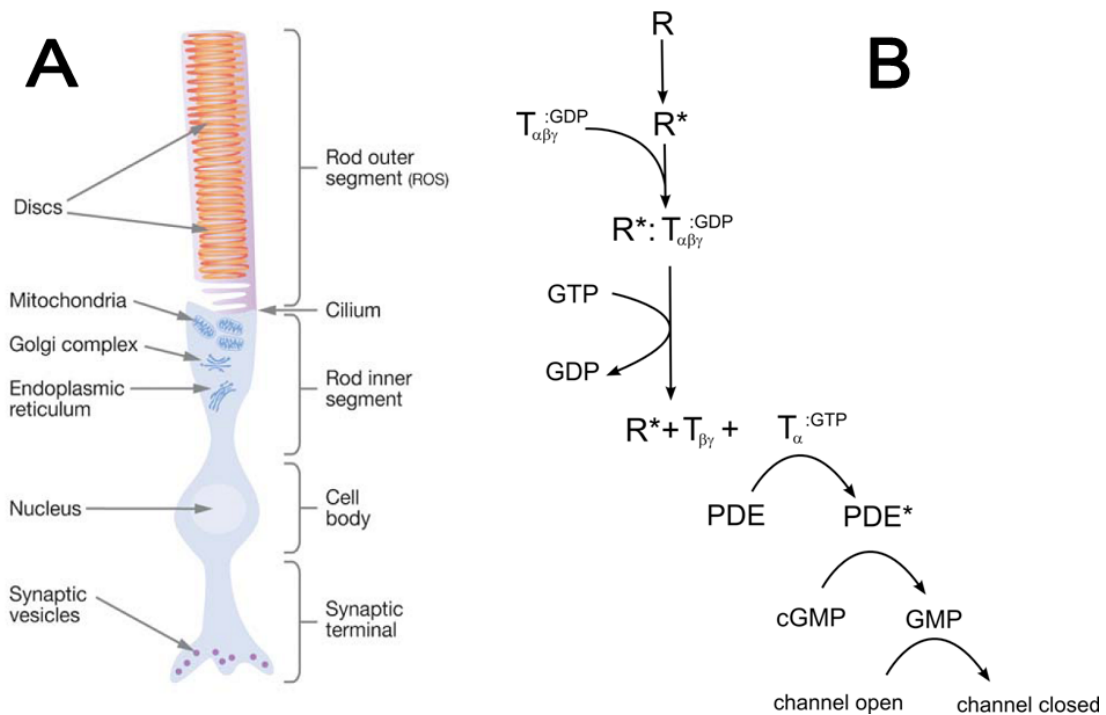
Biology/sequence

Figure 8 **A** Composition of a Rod cell. Rhodopsin is located in the discs in the outer segment. Figure taken from (34). **B** Scheme of the visual signal transduction pathway.

Rhodopsin is the visual pigment in the rod cell of the vertebrate eye. Rod cells are responsible for dim light vision and therefore highly light sensitive. The schematic composition of a rod cell is shown in Figure 8A. Rhodopsin is located in the discs of the rod outer segment. It is the main protein component of the rod outer segment (ROS) membrane (>90%) (34).

When rhodopsin is activated by light, it triggers a signaling pathway which in the end results in a hyperpolarization of the rod cell. This inhibits the release of glutamate into the synaptic gap and transduces the signal to the neurons of the retina. A scheme of the visual signal transduction pathway in the rod cell is shown in Figure 8B.

In the first step rhodopsin is activated by light and forms the signaling state Meta_{II} or R*. The G-protein transducin binds to R* and releases a GDP nucleotide. Then the heterotrimeric transducin binds a GTP nucleotide and dissociates into its α unit and the βγ-unit. The α-unit dissociates from R* and activates the enzyme phosphodiesterase (PDE). In its active state PDE catalyzes the reaction from cGMP to GMP. As cGMP is the substrate of a cation channel in the cell membrane which leads to its opening, the reduction of cGMP in the cytosol results in a closure of the channel and the hyperpolarization of the rod cell. Note that in different steps of the phototransduction cascade the signal gets amplified: One R* activates several transducins, one activated Gα activates only one PDE, which itself hydrolyses several cGMP (35). This leads to an overall amplification factor of around 10⁷ (this means the activation of one rhodopsin prevents the entry of around 10⁷ cations into the rod cell) (36), partially explaining the high light sensitivity of dim light vision. Another point increasing the light sensitivity of

Chapter 1

the rod cell is the extraordinary low residual activity of rhodopsin. It has been estimated that the decay of rhodopsin via thermal retinal isomerization at physiological temperatures has a lifetime of between 420 and 470 years (36, 37). After activation, R* gets shut down in a two step process involving the phosphorylation of rhodopsin by rhodopsin kinase and the binding of arrestin, which completely deactivates the receptor.

Besides its role in vision, rhodopsin is also an important model system for G-protein coupled receptors (GPCRs) in general. There are ~500 genes in the human genome encoding sensory GPCRs, which regulate a wide range of physiological processes (34) and are therefore targets of more than 30% of the therapeutically relevant drugs in humans (38).

In this study we investigate the activation kinetics of bovine rhodopsin in native disc membranes. The amino acid sequence of bovine rhodopsin is shown in Figure 9. Colored cylinders highlight the α -helical secondary structure of the receptor. Rhodopsin is a transmembrane protein with 7 transmembrane helices and binds 11-cis retinal as a chromophore via a protonated Schiff base linkage to Lys 296. The chemical structure of the chromophore in its 11-cis configuration is shown as an inset in Figure 9. The apo-protein without the bound retinal is called opsin.

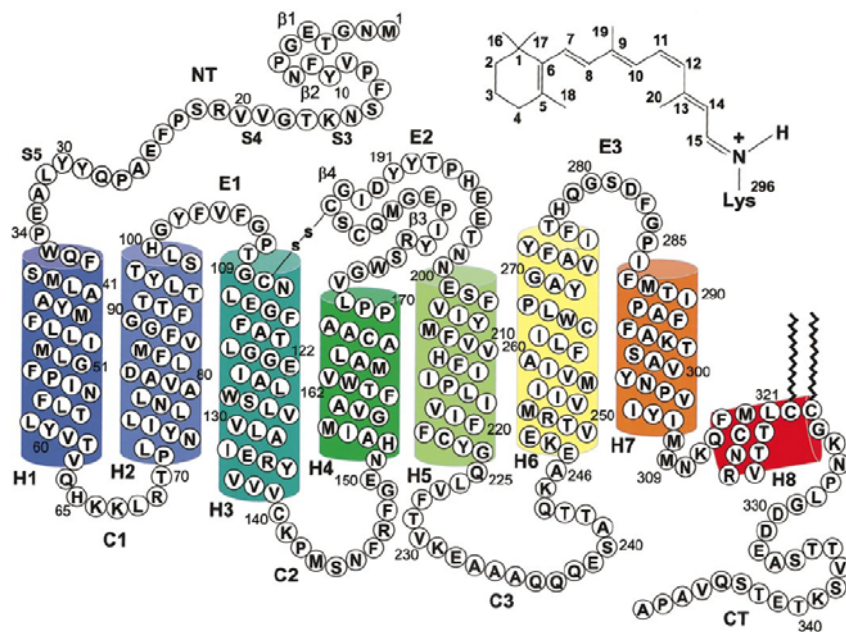


Figure 9 Amino acid sequence of bovine rhodopsin taken from (36). The helices are shown as colored cylinders. The inset on the right upper corner shows the chemical structure of the 11-cis retinal bound to Lys296.

Structure

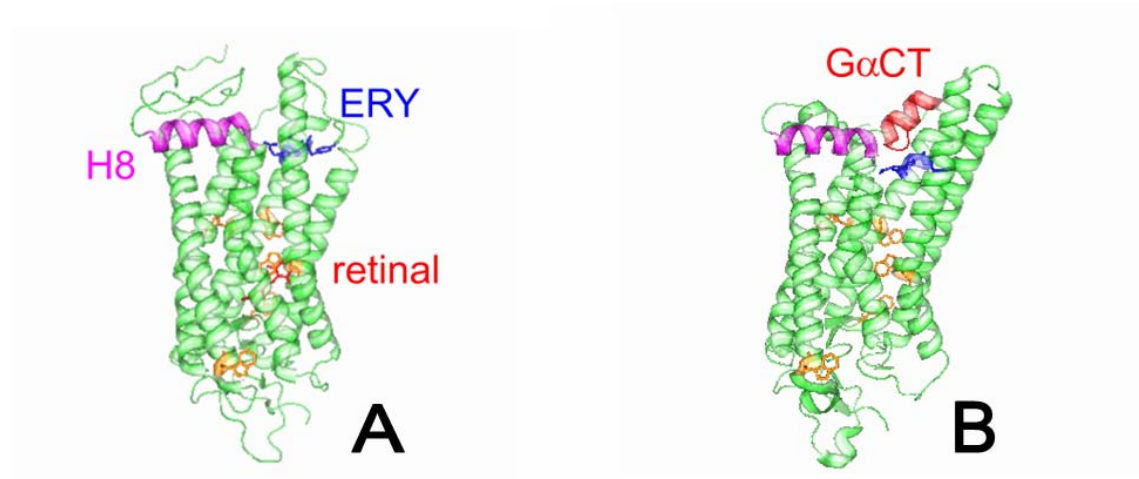


Figure 10 **A** Secondary structure of bovine rhodopsin based on the Protein Data Bank file 1U19.pdb (resolution 2.2 Å) (39). The retinal (red), the functionally important ERY motif (blue) and the 5 tryptophans (orange) are shown as sticks, the helix H8 is colored in magenta. **B** secondary structure of bovine opsin in complex with a synthetic peptide called GαCT based on the Protein Data Bank file 3DQB.pdb (resolution 3.2 Å) (40). The 11 amino acids long peptide, which is similar to the C-terminal end of transducin, is shown in red.

The crystal structure of bovine rhodopsin is shown in Figure 10A (39). Actually it was the first GPCR whose atomic structure has been solved (41), but recently also the structures of squid rhodopsin. The turkey β_1 - and the human β_2 -adrenergic receptor and the human A_{2A} adenosine receptor have been determined (42-46). For a detailed review of the atomic details of the rhodopsin crystal structure see (36). Note that the cytoplasmic surface, which is the binding interface for the G-protein transducin, is on top of the Figure 10.

One part of this binding interface is the small α -helix H8 which runs parallel to the cytoplasmic surface from N310 to C322. It acts as a membrane-dependent conformational switch and contributes to the highly conserved NPxxY(x)_{5,6}F motif via F313 (47, 48). Furthermore there are 5 tryptophans in the sequence of rhodopsin, they are highlighted in orange in Figure 10. One of them, W265 lies in the retinal binding pocket in direct contact with the chromophore and is supposed to reorient upon photoactivation of rhodopsin (49, 50).

Recently also the crystal structure of opsin in complex with a 11 amino acids long synthetic peptide (GαCT), which is similar to the C-terminal end of transducin has been solved and is shown in Figure 10B (40). The structure is very similar to the structure of opsin crystallized without the peptide (51). As GαCT stabilizes Meta_{II} the authors suggest that the protein conformation of the opsin-peptide complex is similar to the signaling state of the photoreceptor. There are several differences between the structures of rhodopsin and the peptide-opsin complex regarding for example the length of the transmembrane helices, but the most important difference is the packing of the helices on the cytoplasmic surface, which is shown in Figure 11. To make way for the peptide the helices 5, 6 and 7 have to reorient. Especially helix 6 tilts out of the helix bundle by 6-7 Å. This light-induced tilt is consistent with several spectroscopic studies on Meta_{II} (52-56), supporting the view that the opsin-peptide crystal resembles the active state conformation. Another important

prerequisite for rhodopsin activation is supposed to be the breakage of the ionic lock between Glu134 and Arg135 in the highly conserved ERY motif on the cytoplasmic end of helix 3 and the resulting proton uptake from the solvent by Glu134 (57, 58). Indeed this ionic lock, which is present in the dark state crystal (39) is broken in the peptide-opsin structure (40). On the other hand a fluorescence study on the binding properties of a similar peptide as used in (40) with dye labeled rhodopsin detected clear differences in the peptide–Meta_{II} interactions upon retinal cleavage by hydroxylamine, suggesting major structural differences between peptide-Meta_{II} and peptide-opsin complexes (53).

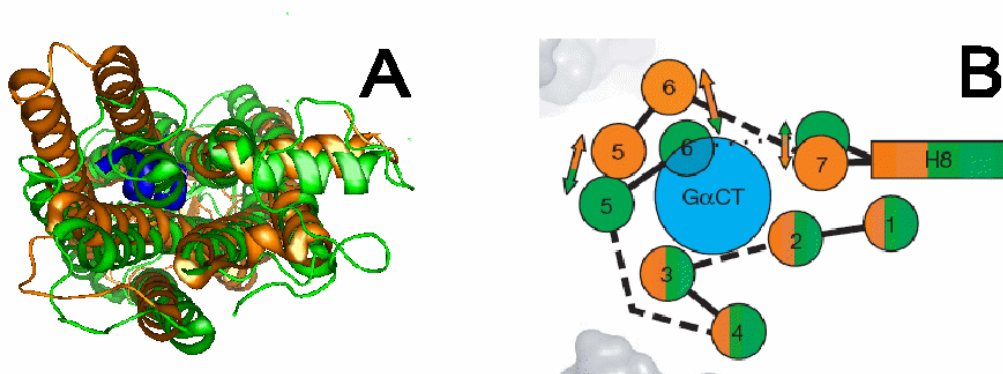


Figure 11 **A** Overlay of the secondary structures of the cytoplasmic surface of rhodopsin (green) and opsin (orange) in complex with the peptide G α CT (blue) based on the Protein Data Bank files 1U19.pdb (39) and 3DQB.pdb (40). **B** Schematic representation of the structural differences between the crystal structure of rhodopsin (green) and opsin (orange) in complex with the peptide G α CT (blue) as shown in panel A. The figure is taken from (40)

Photoactivation cascade

The absorption of light by rhodopsin induces a rapid isomerization (200 fs) of the 11-cis retinal to the all-trans form. This triggers several thermal relaxations leading to the formation of the signaling state Meta_{II} in several ms. The different photointermediates, their absorption maxima and the time constants of the corresponding transitions are shown in Figure 12. In the transition from Meta_I to Meta_{II} the Schiff base linkage is deprotonated causing a major blue shift of the absorption spectrum from 480 nm in Meta_I to 380 nm in Meta_{II}. Figure 13 shows the UV-VIS absorption spectra of Rhodopsin and Meta_{II}. Due to back reactions, Meta_I and Meta_{II} form a temperature, pH and salt dependent equilibrium (59). Depending on the conditions the Meta_I/Meta_{II}-equilibrium decays either directly to opsin and all-trans retinal or via the metastable intermediate Meta_{III} (for a detailed review on Meta_{III} see (60)). The chemical structure of the retinal and the Schiff base in rhodopsin, the early photointermediates from photo to Meta_I, Meta_{II} and all trans retinal+opsin are also shown in Figure 12. In the rod cell after photoactivation, shut down and retinal hydrolysis of rhodopsin, opsin is recycled by reconstitution with fresh 11-cis retinal in a reaction pathway called retinoid cycle (for details see review (61)).

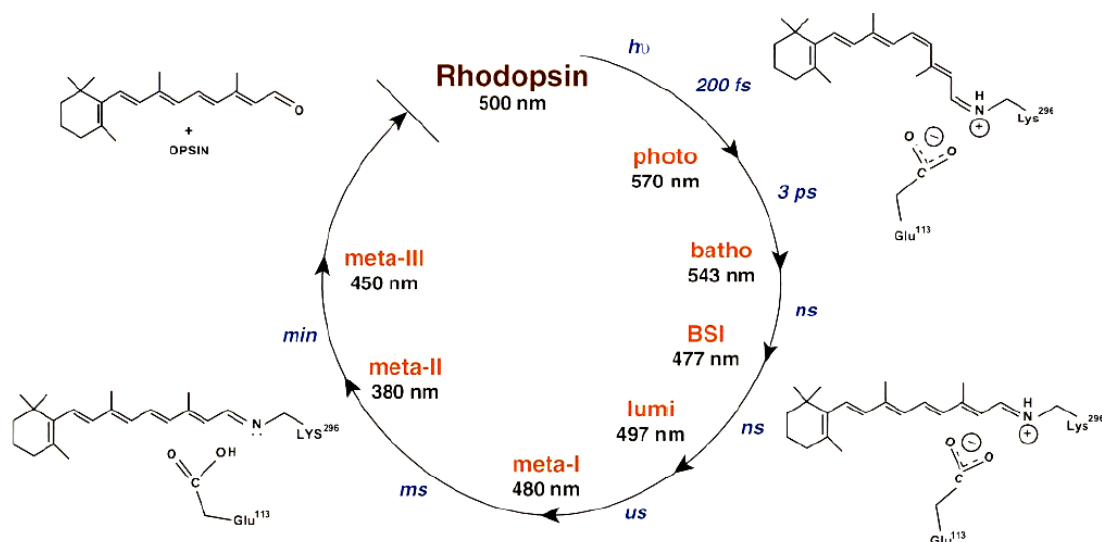


Figure 12 Photoactivation scheme of rhodopsin showing the names of the intermediates, their absorption maxima and the apparent rate constants for the transitions. The chemical structures of the retinal and Glu113 are drawn clockwise for the states rhodopsin (protonated 11-cis retinal), the early photointermediates (protonated all-trans retinal), Meta_I (deprotonated all-trans retinal) and opsin + all trans retinal. The figure is taken from (36).

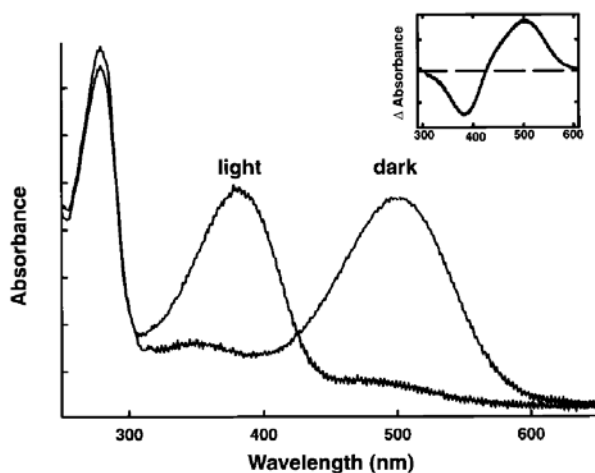


Figure 13 UV-VIS Absorption spectra of rhodopsin and Meta_{II} taken from (36). The inset shows the rhodopsin- Meta_{II} difference spectrum.

Steady state investigations of Meta_I and Meta_{II} by several biophysical methods such as electron microscopy (62), ESR- (52) and FTIR-spectroscopy (63) and fluorescence depolarization experiments (64) suggested that the Meta_I to Meta_{II} transition is accompanied by major conformational changes of the protein, which enable the docking and activation of the G-protein transducin. Several studies which used C316 for site-specific labeling with fluorescence- or ESR-labels indicated light-induced structural changes in H8 (64-66). In particular a fluorescence study using the dye Alexa594-maleimide bound to C316 detected a 20% increase in the fluorescence quantum yield of the dye upon photoactivation of rhodopsin (65).

Studies on the tryptophan fluorescence in rhodopsin showed an increase of the fluorescence quantum yield by a factor of 2-4 in the Meta_{II}/opsin transition (67, 68) and a

slightly smaller quantum yield in Meta_{II} than in rhodopsin (67). Furthermore an analysis of the tryptophan absorption spectra in rhodopsin and Meta_{II} showed small light-induced changes in the extinction coefficient of W265 and W126 presumably caused by structural or environmental changes (69).

Nevertheless the sequence of the molecular events during the activation of rhodopsin is still unclear, partially because the number of time-resolved techniques applied so far to rhodopsin to measure directly the kinetics of the photoactivation process is limited to transient UV-VIS-absorption and ESR-spectroscopy. Transient absorption measurements of rhodopsin in micelles showed that under these conditions the proton uptake from the solvent is not coupled to the deprotonation of the Schiff base, suggesting two different spectrally indistinguishable Meta_{II} states with different protonation state (70). Time resolved ESR-studies of site-directed spin-labeled rhodopsin suggested structural changes in parallel with Schiff base deprotonation in native ROS membranes (66) and in parallel with proton uptake in micelles (71).

LOV2 / Phototropin

Biology/sequence

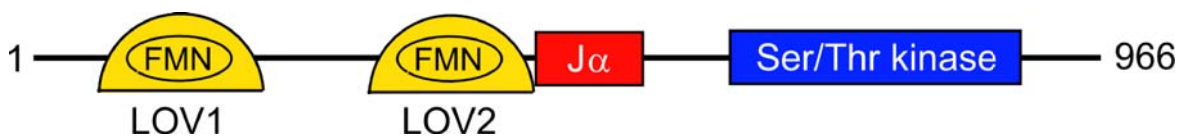


Figure 14 Schematic representation of the functional domains in oat phototropin1. The LOV1 and LOV2 domains are shown in yellow, the J α helix domain following the LOV2 domain is shown in red and the Ser/Thr kinase domain is shown in blue. Drawing adapted from (72).

LOV1 and LOV2 are the light sensing flavin binding domains of the photoreceptor phototropin. LOV is an acronym for light/oxygen/voltage pointing to the broad range of stimuli sensed by these domains. Phototropins mediate phototropism, the light directed growth of plants or fungi, but also light induced stomatal opening and chloroplast movement in response to changes in the light intensity, which help to regulate the photosynthetic efficiency of a plant (73-77). In *Arabidopsis* two different phototropins called phototropin1 (phot1) and phototropin2 (phot2) are present. While phot1 is responsible for phototropism at low light intensities phot2 is suggested to be responsible for high light avoidance responses (78).

There are also photosensor domains containing a photoactive flavin with structure and photochemistry very similar to LOV1 and LOV2 in other proteins than phototropin. In general these LOV domains are coupled to effector domains and are therefore part of large multidomain proteins (with the exception of *Neurospora* VVD and *Arabidopsis* PAS/LOV which are single LOV domain proteins). These proteins can be categorized by their function as proteins regulating circadian rhythms, LOV-histidine kinases, LOV-STAS proteins (LOV-sulfate transporter and anti-sigma factor antagonist) and LOV phosphodiesterases (79). Recently a LOV-histidine kinase was found in *Brucella abortus*, regulating the virulence of the pathogen (80).

In this study we investigated the LOV2 domain from *Avena sativa* (oat) phototropin1. Figure 14 shows the composition of the 996 amino acid protein. On the N-terminal side

Chapter 1

are the light sensing LOV1 and LOV2 domains, on the C-terminal side there is a Ser/Thr kinase domain. Light activation of the LOV2 domain leads to an autophosphorylation of the kinase domain, whereas the LOV1 domain is suggested to act as a dimerization site (81, 82). Figure 15A shows the amino acid sequence of the LOV2 fusion protein investigated in this study. It consists of the LOV2 domain itself plus the following 30 residues on the C-terminal side including a 20 amino acids long amphipathic α -helix called $J\alpha$ (83). Furthermore there are 46 non native amino acids which act as a calmodulin binding site, necessary for protein purification. The chromophore of the LOV domains is flavinmononucleotide (FMN) which is bound noncovalently to the protein. The chemical structure of the isoalloxazine ring of FMN is shown in Figure 1. Figure 15 B shows an amino acid sequence alignment of the extended LOV2 domains from oat phototropin1, *Adiantum capillus-veneris* (fern) phy3 and the LOV1 domain from *Chlamydomonas reinhardtii* phototropin. Phy3 is a chimeric photoreceptor with homology to phytochrome at its N-terminal end and a phototropin at its C-terminal end. For all three LOV domains the crystal structures have been solved (84-86). The arrow marks a conserved cysteine residue necessary for the photoactivity of the LOV domains.

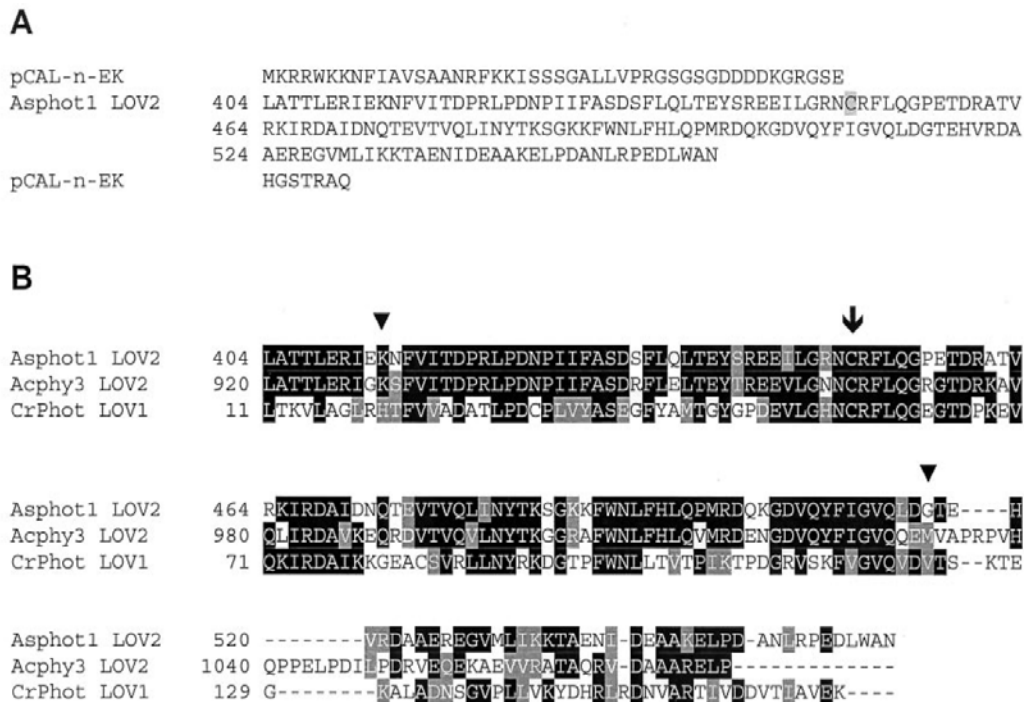


Figure 15 A Amino acid sequence of the LOV2 fusion protein examined in this thesis taken from (87). In the first and last line are the N- and C- terminal extensions encoding the calmodulin binding site. The three lines in between show the sequence of the oat phototropin1 (Asphot1) domain including LOV2 and the $J\alpha$ -helix. **B** Sequence alignment of LOV domains from different organism also taken from (87). The first line shows the sequence of the LOV2- $J\alpha$ domain of oat phot1 (Asphot1), the second the corresponding sequence from fern phy3 LOV2 (Acphy3) domain and the third line the sequence of *Chlamydomonas reinhardtii* phot LOV1 (CrPhot). Conserved residues are shaded. The segment of phy3 studied by crystallography is indicated by arrowheads, its chromophore binding pocket is shown in Figure 19. The conserved cysteine necessary for the light induced flavin-cysteinyl adduct formation in LOV2 and LOV1 domains is marked by an arrow.

Structure

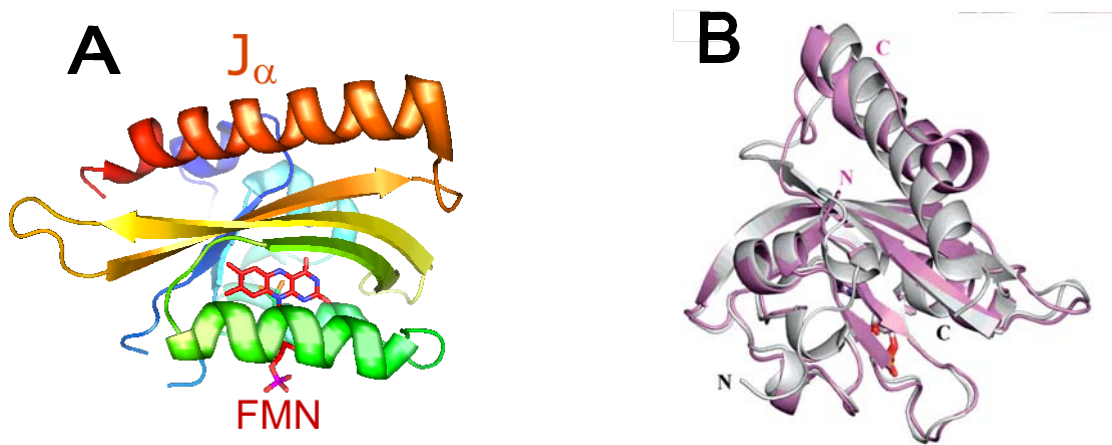


Figure 16 **A** Secondary structure of the oat phot1 LOV2-J α domain based on the Protein Data Bank file 2V0U.pdb (86). The chromophore is shown as sticks; the orange helix at the top of the structure is the J α -helix. **B** Joint presentation of the X-ray structure from panel A (grey) and the NMR-structure (magenta) from (83) taken from (86). The C- and N- termini of both structures are labeled; the chromophore is shown as sticks.

The atomic structure of the oat LOV2 domain including the J α -helix investigated in this study has been solved by NMR-spectroscopy (83) and X-ray crystallography (86). Figure 16A shows the crystal structure based on the Protein Data Bank file 2V0U.pdb with the chromophore shown as sticks. Figure 16B is an overlay of the NMR- (magenta) and X-ray-structure (grey). They resemble each other to a high degree with some differences for the J α -helix, which is bent in the NMR-structure but straight in crystals.

The LOV domains are a subset of the PAS-domain superfamily. The LOV2 domain crystal structure closely resembles that of other PAS-domains including PYP, HERG and FixL (84). The secondary structure of the domain consists of a 5-stranded antiparallel β -sheet and 4 α -helices forming the binding pocket of the chromophore, which sticks into the protein and is stabilized by an extended hydrogen-bonding network as well as by non-polar interactions. On the other side of the central β -sheet the C-terminal amphipathic J α -helix is located and stabilized by hydrophobic interactions with the β -sheet (83, 88). Note that in PYP, the other PAS domain protein investigated in this study, the central β -sheet divides the photoreceptor into two parts, the chromophore binding region and the N-terminal cap, a 26 amino acid long domain consisting mainly of two short α -helices. In this respect the composition of the LOV-J α construct is quite similar to PYP with the C-terminal α -helix J α taking the role of the N-terminal cap.

Photocycle

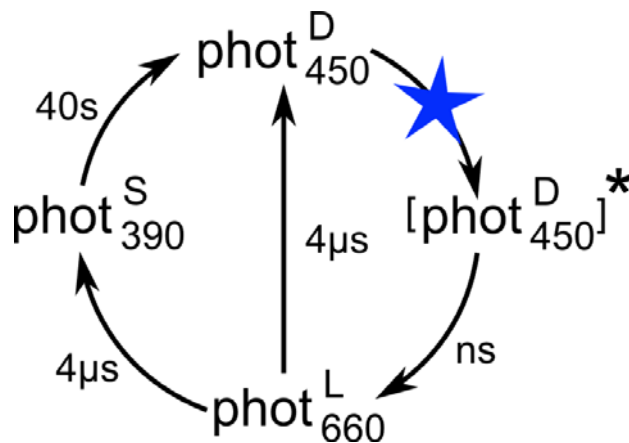


Figure 17 Photocycle of oat phot1 LOV2.

The photocycle of LOV2 is shown in Figure 17. In the dark state $\text{phot}^{\text{D}}_{450}$, the photoreceptor has an absorption maximum of 450 nm. The absorption of light brings the FMN to its excited singlet state. With a time constant in the range of ns an excited triplet state, called $\text{phot}^{\text{L}}_{660}$ with an absorption maximum of 660 nm is formed via intersystem crossing (89). With a time constant of 4 μs $\text{phot}^{\text{L}}_{660}$ decays either back to ground state or to the long living intermediate $\text{phot}^{\text{S}}_{390}$ with an absorption maximum at 390 nm. The transition to $\text{phot}^{\text{S}}_{390}$ is associated with the formation of a Cys-C4a flavin-cysteinyl adduct between a conserved cysteine and FMN (2, 90-92) and is slowed down nearly 5-fold in D_2O suggesting a proton transfer involved in the rate limiting step of the reaction (87). $\text{Phot}^{\text{S}}_{390}$ is the longest living intermediate of the LOV2 photocycle and is therefore supposed to be the signalling state of the photoreceptor domain. It recovers to the ground state with a time constant of ~ 40 sec. The UV-VIS absorption spectra of the dark state and the photointermediates are shown in Figure 18.

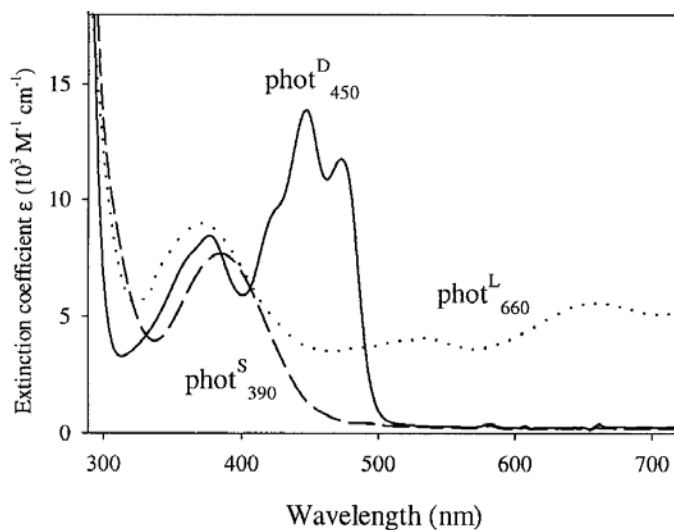


Figure 18 UV-VIS absorption spectra of the ground state ($\text{phot}^{\text{D}}_{450}$) and the two photointermediates $\text{phot}^{\text{L}}_{660}$ and $\text{phot}^{\text{S}}_{390}$ (89)

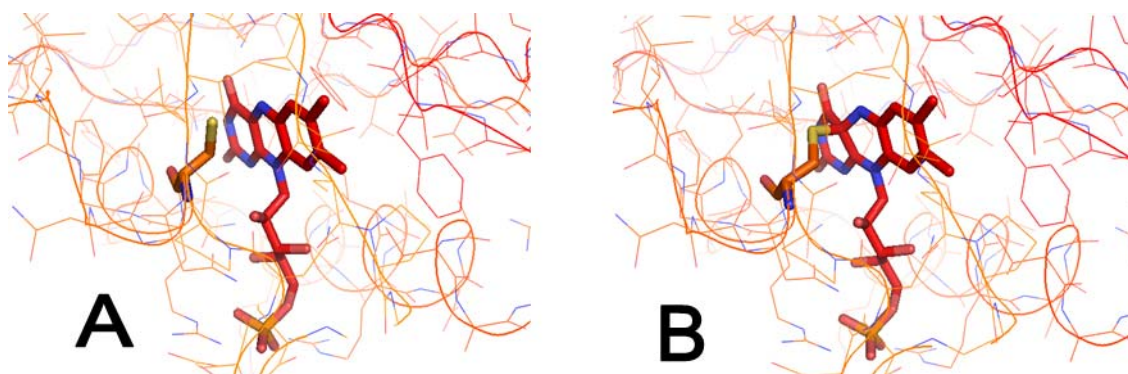


Figure 19 Crystal structure of the binding pocket of *Ac phy3* LOV2 of the dark state based on the Protein Data Bank file 1G28.pdb (A) (84) and in the light activated state based on the Protein Data Bank file 1JNU.pdb (B) (2). The chromophore C966 are shown as sticks.

The detailed reaction pathway for the flavin-cysteinyl adduct formation is still under debate. Proposed models either involve proton transfer between the sulfhydryl group of the cysteine and N5 of FMN prior to the formation of the C-S bond (84, 89, 93), or the involvement of a flavosemi-quinone free radical and reaction with a sulphur radical (94-96). For a detailed review of the LOV photochemistry see (97).

The crystal structure of the binding pocket of LOV2 from fern *phy3* in the ground state and the photoactivated state is shown in Figure 19. It illustrates the light induced formation of the transient flavin-cysteinyl adduct. For oat *phot1* LOV2-J α the crystal structures of *phot*^D₄₅₀ and *phot*^S₃₉₀ were also solved recently (86). The light induced flavin-cysteinyl adduct formation is also present in this system, but there is a structural heterogeneity for the conformation of the conserved cysteine in the dark state, which was also detected in crystals of *Chlamydomonas phot1*-LOV1 (85). Despite some rearrangements in the chromophore binding pocket no global light-induced conformational changes could be detected in fern *phy3* LOV2 as well as in oat *phot1* LOV2-J α crystals. But several experiments in solution showed, that the photoactivation of oat LOV2-J α is associated with major changes in the protein conformation. FTIR spectroscopy experiments indicated changes in the protein structure (91) and circular dichroism spectroscopy measurements detected a light induced loss in α -helical content (87). NMR experiments directly showed that illumination is associated with an unfolding of the C-terminal J α -helix including conformational changes for the two tryptophans W491 and W557 in the investigated domain (83). Furthermore the amino acids essential for the interaction between the β -sheet and the J α -helix were identified (88) and the free energy necessary for the unfolding process was determined (72). A scheme illustrating the light induced structural changes of oat *phot1* LOV2-J α is shown in Figure 20. The kinetics of the light-triggered unfolding process was investigated using transient optical rotatory dispersion (ORD) measurements and a transition in the far-UV (230 nm) appearing with a time constant $\sim 90\mu\text{s}$ was found (98). However the amplitude of this transition barely exceeded the noise level of the data reducing the significance of the results and motivating the search for new methods to probe the kinetics of the light-induced conformational change in LOV2-J α .

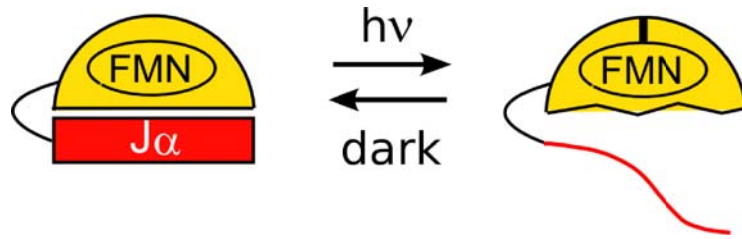


Figure 20 Schematic representation of the light-induced conformational changes in the oat phot1 LOV2- $J\alpha$ domain. Upon illumination the chromophore forms a covalent bond with a conserved cysteine and the $J\alpha$ -helix detaches from the central β -sheet and unfolds. Drawing adapted from (72).

Methods

Single Photon Counting

Set-up

Fluorescence spectroscopy is a widely used method in the field of molecular biophysics. In protein biophysics one can either study the intrinsic protein fluorescence or attach a fluorescence label to the investigated molecule. The intrinsic protein fluorescence results mainly from the emission of the amino acid tryptophan, which absorbs and fluoresces in the near UV ($\lambda_{\text{max}}(\text{abs}) \sim 280 \text{ nm}$, $\lambda_{\text{max}}(\text{em}) \sim 320\text{-}350 \text{ nm}$). Fluorescence labels are available in a wide spectral range from the UV to the near infrared (for details see the MolProbes catalog/handbook). In general fluorescence dyes are coupled to a reactive group, which forms a covalent bond with the protein.

To get information about the investigated system one can either analyze the fluorescence emission spectra and fluorescence quantum yields in a steady state fluorescence spectrometer, or measure the kinetics of the fluorescence decay with time resolved techniques. The latter possibility requires a more complicated and costly set-up and is therefore not as widespread as steady-state techniques, but it gives much more information about the fluorescence properties of the system.

For both, tryptophan and label emission, the fluorescence lifetime is in the range of nanoseconds. To measure directly the fluorescence decay in this time regime the method of single photon counting is used. This technique enables a time resolution in the range of picoseconds by measuring the delay between excitation pulses and resulting single photon emission events. The set-up for the single photon counting experiments, used for the tryptophan fluorescence of photoactive yellow protein described in this thesis, is shown in Figure 21.

As light source a Ti:sapphire laser system (Tsunami, Spectra Physics) is used. The Ti:sapphire laser itself is pumped by a frequency doubled diode pumped Nd:YVO₄ –laser (Millenia Vs, Spectra Physics). The output power of the system is 5 W. The pulse width is 2 ps at a frequency of 80 MHz. The output wavelength is tunable between 900 and 1200 nm. In a first step the pulse rate is reduced to 4 MHz by a pulse picker (No. 3980, Spectra Physics). This ensures the complete decay of the fluorescence between two excitation pulses. Then the light passes a frequency tripler (GWU-23-PL, Spectra Physics) to enable the excitation of tryptophan at $\sim 300 \text{ nm}$. The frequency tripled light then passes a beam splitter. One part of the beam is focused on a photo diode (DET210, Thorlabs) and converted to a voltage pulse which acts as a trigger signal for the delay measurement. The other part of the beam excites the sample. When a photon is emitted by the sample and reaches the Microchannel-plate-photomultiplier (PM) (R3809U, Hamamatsu), the resulting voltage pulse acts as a stop pulse for the delay measurement. Note that the essence of the single photon counting method is that only one emitted photon per excitation pulse is measured. If more than one photon reaches the photomultiplier only the first one will be recognized, due the dead time of the detection electronics. To measure the true fluorescence decay it is therefore necessary to ensure, that the probability of more than one photon reaching the PM per excitation pulse is low. This is done by reducing the excitation pulse power via neutral density filters down to a value such that the number of detected photons (stop pulses) is 1% or less of the number of excitation pulses (start pulses). Also part of the set-up are cut off filters to separate the fluorescence light from scattered excitation light and two linear polarizer for fluorescence anisotropy decay measurements. For technical reasons the fluorescence pulse is the start signal and the following photodiode pulse is the stop signal of the delay measurement.

Chapter 1

Figure 22 shows the electronics of the “clock” used in single photon counting experiments. First the start and stop pulses are amplified by a 1GHz-preamplifier (No. 9360, EG&G Ortec), then they reach a constant fraction discriminator (TC 453, Tennelec), which sets the trigger level. Start pulses which exceed this level trigger the charging of a capacitor in the time to amplitude converter (No. 457, EG&G Ortec). The charging is stopped by the stop pulse. The voltage at the capacitor is then a measure of the delay between the two pulses. It is converted by an analog digital transformer (No. 8715, Canberra) and read out by a measuring card (Accuspec/B, Canberra), which acts as a multichannel analyzer, and in the channel associated with the specific time delay one count is added. To get a fluorescence decay curve this experiment has to be repeated many times. In the end one gets a histogram of the fluorescence decay which is read out by a PC for storage and analysis.

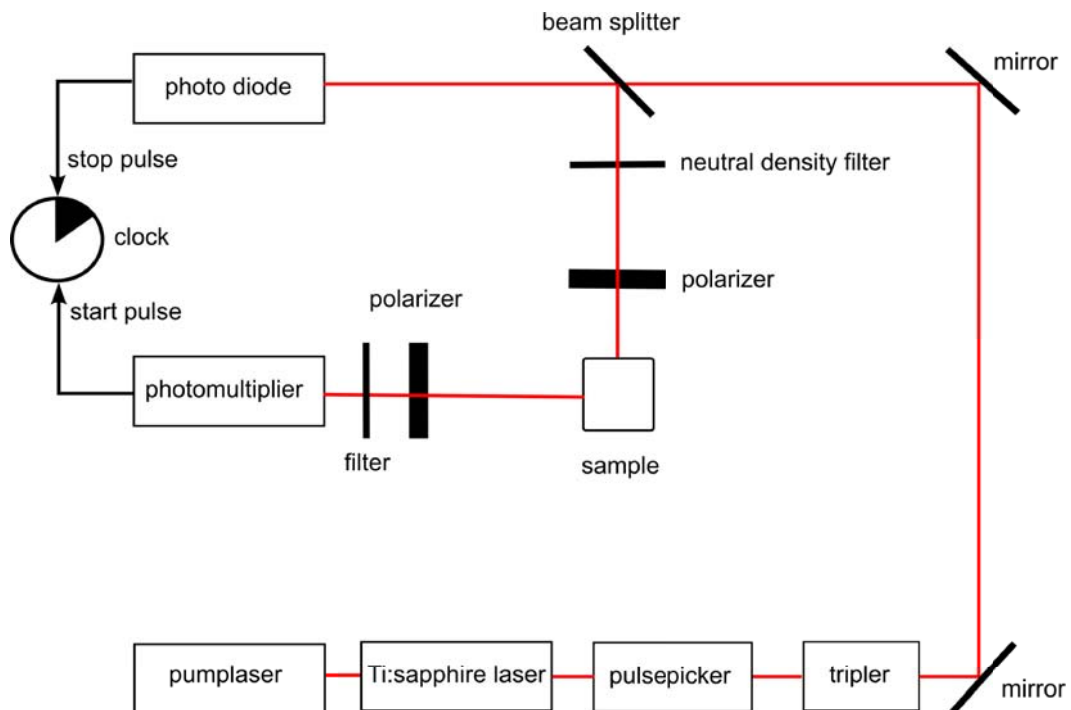


Figure 21 Set-up for single photon counting experiments described in this thesis.

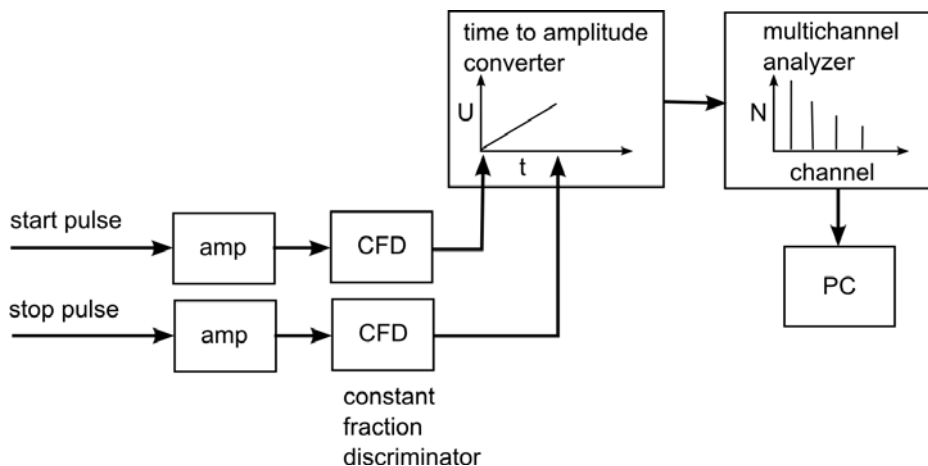


Figure 22 Schematic representation of the electronics for single photon counting measurements.

Data analysis

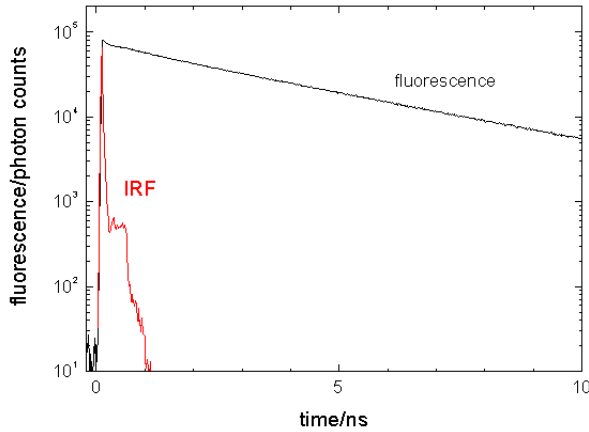


Figure 23 Fluorescence decay curve of fluorescein bound to the PYP (black) and the instrument response function measured with a highly scattering solution of DMPC vesicles.

A typical fluorescence decay curve measured with a single photon counting apparatus is shown in Figure 23. Also shown is the instrument response function (IRF), which is derived from a single photon counting experiment of a non fluorescent but highly scattering sample. The IRF represents the shape of the exciting pulse, which is broadened by the detection electronics (with our apparatus we get typically a IRF with a full width at half maximum around 70 ps). Furthermore the IRF serves as the time zero point for the measurement. The fluorescence curve $I(t)$ measured by single photon counting is a convolution of the IRF $L(t)$ (L amp pulse) with the true fluorescence decay $F(t)$:

$$I(t) = \int_{-\infty}^t L(t')F(t-t')dt'$$

In general $F(t)$ can be assumed to be a sum of exponentials:

$$F(t) = \sum_{i=1}^n c_i e^{-t/\tau_i}$$

To fit the data the model curve $F(t)$ must be convoluted numerically with $L(t)$ in every iteration step. Then $F_{\text{conv}}(t)$ is compared numerically with the measured fluorescence decay $I(t)$ by calculating the reduced χ^2 value

$$\chi^2 = \frac{1}{N-n-1} \sum_{i=1}^N \frac{(I(t_i) - F_{\text{conv}}(t_i))^2}{s(t_i)^2}$$

with N the number of channels of the SPC apparatus, n the number of fitting parameters and s the standard deviation (note $s(t_i)^2 = I(t_i)$ in SPC experiments). The parameters of $F(t)$ are varied in between iteration steps to minimize the χ^2 value. For the fitting procedure of the SPC fluorescence decay curves the commercially available software GLOBALS unlimited was used.

Time resolved anisotropy decay

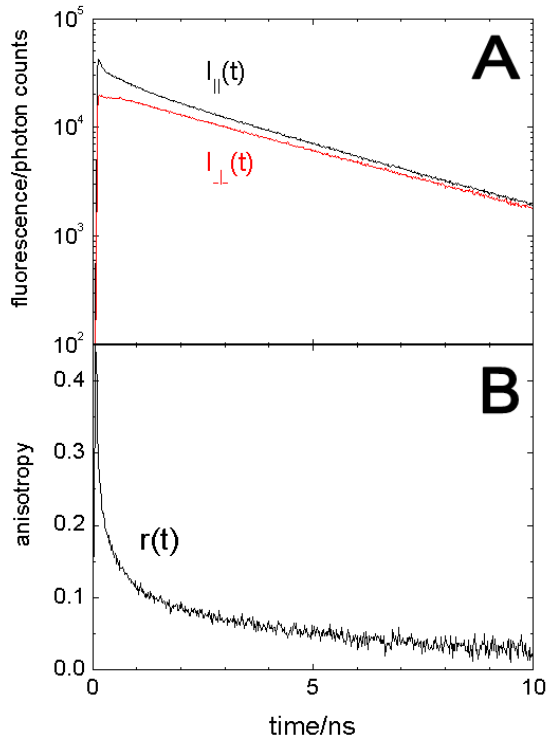


Figure 24 **A** Fluorescence decay curve of fluorescein bound to PYP measured with detector polarization plane parallel (black) and perpendicular (red) to the polarization plane of the exciting pulse. **B** Anisotropy decay calculated from the fluorescence decay curves in A according to Eq. 1.

With this technique the rotational diffusion of a fluorophore can be probed. Therefore the sample is excited with linear polarized light. The fluorescence emission also passes a linear polarizer before reaching the detector. The anisotropy is calculated from the fluorescence decay curves with polarization plane parallel $I_{\parallel}(t)$ and perpendicular $I_{\perp}(t)$ to polarization plane of the excitation pulse:

$$r(t) = \frac{I_{\parallel}(t) - I_{\perp}(t)}{I_{\parallel}(t) + 2I_{\perp}(t)} \quad (1)$$

An example of $I_{\parallel}(t)$, $I_{\perp}(t)$ and the resulting anisotropy decay $r(t)$ is shown in Figure 24. For spherical rotors the anisotropy decays monoexponentially

$$r(t) = r(0) e^{-t/\tau_c} \quad (2)$$

with $r(0)$ the maximal anisotropy at $t=0$. $r(0)=0.4$ if the transition dipole moments of the absorption and the emission have same orientation. τ_c is the rotational correlation time

$$\tau_c = \frac{\eta V}{kT}$$

with V the volume of the rotor, η the viscosity of the solvent, k the Boltzmann constant and T the temperature. Eq. 2 is derived from the solution of the rotational diffusion equation. In biomolecules the fluorescence anisotropy often decays with more than one exponential due to a hindered segmental motion of the fluorophore itself or to the anisotropic diffusion of a non-spherical protein (99). Note that for data analysis of the measured anisotropy decay curves, the convolution of $I_{\parallel}(t)$ and $I_{\perp}(t)$ with the IRF must be taken into account.

Transient Absorption Spectroscopy

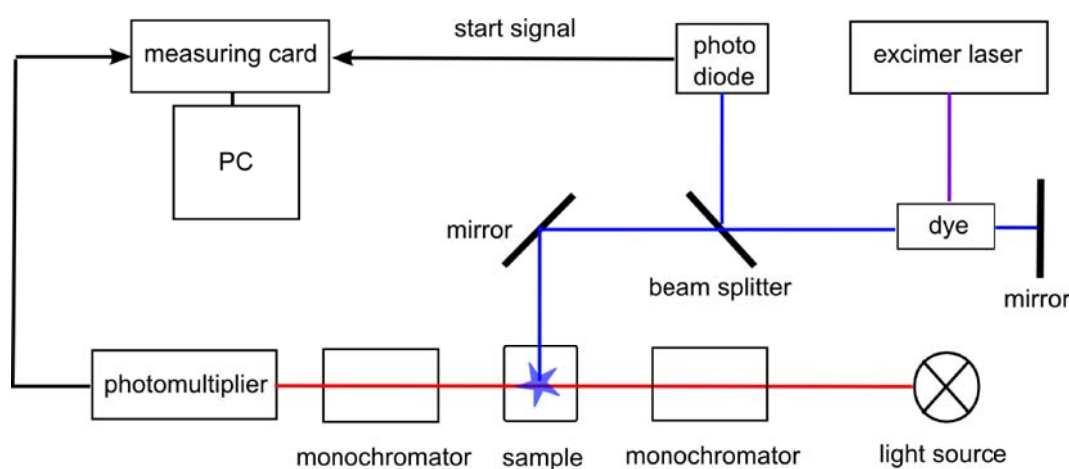


Figure 25 Set-up for the transient absorption spectroscopy experiments described in this thesis

To investigate the photocycle kinetics of photoreceptors in the time range from 100 ns to seconds the method of transient flash spectroscopy is used. In most cases the transient absorption changes of the chromophore are probed. Another application is the measurement of proton uptake and release kinetics using transient absorption changes of a pH indicator dye added to the protein solution.

The set-up for the transient absorption measurements described in this thesis is shown in Figure 25. To trigger the photocycle intense laser flashes of variable wavelength with energy in the range of several mJ and a pulse width of ~ 10 ns are used. They are generated by pumping a laser dye by intense excimer laser pulses. In our apparatus we use an XeCl laser (EMG 50, Lambda Physics) with an pulse power of 100 mJ at 308 nm as a pump laser. The 308 nm flash then hits a cuvette with a laser dye dissolved in ethanol. To excite different photoreceptors excitation pulses of different wavelengths are needed. In the experiments described in this thesis the dyes Coumarin 2, Coumarin 102 and Coumarin 307 with emission wavelengths of 450, 460 and 500 nm are used. All three dyes created excitation flashes with an energy between 10 to 15 mJ. The flash is then focused on the sample in a micro fluorescence cuvette of 3 mm pathlength (Helma), which is placed in a thermostatted sample holder. The measuring light passes the cuvette perpendicular to the direction of the excitation flash. As the light source of the measuring light a 100 W Halogen lamp is used. To select a specific wavelength from the broad emission spectrum of the Halogen lamp the measuring light first passes a monochromator (SA H10 VIS,

Chapter 1

Jobin-Yvon) before it hits the sample. For our experiments we used a monochromator slit width of 2 mm which results in a spectral bandwidth of 12 nm. After it went through the sample cuvette the measuring light passes a second monochromator (SA H10 VIS, Jobin-Yvon) and is detected by a photomultiplier tube (S4710, Hamamatsu). The second monochromator is used to cut off scattering light from the excitation flash and possible fluorescence light excited by the flash.

When a measurement is started, first the photomultiplier current before the flash is recorded by a two channel 40 MHz A/D converter (T12840 Geitmann GmbH) with 8-bit-resolution and 128-kbyte memory which is connected to a PC. Then an excitation flash is initiated. As a trigger signal for the recording of the transient absorption changes a voltage pulse from a photodiode is used which detects a small fraction of the exciting flash which is reflected out of the beam by a glass plate. The evolution of the photomultiplier current is then recorded by the two channels of the A/D converter with different time bases but overlapping time frames and a linear time scale. Both channels have 65,536 channels, the sampling time of the channels can be chosen between 50 ns and 4 ms. In this way the reaction kinetics in the time window from 50 ns to 260 seconds can be recorded with a single flash.

From the photomultiplier current before (I_0) and after the flash ($I(t)$) the light induced absorption changes are calculated according to Lambert-Beer law via:

$$\Delta A = -\log \frac{I(t)}{I_0}$$

The huge dataset (8MB) from the two channels with linear time scales are then merged together numerically to one dataset with logarithmic timescale (100 data points per decade) by averaging over several channels (see Figure 26). Note that this procedure results in a decreasing noise level for data points late in the photoactivation pathway.

To decrease the noise level further the experiment is repeated many times and the resulting transient absorption curves are averaged. Typically averages over 10 shots are acquired.

The emission intensity of the Halogen lamp is low at wavelength below 400 nm. Thus we modified the set-up for the transient absorption measurements at 360 nm on rhodopsin in ROS membranes as shown in Figure 27. As light source we used an LED emitting at 360 nm with a band width of 10 nm. As the emitted LED light is already monochromatic, we placed the LED directly before the sample holder. The second monochromator before the PM is either retained or replaced by a bandpass filter (UG11, Schott) which efficiently blocked stray light from the excitation flash at 500 nm. With this redevelopment it was possible to record transient absorption traces with very low noise level in the UV region of highly scattering samples with single shots (see Chapter 6).

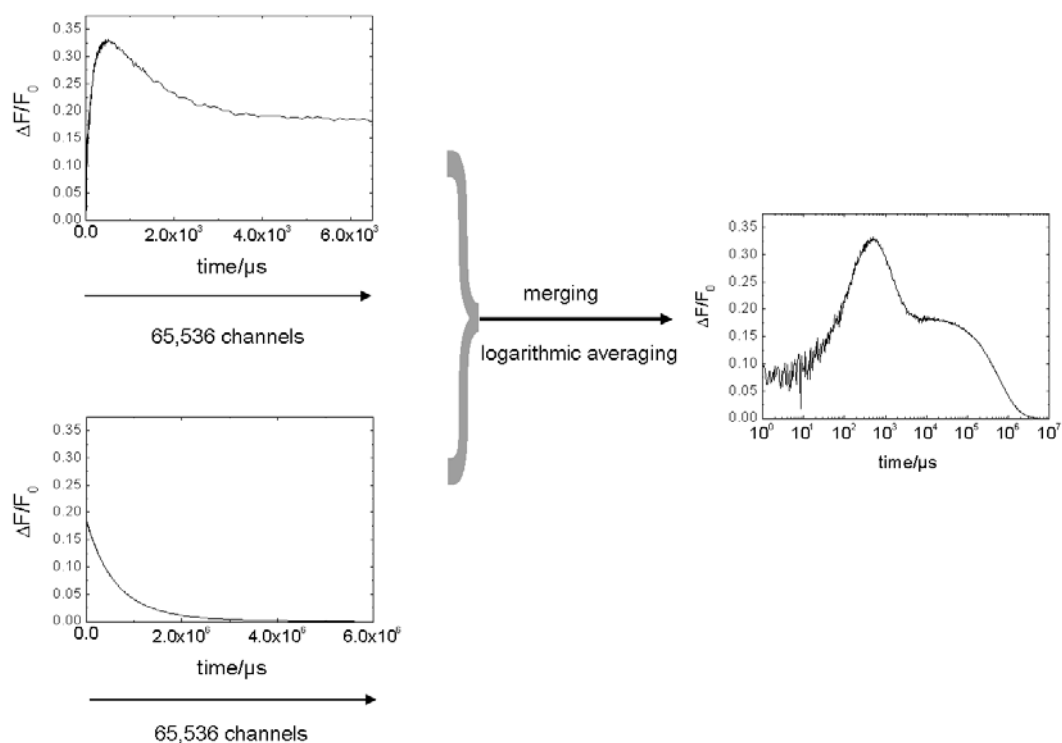


Figure 26 Data acquisition for transient absorption/fluorescence spectroscopy in the time range from μs to seconds.

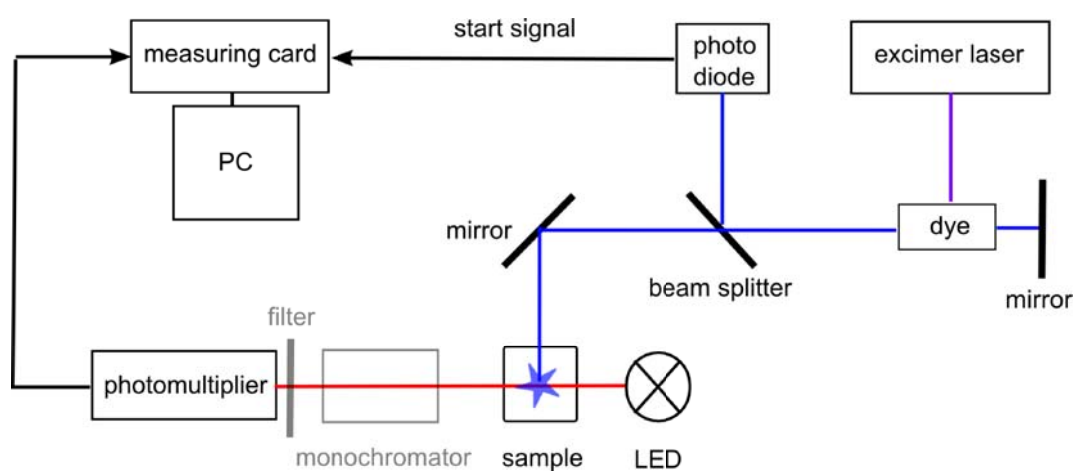


Figure 27 Set-up for the transient absorption spectroscopy experiments with an LED as light source. As in this measurement either a bandpass filter or a monochromator was used to block-off stray light from the excitation flash these two components are drawn in grey.

Data analysis

In general the transient absorption data are fitted with a sum of exponentials. This can be justified in the following way:

The transient absorbance change $\Delta A(\lambda, t)$ is given by:

$$\Delta A(\lambda, t) = \sum_i (A_i(\lambda) - A_0(\lambda)) n_i(t)$$

where $A_i(\lambda, t)$ is the spectrum of intermediate i , $A_0(\lambda)$ is the spectrum of the dark state and $n_i(t)$ is the relative concentration of intermediate i . The relative concentrations are defined as $n_i(t) = c_i(t)/c_0$ with $c_i(t)$ the concentration of the i^{th} intermediate and c_0 the concentration of the protein in the ground state before the flash. For photocycle models with first-order kinetics the solution of the corresponding coupled differential equations is given by a sum of exponentials

$$n_i(t) = \sum_{j=1}^r C_{ij} e^{-t/\tau_j}$$

where r is the number of exponential components j necessary to fit the time traces. This leads to

$$\Delta A(\lambda, t) = \sum_{j=1}^r B_j(\lambda) e^{-t/\tau_j}$$

where the amplitude spectra $B_j(\lambda)$ are defined as

$$B_j(\lambda) = \sum_i (A_i(\lambda) - A_0(\lambda)) C_{ij}$$

For a simple sequential photocycle, $B_j(\lambda)$ is the difference spectrum of the two intermediates in the j^{th} transition.

Transient Fluorescence Spectroscopy

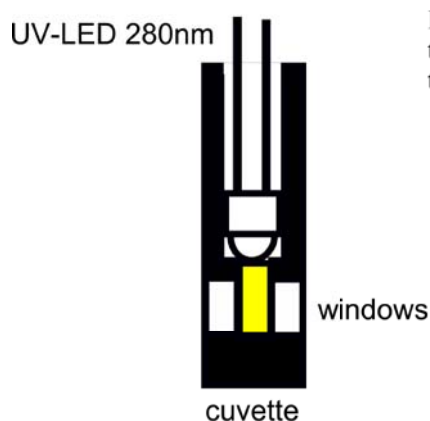


Figure 28 Set-up for the tryptophan fluorescence excitation in the transient fluorescence experiments. The UV-LED is placed directly in the cuvette illuminating the sample from above.

The main technical development in the course of this thesis was the modification of the apparatus for transient absorption spectroscopy to do transient fluorescence measurements. The detected light intensities are generally much lower in fluorescence than in absorption experiments, due to the isotropic fluorescence emission and quantum yields which usually are well below 1 depending on the investigated fluorophore. To do transient fluorescence measurements in the time range of μs it is therefore necessary to use high intensity excitation light sources and to harvest the emitted fluorescence light efficiently. Another prerequisite is a high output stability of the excitation light source, because oscillations in the light flux can easily disrupt weak transient signals.

The development of UV-LEDs emitting at 280 nm, which are on the market since some years made transient tryptophan fluorescence experiments feasible. These light sources have an output power of around $500 \mu\text{W}$, are monochromatic with a bandwidth of 10 nm and are so small that they can be placed in close contact to the sample, minimizing light intensity losses by optical imaging systems.

For transient tryptophan fluorescence experiments we thus placed the LED right into a micro cuvette with 3 mm path length (105.251-QS, Helma), where it illuminates the sample from above as shown in Figure 28.

The complete set-up for the transient fluorescence measurements is shown in Figure 29. It is nearly the same as for the transient absorption experiments, only the measuring light source has been replaced by the UV-LED, and the monochromator before the PM by a combination of 2 filters: A bandpass filter (UG11) cuts off stray light from the excitation flash and a long pass filter (WG305 or WG320) cuts off stray light from the UV-LED. This filter combination, which results in a bandpass between 305 nm and 400 nm transmits of the whole tryptophan emission band and maximizes the number of photons reaching the photomultiplier in comparison to a monochromator, which selects a narrow wavelength region.

For measurements with the fluorescence label Alexa594 attached to rhodopsin, which absorbs at ~ 600 nm, we used a high power LED emitting at 590 nm. It was placed in front of the sample holder as shown in Figure 30. This enabled us to use an additional color filter, which was placed between LED and the cuvette, to modify the spectrum of the excitation light.

Chapter 1

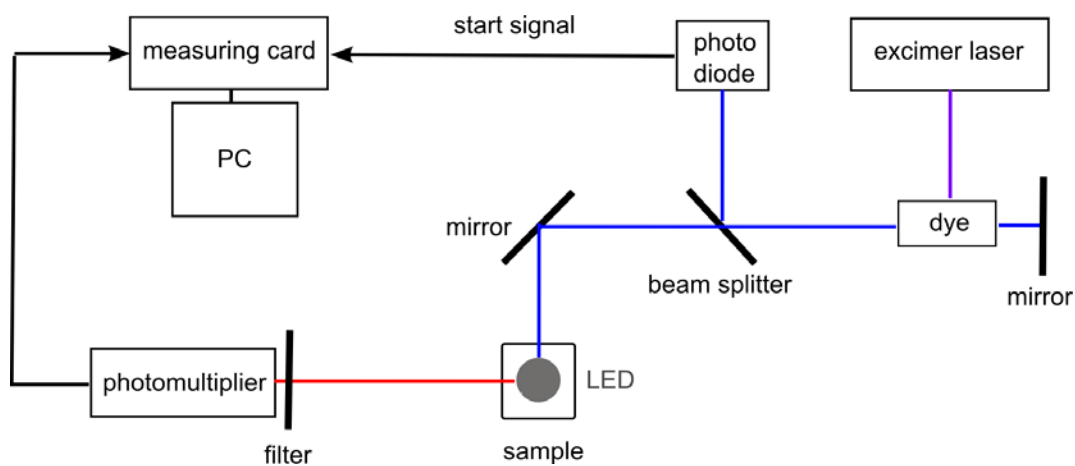


Figure 29 Set-up for the transient tryptophan fluorescence experiments described in this thesis.

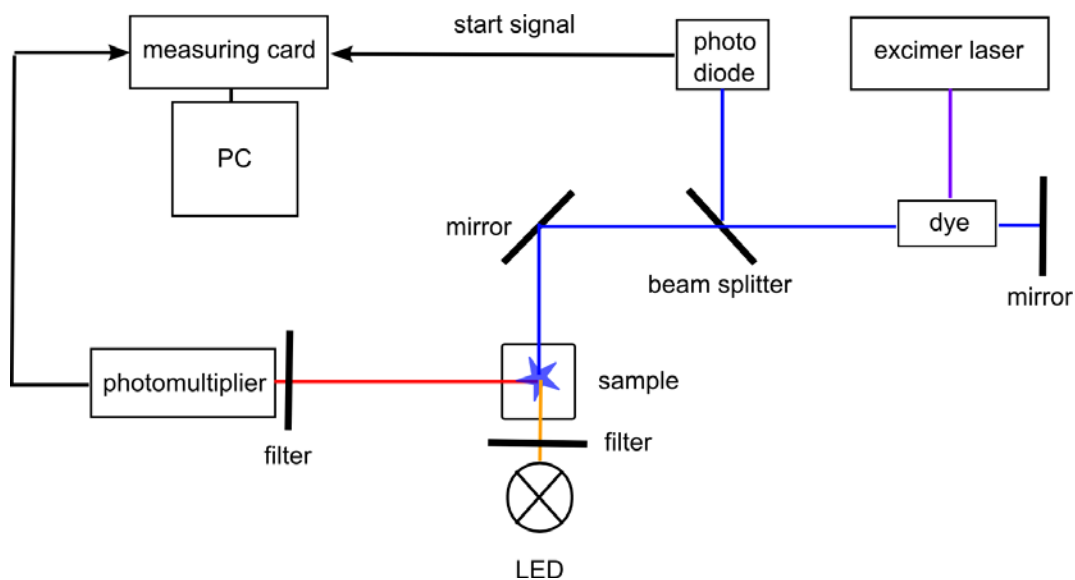


Figure 30 Set-up for the transient Alexa594 fluorescence experiments described in this thesis.

In analogy to the transient absorption signal the transient fluorescence signal is calculated from the PM currents I_0 and $I(t)$ before and shortly after the excitation flash:

$$\frac{\Delta F(t)}{F_0} = \frac{F(t) - F_0}{F_0} = \frac{I(t) - I_0}{I_0} \quad (3)$$

Data analysis

The PM current I is proportional to the number of detected photons which is itself proportional to the product of the number of the excited fluorophores n_i and the fluorescence quantum yield Φ_i in the intermediate i in the photoactivation process:

$$I \propto \sum_i \Phi_i n_i \propto \sum_i \Phi_i (1 - 10^{-A_i}) = \sum_i \Phi_i (1 - 10^{-A}) \quad (4)$$

In the last step we assumed that the absorption A_i of the fluorophore does not change during the photoactivation. After the flash a fraction of the initial ground state population enters the photoactivation pathway with several intermediates i with fluorescence lifetimes τ_i . The normalized fluorescence change $\Delta F/F_0 = (F - F_0)/F_0 = (I - I_0)/I_0$ represents the time resolved fluorescence difference. Using the equations 3 and 4 and the fact that Φ_i is proportional to τ_i we find:

$$\frac{\Delta F(t)}{F_0} = \frac{\sum_i c_i(t)(\tau_i - \tau_0)}{c_0 \tau_0}$$

$c_i(t)$ is the concentration of molecules in intermediate i at time t . c_0 is the initial concentration of molecules in the ground state at $t=0$ before the flash and τ_0 the fluorescence lifetime of the ground state.

Motivation and goals of this work

Photoreceptors transduce the incoming light signal to a biological signal. This is done by light-induced changes of the protein conformation which brings the receptor to its active state. The primary light-induced step is usually a very fast change in the chromophore configuration – for example an isomerization –, which is followed by a series of slower relaxations in the dark, usually in the μs to ms time range. We used time-resolved spectroscopic techniques in the time range from ps to seconds to either characterize the conformational changes or to resolve the kinetics of the transitions of the activation process.

This thesis is mainly focused on investigations of PYP from *H. halophila* (chapter 2 to 5). This photoreceptor system has been studied in detail but fundamental questions concerning the protein functioning are still not answered. It is well established that there are big light-induced conformational changes in PYP but the mechanism of the photoactivation process and the structure of the putative signaling state I_2' are still unknown.

One goal of our investigations was to use the emission of the single tryptophan W119 in PYP to get new information about the structure of various photointermediates of PYP (chapter 2 and 3). W119 is located at the interface between the central β -sheet and the N-terminal cap and might be a good probe to investigate conformational changes in this region of the protein. A previous study already detected changes in the tryptophan fluorescence quantum yield between the dark state P and a photostationary equilibrium of intermediates under background illumination. Our approach was to use time-resolved techniques to measure directly the fluorescence lifetime of the ground state and the various photointermediates and to build a model which can explain the experimental results. The two methods we used were time correlated single photon counting which measures the fluorescence decay of stationary states in the time range of ps to ns and transient fluorescence spectroscopy which probes the fluorescence quantum yield during the photocycle of the photoreceptor with a time resolution of μs to seconds.

Another aim of this thesis was to use time resolved spectroscopic methods to investigate the interactions between the N-terminal cap and the PAS-core of PYP during the photocycle (chapter 4 and 5). There are several studies which indicate that the light-induced structural changes in PYP are concentrated in the N-terminal domain which is at least 15 Å away from the chromophore binding pocket on the opposite side of the central β -sheet. For an understanding of the mechanism of photoactivation of PYP, PAS-domain signaling and protein signal transduction in general it is of great interest how the structural signal is transmitted to this region.

It is known that the recovery kinetics of PYP is influenced by the salt concentration of the solvent and that this salt dependency is abolished in PYP constructs lacking the N-terminal cap. This suggests that the salt effect is mediated by ionic interactions between the N-terminal cap and the PAS-core of the photoreceptor. Our aim was to investigate the effect of the salt concentration on the photoactivation kinetics and the concentrations of the intermediates during the photocycle (chapter 4). The methods we used for this were transient absorption spectroscopy of the chromophore and single photon counting experiments on the tryptophan fluorescence decay. Furthermore we investigated the PYP mutants K110A and E12A in which the salt bridge K110/E12 between N-terminal cap and PAS-core is deleted.

Another approach to investigate the PAS-domain/N-terminal cap interaction in PYP was

Chapter 1

to introduce cysteine residues in the amino acid sequence of the N-terminal cap to enable site-specific labeling with the thiol reactive dye IAF (chapter 5). Measuring the transient changes of the label absorption caused by perturbations of the label environment allows to resolve the kinetics of the conformational change at the specific sites in the N-terminal cap. So far only the kinetics of global conformational changes in PYP without any spatial resolution have been determined, therefore this approach was thought to give more detailed insights in the photoactivation mechanism.

The second photoreceptor system we investigated in this thesis was the G-protein coupled receptor rhodopsin (chapter 6). We used the method of transient fluorescence spectroscopy to resolve the kinetics of the photoactivation and to get new information about the sequence of molecular events involved in this process. The distinct molecular events known to date are the deprotonation of the chromophore, proton uptake from the solvent and conformational change on the cytoplasmic surface of rhodopsin, which enables the binding and activation of transducin. The first two events can be monitored with high time resolution by transient absorption spectroscopy. The only time resolved technique used so far to probe the kinetics of the conformational change is time resolved ESR-spectroscopy of site specific spin-labeled rhodopsin which suffers however from a low signal to noise ratio reducing the time resolution to ms.

We wanted to use the transient fluorescence of the native tryptophan residues in rhodopsin and a fluorescence label attached to C316 in H8 to resolve the conformational changes with a μs time resolution. This approach was promising as previous experiments already showed that photoactivation leads to a reorientation of W265 in the retinal binding pocket and to changes in the fluorescence quantum yield of a dye attached at C316.

The LOV2-J α domain of phototropin1 from *Avena sativa* is the third photoreceptor system investigated in this thesis (chapter 7). The LOV domains are also part of the PAS-domain family and therefore LOV2-J α shares some structural similarity with PYP. Furthermore their mechanism of photoactivation seems to be similar as in both systems illumination leads to major structural changes in α -helical domains (J α and N-terminal cap), which are packed against the central β -sheet of the PAS-domain.

NMR spectroscopy experiments already showed changes in the conformation of two tryptophan residues in LOV2-J α upon photoactivation. We wanted to investigate the influence of this conformational change on the fluorescence properties of the tryptophans in LOV2-J α and to resolve the kinetics of the light-induced conformational change by transient tryptophan fluorescence spectroscopy. It is an interesting question if the kinetics of light-induced changes of the tryptophan conformation are coupled to the formation of the long living photointermediate phot^S₃₉₀ which rises with a time constant of 4 μs or if there are any delays between these processes.

References

1. Van der Horst, M. A., and K. J. Hellingwerf. 2004. Photoreceptor proteins, "star actors of modern times": A review of the functional dynamics in the structure of representative members of six different photoreceptor families. *Accounts of Chemical Research* 37:13-20.
2. Crosson, S., and K. Moffat. 2002. Photoexcited structure of a plant photoreceptor domain reveals a light-driven molecular switch. *Plant Cell* 14:1067-1075.
3. Kumauchi, M., M. T. Hara, P. Stalcup, A. H. Xie, and W. D. Hoff. 2008. Identification of six new photoactive yellow proteins - Diversity and structure-function relationships in a bacterial blue light photoreceptor. *Photochemistry and Photobiology* 84:956-969.
4. Jiang, Z. Y., L. R. Swem, B. G. Rushing, S. Devanathan, G. Tollin, and C. E. Bauer. 1999. Bacterial photoreceptor with similarity to photoactive yellow protein and plant phytochromes. *Science* 285:406-409.
5. Getzoff, E. D., K. N. Gutwin, and U. K. Genick. 2003. Anticipatory active-site motions and chromophore distortion prime photoreceptor PYP for light activation. *Nature Structural Biology* 10:663-668.
6. Düx, P., G. Rubinstenn, G. W. Vuister, R. Boelens, F. A. A. Mulder, K. Hard, W. D. Hoff, A. R. Kroon, W. Crielaard, K. J. Hellingwerf, and R. Kaptein. 1998. Solution structure and backbone dynamics of the photoactive yellow protein. *Biochemistry* 37:12689-12699.
7. Pellequer, J. L., K. A. Wager-Smith, S. A. Kay, and E. D. Getzoff. 1998. Photoactive yellow protein: A structural prototype for the three-dimensional fold of the PAS domain superfamily. *Proceedings of the National Academy of Sciences of the United States of America* 95:5884-5890.
8. Borgstahl, G. E. O., D. R. Williams, and E. D. Getzoff. 1995. 1.4 Å structure of photoactive yellow protein, a cytosolic photoreceptor: unusual fold, active site, and chromophore. *Biochemistry* 34:6278-6287.
9. Taylor, B. L., and I. B. Zhulin. 1999. PAS domains: Internal sensors of oxygen, redox potential, and light. *Microbiology and Molecular Biology Reviews* 63:479-506.
10. van der Horst, M. A., J. Hendiks, J. Vreede, S. Yermenko, W. Crielaard, and K. J. Hellingwerf. 2005. Photoactive Yellow Protein, the Xantopsin. In *Handbook of Photosensory Receptors*. W. R. Briggs, and J. L. Spudich, editors. Wiley-VCH, Weinheim. 391-418.
11. Fisher, S. Z., S. Anderson, R. Henning, K. Moffat, P. Langan, P. Thiyagarajan, and A. J. Schultz. 2007. Neutron and X-ray structural studies of short hydrogen bonds in photoactive yellow protein (PYP). *Acta Crystallographica Section D-Biological Crystallography* 63:1178-1184.

Chapter 1

12. Yamaguchi, S., H. Kamikubo, K. Kurihara, R. Kuroki, N. Niimura, N. Shimizu, Y. Yamazaki, and M. Kataoka. 2009. Low-barrier hydrogen bond in photoactive yellow protein. *Proceedings of the National Academy of Sciences of the United States of America* 106:440-444.
13. Genick, U. K., S. Devanathan, T. E. Meyer, I. L. Canestrelli, E. Williams, M. A. Cusanovich, G. Tollin, and E. D. Getzoff. 1997. Active site mutants implicate key residues for control of color and light cycle kinetics of photoactive yellow protein. *Biochemistry* 36:8-14.
14. Brudler, R., T. E. Meyer, U. K. Genick, S. Devanathan, T. T. Woo, D. P. Millar, K. Gerwert, M. A. Cusanovich, G. Tollin, and E. D. Getzoff. 2000. Coupling of hydrogen bonding to chromophore conformation and function in photoactive yellow protein. *Biochemistry* 39:13478-13486.
15. Borucki, B., C. P. Joshi, H. Otto, M. A. Cusanovich, and M. P. Heyn. 2006. The transient accumulation of the signaling state of photoactive yellow protein is controlled by the external pH. *Biophysical Journal* 91:2991-3001.
16. Joshi, C. P., B. Borucki, H. Otto, T. E. Meyer, M. A. Cusanovich, and M. P. Heyn. 2006. Photocycle and photoreversal of photoactive yellow protein at alkaline pH: Kinetics, intermediates, and equilibria. *Biochemistry* 45:7057-7068.
17. Joshi, C. P., B. Borucki, H. Otto, T. E. Meyer, M. A. Cusanovich, and M. P. Heyn. 2005. Photoreversal kinetics of the I-1 and I-2 intermediates in the photocycle of photoactive yellow protein by double flash experiments with variable time delay. *Biochemistry* 44:656-665.
18. Groot, M. L., L. J. van Wilderen, D. S. Larsen, M. A. van der Horst, I. H. van Stokkum, K. J. Hellingwerf and R. van Grondelle. 2003. Initial steps of signal generation in photoactive yellow protein revealed with femtosecond mid-infrared spectroscopy. *Biochemistry* 42:10054-10059.
19. Brudler, R., R. Rammelsberg, T. T. Woo, E. D. Getzoff, and K. Gerwert. 2001. Structure of the I-1 early intermediate of photoactive yellow protein by FTIR spectroscopy. *Nature Structural Biology* 8:265-270.
20. Borucki, B., S. Devanathan, H. Otto, M. A. Cusanovich, G. Tollin, and M. P. Heyn. 2002. Kinetics of proton uptake and dye binding by photoactive yellow protein in wild type and in the E46Q and E46A mutants. *Biochemistry* 41:10026-10037.
21. Chen, E. F., T. Gensch, A. B. Gross, J. Hendriks, K. J. Hellingwerf, and D. S. Kliger. 2003. Dynamics of protein and chromophore structural changes in the photocycle of photoactive yellow protein monitored by time-resolved optical rotatory dispersion. *Biochemistry* 42:2062-2071.
22. Hendriks, J., T. Gensch, L. Hviid, M. A. van der Horst, K. J. Hellingwerf, and J. J. van Thor. 2002. Transient exposure of hydrophobic surface in the photoactive yellow protein monitored with Nile red. *Biophysical Journal* 82:1632-1643.

Chapter 1

23. Genick, U. K., G. E. O. Borgstahl, K. Ng, Z. Ren, C. Pradervand, P. M. Burke, V. Srajer, T. Y. Teng, W. Schildkamp, D. E. McRee, K. Moffat, and E. D. Getzoff. 1997. Structure of a protein photocycle intermediate by millisecond time-resolved crystallography. *Science* 275:1471-1475.
24. Ihee, H., S. Rajagopal, V. Srajer, R. Pahl, S. Anderson, M. Schmidt, F. Schotte, P. A. Anfinrud, M. Wulff, and K. Moffat. 2005. Visualizing reaction pathways in photoactive yellow protein from nanoseconds to seconds. *Proceedings of the National Academy of Sciences of the United States of America* 102:7145-7150.
25. Anderson, S., S. Crosson, and K. Moffat. 2004. Short hydrogen bonds in photoactive yellow protein. *Acta Crystallographica Section D-Biological Crystallography* 60:1008-1016.
26. van der Horst, M. A., I. H. van Stokkum, W. Crielaard, and K. J. Hellingwerf. 2001. The role of the N-terminal domain of photoactive yellow protein in the transient partial unfolding during signalling state formation. *FEBS Letters* 497:26-30.
27. Rubinstenn, G., G. W. Vuister, F. A. A. Mulder, P. E. Düx, R. Boelens, K. J. Hellingwerf, and R. Kaptein. 1998. Structural and dynamic changes of photoactive yellow protein during its photocycle in solution. *Nature Structural Biology* 5:568-570.
28. Craven, C. J., N. M. Derix, J. Hendriks, R. Boelens, K. J. Hellingwerf, and R. Kaptein. 2000. Probing the nature of the blue-shifted intermediate of photoactive yellow protein in solution by NMR: Hydrogen-deuterium exchange data and pH studies. *Biochemistry* 39:14392-14399.
29. Imamoto, Y., H. Kamikubo, M. Harigai, N. Shimizu, and M. Kataoka. 2002. Light-induced global conformational change of photoactive yellow protein in solution. *Biochemistry* 41:13595-13601.
30. Harigai, M., Y. Imamoto, H. Kamikubo, Y. Yamazaki, and M. Kataoka. 2003. Role of an N-terminal loop in the secondary structural change of photoactive yellow protein. *Biochemistry* 42:13893-13900.
31. Borucki, B., J. A. Kyndt, C. P. Joshi, H. Otto, T. E. Meyer, M. A. Cusanovich, and M. P. Heyn. 2005. Effect of salt and pH on the activation of photoactive yellow protein and gateway mutants Y98Q and Y98F. *Biochemistry* 44:13650-13663.
32. Gensch, T., J. Hendriks, and K. J. Hellingwerf. 2004. Tryptophan fluorescence monitors structural changes accompanying signalling state formation in the photocycle of photoactive yellow protein. *Photochemical & Photobiological Sciences* 3:531-536.
33. Bernard, C., K. Houben, N. M. Derix, D. Marks, M. A. van der Horst, K. J. Hellingwerf, R. Boelens, R. Kaptein, and N. A. J. van Nuland. 2005. The solution structure of a transient photoreceptor intermediate: Delta 25 photoactive yellow protein. *Structure* 13:953-962.

Chapter 1

34. Palczewski, K. 2006. G protein-coupled receptor rhodopsin. *Annual Review of Biochemistry* 75:743-767.
35. Lamb, T. D. 1996. Gain and kinetics of activation in the G-protein cascade of phototransduction. *Proceedings of the National Academy of Sciences of the United States of America* 93:566-570.
36. Menon, S. T., M. Han, and T. P. Sakmar. 2001. Rhodopsin: Structural basis of molecular physiology. *Physiological Reviews* 81:1659-1688.
37. Baylor, D. A. 1987. Photoreceptor signals and vision. *Investigative Ophthalmology & Visual Science* 28:34-49.
38. Morris, M. B., S. Dastmalchi, and W. B. 2009. Rhodopsin: Structure, signal transduction and oligomerisation. In *The International Journal of Biochemistry & Cell Biology* 41:721-724.
39. Okada, T., M. Sugihara, A. N. Bondar, M. Elstner, P. Entel, and V. Buss. 2004. The retinal conformation and its environment in rhodopsin in light of a new 2.2 angstrom crystal structure. *Journal of Molecular Biology* 342:571-583.
40. Scheerer, P., J. H. Park, P. W. Hildebrand, Y. J. Kim, N. Krauss, H. W. Choe, K. P. Hofmann, and O. P. Ernst. 2008. Crystal structure of opsin in its G-protein-interacting conformation. *Nature* 455:497-U430.
41. Palczewski, K., T. Kumasaka, T. Hori, C. A. Behnke, H. Motoshima, B. A. Fox, I. Le Trong, D. C. Teller, T. Okada, R. E. Stenkamp, M. Yamamoto, and M. Miyano. 2000. Crystal structure of rhodopsin: A G protein-coupled receptor. *Science* 289:739-745.
42. Rasmussen, S. G. F., H. J. Choi, D. M. Rosenbaum, T. S. Kobilka, F. S. Thian, P. C. Edwards, M. Burghammer, V. R. P. Ratnala, R. Sanishvili, R. F. Fischetti, G. F. X. Schertler, W. I. Weis, and B. K. Kobilka. 2007. Crystal structure of the human beta(2) adrenergic G-protein-coupled receptor. *Nature* 450:383-387.
43. Cherezov, V., D. M. Rosenbaum, M. A. Hanson, S. G. F. Rasmussen, F. S. Thian, T. S. Kobilka, H. J. Choi, P. Kuhn, W. I. Weis, B. K. Kobilka, and R. C. Stevens. 2007. High-resolution crystal structure of an engineered human beta(2)-adrenergic G protein-coupled receptor. *Science* 318:1258-1265.
44. Hanson, M. A., V. Cherezov, M. T. Griffith, C. B. Roth, V. P. Jaakola, E. Y. T. Chien, J. Velasquez, P. Kuhn, and R. C. Stevens. 2008. A specific cholesterol binding site is established by the 2.8 angstrom structure of the human beta(2)-adrenergic receptor. *Structure* 16:897-905.
45. Jaakola, V. P., M. T. Griffith, M. A. Hanson, V. Cherezov, E. Y. T. Chien, J. R. Lane, A. P. Ijzerman, and R. C. Stevens. 2008. The 2.6 Angstrom Crystal Structure of a Human A(2A) Adenosine Receptor Bound to an Antagonist. *Science* 322:1211-1217.

Chapter 1

46. Murakami, M., and T. Kouyama. 2008. Crystal structure of squid rhodopsin. *Nature* 453:363-367.
47. Krishna, A. G., S. T. Menon, T. J. Terry, and T. P. Sakmar. 2002. Evidence that helix 8 of rhodopsin acts as a membrane-dependent conformational switch. *Biochemistry* 41:8298-8309.
48. Fritze, O., S. Filipek, V. Kuksa, K. Palczewski, K. P. Hofmann, and O. P. Ernst. 2003. Role of the conserved NPxxY(x)(5,6)F motif in the rhodopsin ground state and during activation. *Proceedings of the National Academy of Sciences of the United States of America* 100:2290-2295.
49. Crocker, E., M. Eilers, S. Ahuja, V. Hornak, A. Hirshfeld, M. Sheves, and S. O. Smith. 2006. Location of Trp265 in metarhodopsin II: Implications for the activation mechanism of the visual receptor rhodopsin. *Journal of Molecular Biology* 357:163-172.
50. Chabre, M., and J. Breton. 1979. Orientation of aromatic residues in rhodopsin. Rotation of one tryptophan upon the meta I to meta II transition after illumination. *Vision Research* 19:1005-1018.
51. Park, J. H., P. Scheerer, K. P. Hofmann, H. W. Choe, and O. P. Ernst. 2008. Crystal structure of the ligand-free G-protein-coupled receptor opsin. *Nature* 454:183-187.
52. Altenbach, C., A. K. Kusnetzow, O. P. Ernst, K. P. Hofmann, and W. L. Hubbell. 2008. High-resolution distance mapping in rhodopsin reveals the pattern of helix movement due to activation. *Proceedings of the National Academy of Sciences of the United States of America* 105:7439-7444.
53. Janz, J. M., and D. L. Farrens. 2004. Rhodopsin activation exposes a key hydrophobic binding site for the transducin alpha-subunit C terminus. *Journal of Biological Chemistry* 279:29767-29773.
54. Sheikh, S. P., T. A. Zvyaga, O. Lichtarge, T. P. Sakmar, and H. R. Bourne. 1996. Rhodopsin activation blocked by metal-ion-binding sites linking transmembrane helices C and F. *Nature* 383:347-350.
55. Farrens, D. L., C. Altenbach, K. Yang, W. L. Hubbell, and H. G. Khorana. 1996. Requirement of rigid-body motion of transmembrane helices for light activation of rhodopsin. *Science* 274:768-770.
56. Acharya, S., Y. Saad, and S. S. Karnik. 1997. Transducin-alpha C-terminal peptide binding site consists of C-D and E-F loops of rhodopsin. *Journal of Biological Chemistry* 272:6519-6524.
57. Arnis, S., K. Fahmy, K. P. Hofmann, and T. P. Sakmar. 1994. A conserved carboxylic acid group mediates light-dependent proton uptake and signaling by rhodopsin. *Journal of Biological Chemistry* 269:23879-23881.

Chapter 1

58. Vogel, R., M. Mahalingam, S. Luedke, T. Huber, F. Siebert, and T. P. Sakmar. 2008. Functional role of the "Ionic Lock" - An interhelical hydrogen-bond network in family a heptahelical receptors. *Journal of Molecular Biology* 380:648-655.
59. Vogel, R. 2004. Influence of salts on rhodopsin photoproduct equilibria and protein stability. *Current Opinion in Colloid & Interface Science* 9:133-138.
60. Bartl, F. J., and R. Vogel. 2007. Structural and functional properties of metarhodopsin III: Recent spectroscopic studies on deactivation pathways of rhodopsin. *Physical Chemistry Chemical Physics* 9:1648-1658.
61. Lamb, T. D., and E. N. Pugh. 2004. Dark adaptation and the retinoid cycle of vision. *Progress in Retinal and Eye Research* 23:307-380.
62. Ruprecht, J. J., T. Mielke, R. Vogel, C. Villa, and G. F. X. Schertler. 2004. Electron crystallography reveals the structure of metarhodopsin I. *Embo Journal* 23:3609-3620.
63. Vogel, R., and F. Siebert. 2003. Fourier transform IR spectroscopy study for new insights into molecular properties and activation mechanisms of visual pigment rhodopsin. *Biopolymers* 72:133-148.
64. Mielke, T., U. Alexiev, M. Gläsel, H. Otto, and M. P. Heyn. 2002. Light-induced changes in the structure and accessibility of the cytoplasmic loops of rhodopsin in the activated M-II state. *Biochemistry* 41:7875-7884.
65. Imamoto, Y., M. Kataoka, F. Tokunaga, and K. Palczewski. 2000. Light-induced conformational changes of rhodopsin probed by fluorescent Alexa594 immobilized on the cytoplasmic surface. *Biochemistry* 39:15225-15233.
66. Farahbakhsh, Z. T., K. Hideg, and W. L. Hubbell. 1993. Photoactivated conformational changes in rhodopsin: a time-resolved spin label study. *Science* 262:1416-1419.
67. Farrens, D. L., and H. G. Khorana. 1995. Structure and function in rhodopsin. Measurement of the rate of metarhodopsin II decay by fluorescence spectroscopy. *Journal of Biological Chemistry* 270:5073-5076.
68. Heck, M., S. A. Schädel, D. Maretzki, F. J. Bartl, E. Ritter, K. Palczewski, and K. P. Hofmann. 2003. Signaling states of rhodopsin - Formation of the storage form, metarhodopsin III, from active metarhodopsin II. *Journal of Biological Chemistry* 278:3162-3169.
69. Lin, S. W., and T. P. Sakmar. 1996. Specific tryptophan UV-absorbance changes are probes of the transition of rhodopsin to its active state. *Biochemistry* 35:11149-11159.
70. Arnis, S., and K. P. Hofmann. 1993. Two different forms of metarhodopsin II: Schiff base deprotonation precedes proton uptake and signaling state. *Proceedings*

Chapter 1

of the National Academy of Sciences of the United States of America 90:7849-7853.

71. Knierim, B., K. P. Hofmann, O. P. Ernst, and W. L. Hubbell. 2007. Sequence of late molecular events in the activation of rhodopsin. *Proceedings of the National Academy of Sciences of the United States of America* 104:20290-20295.
72. Yao, X. L., M. K. Rosen, and K. H. Gardner. 2008. Estimation of the available free energy in a LOV2-J alpha photoswitch. *Nature Chemical Biology* 4:491-497.
73. Huala, E., P. W. Oeller, E. Liscum, I. S. Han, E. Larsen, and W. R. Briggs. 1997. Arabidopsis NPH1: A protein kinase with a putative redox-sensing domain. *Science* 278:2120-2123.
74. Jarillo, J. A., H. Gabrys, J. Capel, J. M. Alonso, J. R. Ecker, and A. R. Cashmore. 2001. Phototropin-related NPL1 controls chloroplast relocation induced by blue light. *Nature* 410:952-954.
75. Christie, J. M., P. Reymond, G. K. Powell, P. Bernasconi, A. A. Raibekas, E. Liscum, and W. R. Briggs. 1998. Arabidopsis NPH1: A flavoprotein with the properties of a photoreceptor for phototropism. *Science* 282:1698-1701.
76. Kagawa, T., T. Sakai, N. Suetsugu, K. Oikawa, S. Ishiguro, T. Kato, S. Tabata, K. Okada, and M. Wada. 2001. Arabidopsis NPL1: A phototropin homolog controlling the chloroplast high-light avoidance response. *Science* 291:2138-2141.
77. Kinoshita, T., M. Doi, N. Suetsugu, T. Kagawa, M. Wada, and K. Shimazaki. 2001. phot1 and phot2 mediate blue light regulation of stomatal opening. *Nature* 414:656-660.
78. Christie, J. M., and W. R. Briggs. 2005. Blue Light Sensing and Signaling by the Phototropins. In *Handbook of Photosensory Receptors*. W. R. Briggs, and J. L. Spudich, editors. Wiley-VCH, Weinheim. 277-303.
79. Crosson, S., S. Rajagopal, and K. Moffat. 2003. The LOV domain family: Photoresponsive signaling modules coupled to diverse output domains. *Biochemistry* 42:2-10.
80. Swartz, T. E., T. S. Tseng, M. A. Frederickson, G. Paris, D. J. Commerci, G. Rajashekara, J. G. Kim, M. B. Mudgett, G. A. Splitter, R. A. Ugalde, F. A. Goldbaum, W. R. Briggs, and R. A. Bogomolni. 2007. Blue-light-activated histidine kinases: Two-component sensors in bacteria. *Science* 317:1090-1093.
81. Salomon, M., U. Lempert, and W. Rudiger. 2004. Dimerization of the plant photoreceptor phototropin is probably mediated by the LOV1 domain. *FEBS Letters* 572:8-10.
82. Nakasako, M., K. Zikihara, D. Matsuoka, H. Katsura, and S. Tokutomi. 2008. Structural basis of the LOV1 dimerization of Arabidopsis phototropins 1 and 2.

Chapter 1

Journal of Molecular Biology 381:718-733.

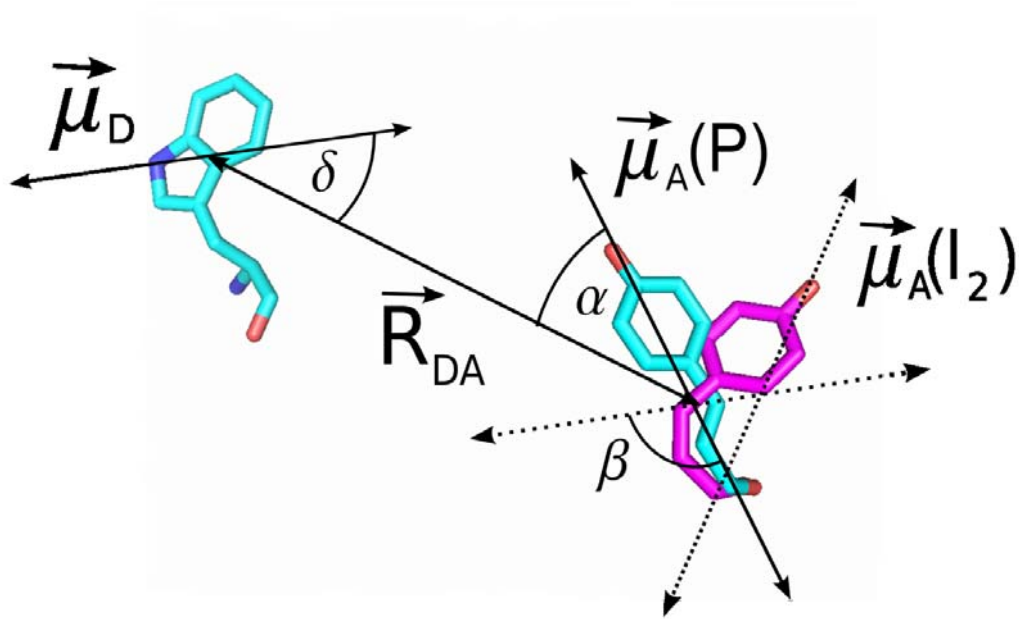
83. Harper, S. M., L. C. Neil, and K. H. Gardner. 2003. Structural basis of a phototropin light switch. *Science* 301:1541-1544.
84. Crosson, S., and K. Moffat. 2001. Structure of a flavin-binding plant photoreceptor domain: Insights into light-mediated signal transduction. *Proceedings of the National Academy of Sciences of the United States of America* 98:2995-3000.
85. Fedorov, R., I. Schlichting, E. Hartmann, T. Domratcheva, M. Fuhrmann, and P. Hegemann. 2003. Crystal structures and molecular mechanism of a light-induced signaling switch: The Phot-LOV1 domain from *Chlamydomonas reinhardtii*. *Biophysical Journal* 84:2474-2482.
86. Halavaty, A. S., and K. Moffat. 2007. N- and C-terminal flanking regions modulate light-induced signal transduction in the LOV2 domain of the blue light sensor phototropin 1 from *Avena sativa*. *Biochemistry* 46:14001-14009.
87. Corchnoy, S. B., T. E. Swartz, J. W. Lewis, I. Szundi, W. R. Briggs, and R. A. Bogomolni. 2003. Intramolecular proton transfers and structural changes during the photocycle of the LOV2 domain of phototropin 1. *Journal of Biological Chemistry* 278:724-731.
88. Harper, S. M., J. M. Christie, and K. H. Gardner. 2004. Disruption of the LOV-J alpha helix interaction activates phototropin kinase activity. *Biochemistry* 43:16184-16192.
89. Swartz, T. E., S. B. Corchnoy, J. M. Christie, J. W. Lewis, I. Szundi, W. R. Briggs, and R. A. Bogomolni. 2001. The photocycle of a flavin-binding domain of the blue light photoreceptor phototropin. *Journal of Biological Chemistry* 276:36493-36500.
90. Salomon, M., J. M. Christie, E. Knieb, U. Lempert, and W. R. Briggs. 2000. Photochemical and mutational analysis of the FMN-binding domains of the plant blue light receptor, phototropin. *Biochemistry* 39:9401-9410.
91. Swartz, T. E., P. J. Wenzel, S. B. Corchnoy, W. R. Briggs, and R. A. Bogomolni. 2002. Vibration spectroscopy reveals light-induced chromophore and protein structural changes in the LOV2 domain of the plant blue-light receptor phototropin 1. *Biochemistry* 41:7183-7189.
92. Salomon, M., W. Eisenreich, H. Durr, E. Schleicher, E. Knieb, V. Massey, W. Rudiger, F. Muller, A. Bacher, and G. Richter. 2001. An optomechanical transducer in the blue light receptor phototropin from *Avena sativa*. *Proceedings of the National Academy of Sciences of the United States of America* 98:12357-12361.
93. Kennis, J. T. M., S. Crosson, M. Gauden, I. H. M. van Stokkum, K. Moffat, and R. van Grondelle. 2003. Primary reactions of the LOV2 domain of phototropin, a

Chapter 1

- plant blue-light photoreceptor. *Biochemistry* 42:3385-3392.
94. Bittl, R., C. W. M. Kay, S. Weber, and P. Hegemann. 2003. Characterization of a flavin radical product in a C57M mutant of a LOV1 domain by electron paramagnetic resonance. *Biochemistry* 42:8506-8512.
 95. Kay, C. W. M., E. Schleicher, A. Kuppig, H. Hofner, W. Rudiger, M. Schleicher, M. Fischer, A. Bacher, S. Weber, and G. Richter. 2003. Blue light perception in plants - Detection and characterization of a light-induced neutral flavin radical in a C450A mutant of phototropin. *Journal of Biological Chemistry* 278:10973-10982.
 96. Kottke, T., J. Heberle, D. Hehn, B. Dick, and P. Hegemann. 2003. Phot-LOV1: Photocycle of a blue-light receptor domain from the green alga *Chlamydomonas reinhardtii*. *Biophysical Journal* 84:1192-1201.
 97. Swartz, T. E., and R. A. Bogomolni. 2005. LOV-domain Photochemistry. In *Handbook of Photosensory Receptors*. W. R. Briggs, and J. L. Spudich, editors. Wiley-VCH, Weinheim. 305-321.
 98. Chen, E. F., T. E. Swartz, R. A. Bogomolni, and D. S. Kliger. 2007. A LOV story: The signaling state of the Phot1 LOV2 photocycle involves chromophore-triggered protein structure relaxation, as probed by far-UV time-resolved optical rotatory dispersion spectroscopy. *Biochemistry* 46:4619-4624.
 99. Lakowicz, J. R. 2006. *Principles of Fluorescence Spectroscopy*. Springer, New York. 383-412.

Chapter 1

Chapter 2



Time-resolved single tryptophan fluorescence in photoactive yellow protein monitors changes in the chromophore structure during the photocycle via energy transfer[†]

Harald Otto[‡], Daniel Hoersch[‡], Terry E. Meyer[§], Michael A. Cusanovich[§], and Maarten P. Heyn^{*‡}

[‡] Biophysics Group, Dept. of Physics, Freie Universität Berlin, Arnimallee 14, 14195 Berlin, Germany

[§] Dept. of Biochemistry and Molecular Biophysics, University of Arizona, Tucson, Arizona, 85721, USA

* Corresponding author; phone: 49-30-83856160; fax: 49-30-83856299;
email: hey@physik.fu-berlin.de

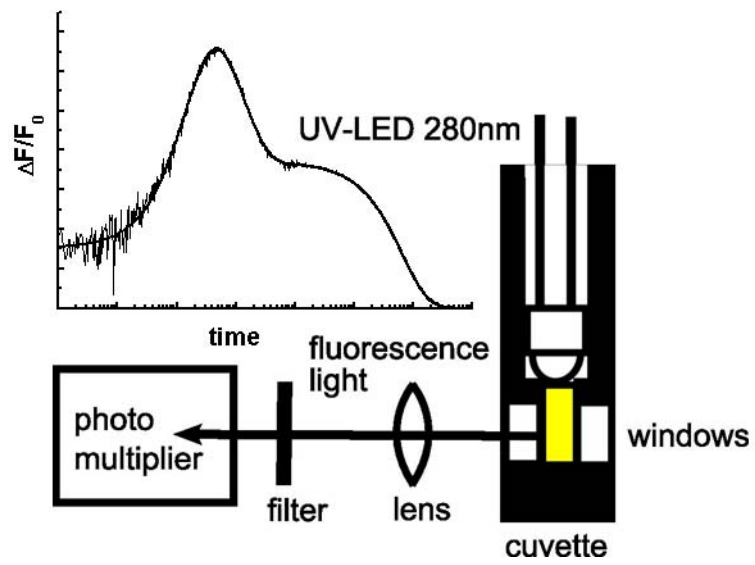
[†] This work was supported by NIH grant GM 66146 (to M.A.C.) and DFG grants He 1382/13-1 and He 1382/14-1 (to M.P.H.)

¹Abbreviations: SVD, singular value decomposition; PYP, photoactive yellow protein; PAS domain, acronym formed from the names of the first three proteins recognized as sharing this sensory domain; LED, light emitting diode; 4HC, 4-hydroxycinnamoyl chromophore;

Published in *Biochemistry* (2005), 43, 16804-16816

The original article is accessible in the World Wide Web via
<http://dx.doi.org/10.1021/bi051448l>

Chapter 3



Distinguishing chromophore structures of photocycle intermediates of the photoreceptor PYP by transient fluorescence and energy transfer[§]

Daniel Hoersch [†], Harald Otto [†], Michael A. Cusanovich [‡], and Maarten P. Heyn ^{* †}

[†] Biophysics Group, Dept. of Physics, Freie Universität Berlin, Arnimallee 14, 14195 Berlin, Germany

[‡] Dept. of Biochemistry and Molecular Biophysics, University of Arizona, Tucson, Arizona, 85721, USA

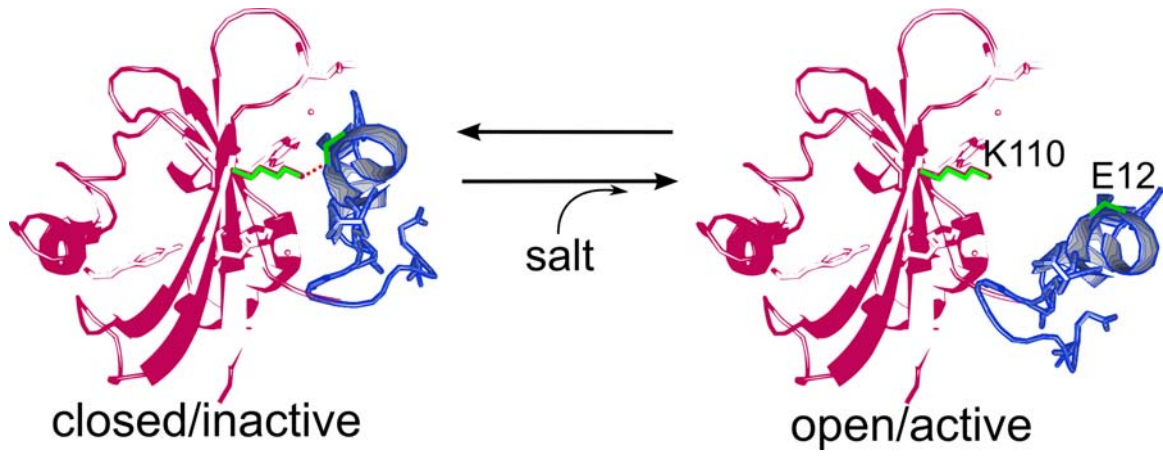
*Corresponding author; phone: 40-30-83856160; fax: 49-30-83856299;
email: heyne@physik.fu-berlin.de

[§] Abbreviations: FRET, fluorescence resonance energy transfer; SVD, singular value decomposition; PAS domain, acronym formed from the names of the first three proteins recognized as sharing this sensory domain; PYP, photoactive yellow protein; LED: light emitting diode; FWHM, full width at half maximum;

Published in *Journal of Physical Chemistry B* (2008), 112, 9118-9125

The original article is accessible in the World Wide Web via
<http://dx.doi.org/10.1021/jp801174z>

Chapter 4



Role of a conserved salt bridge between the PAS core and the N-terminal domain in the activation of the photoreceptor Photoactive Yellow Protein.

Daniel Hoersch*, Harald Otto*, Chandra P. Joshi*, Berthold Borucki*, Michael A. Cusanovich[†] and Maarten P. Heyn*

*Biophysics Group, Dept. of Physics, Freie Universität Berlin, Arnimallee 14, 14195 Berlin, Germany,

[†] Dept. of Biochemistry and Molecular Biophysics, University of Arizona, Tucson, Arizona, 85721, USA

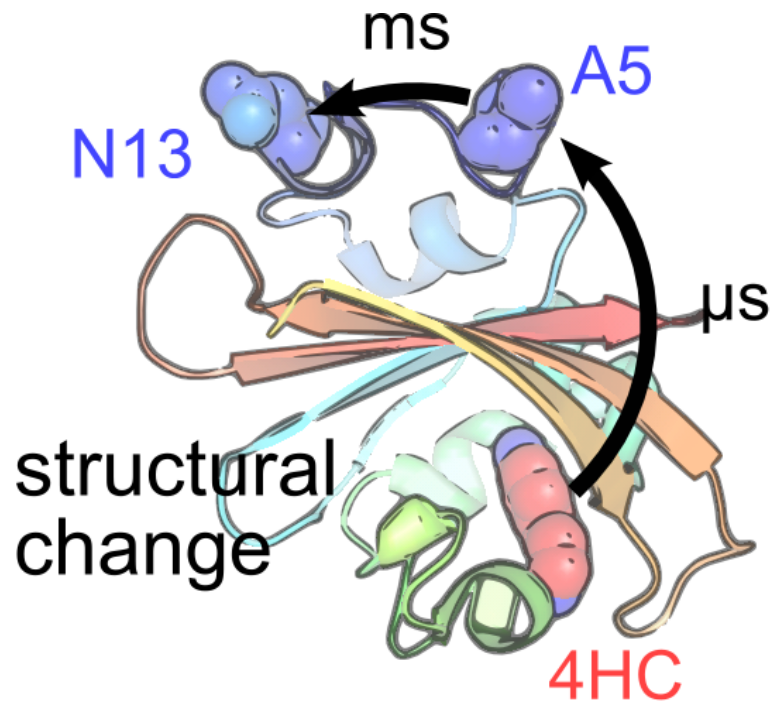
Address correspondence to: Maarten P. Heyn, Biophysics Group, Dept. of Physics, Freie Universität Berlin, Arnimallee 14, 14195 Berlin, Germany. Phone: 49-30-83856160; Fax: 49-30-83856299; E-mail: heyne@physik.fu-berlin.de

Abbreviations: PAS domain, acronym formed from the names of the first three proteins recognized as sharing this sensory domain; PYP, photoactive yellow protein;

Published in *Biophysical Journal* (2007), 93, 1687-1699

The original article is accessible in the World Wide Web via
<http://dx.doi.org/10.1529/biophysj.107.106633>

Chapter 5



Time-resolved spectroscopy of dye-labeled PYP suggests a pathway of light-induced structural changes in the N-terminal cap[†]

*Daniel Hoersch^a, Harald Otto^a, Michael A. Cusanovich^b and Maarten P. Heyn^{*a}*

^a Biophysics Group, Department of Physics, Freie Universität Berlin, Arnimallee 14,
14195

^b Department of Biochemistry and Molecular Biophysics, University of Arizona, Tuscon,
Arizona, 85721

* Corresponding author; phone 49-30-83856160; fax: 49-30-83856299; email
hey@physik.fu-berlin.de

[†] *This work was supported by the DFG grant He1382/14-2 (to M.P.H. and H.O.) and NIH grant GM 66146 (to M.A.C.)*

Physical Chemistry Chemical Physics (2009), DOI: 10.1039/b821345c

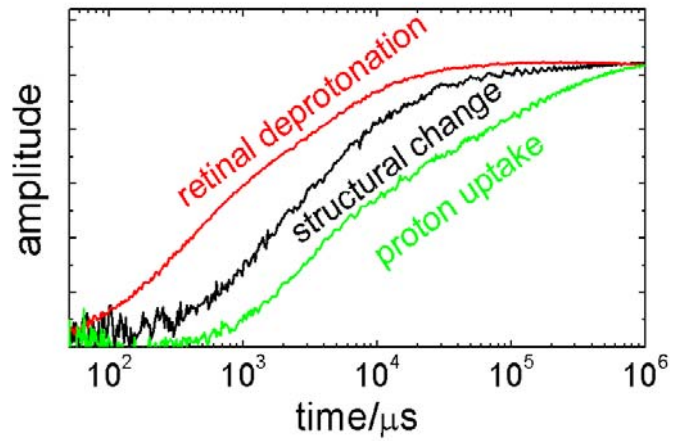
The original article is accessible in the World Wide Web via
<http://dx.doi.org/10.1039/b821345c>

Note added:

Similar light-induced transient absorption changes have been observed with fluorescein covalently bound to cysteine residues of plant photochromes (P. H. Eilfeld et al. JPP B 3, 209 (1989)) and with Agp1 photochrome (B. Borucki, private communication).

Chapter 6

kinetics of
rhodopsin
activation



Monitoring the conformational changes of photoactivated rhodopsin from μs to seconds by transient fluorescence spectroscopy[†]

*Daniel Hoersch, Harald Otto, Ingrid Wallat and Maarten P. Heyn**

Biophysics Group, Dept. of Physics, Freie Universität Berlin, Arnimallee 14, 14195 Berlin, Germany

*Corresponding author; phone 49-30-83856160; fax: 49-30-83856299; email: heyne@physik.fu-berlin.de

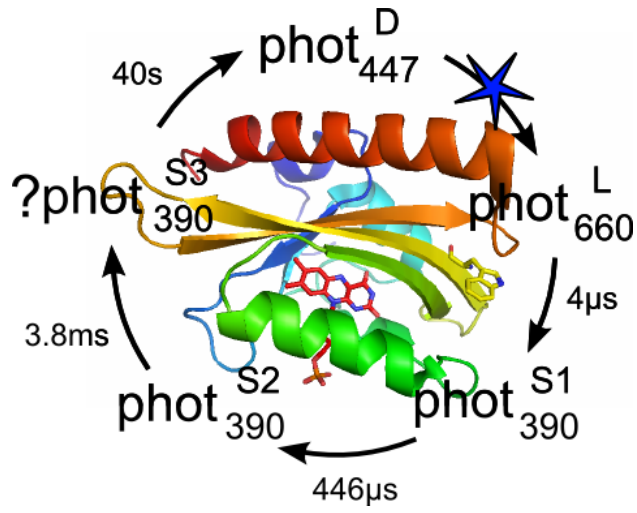
[†] This work was supported by DFG grant He1382/14-2 (to M.P.H. and H.O.)

¹ Abbreviations: DM, dodecyl maltoside; LED, light emitting diode; BCP, bromocresol purple; ROS, rod outer segment; SB, Schiff base; PM, photo multiplier;

Published in *Biochemistry* (2008) 47, 11518-11527

The original article is accessible in the World Wide Web via <http://dx.doi.org/10.1021/bi801397e>

Chapter 7



The kinetics of light induced conformational change in phot1 LOV2-J α probed by transient tryptophan fluorescence

Daniel Hoersch^a, Harald Otto^a, Roberto Bogomolni^b, Farzin Bolourchian^b and Maarten P. Heyn^a

^a Biophysics Group, Department of Physics, Freie Universität Berlin, Arnimallee 14, 14195 Berlin, Germany

^b Department of Chemistry, University of California, Santa Cruz, 1156 High Street, CA 95064, USA

Abstract

We investigated the kinetics of light induced conformational changes of the LOV2-J α domain of oat phototropin1 by transient tryptophan fluorescence spectroscopy from 10 μ s to seconds. The quantum yield of the tryptophan fluorescence is sensitive to the environment and is therefore a good marker for changes in the secondary and tertiary structure of the protein. Upon photoactivation with a blue laser flash at 450 nm the fluorescence quantum yield of the LOV2-J α domain increases biexponentially. The corresponding time constants are 450 μ s for the major component accounting for 86% of the overall amplitude and 3.8 ms for the second minor component. These transitions are not observed in the photocycle of LOV2-J α as probed by transient absorption spectroscopy in the UV-VIS and are presumably coupled to conformational changes of the protein. The mean activation energy of the conformational change was determined to be 18.2 kcal/mol from the temperature dependency of the transient fluorescence signal. This value is nearly the same as the activation energy of 18.5 kcal/mol for the I₂/I₂' transition in the PAS-domain photoreceptor PYP, which we also measured by transient tryptophan fluorescence spectroscopy. This transition is associated with global changes in the protein conformation. Therefore the similarity of the kinetics of the light-induced structural changes in these two photoreceptors is noteworthy and hints presumably to a common PAS-domain signaling mechanism.

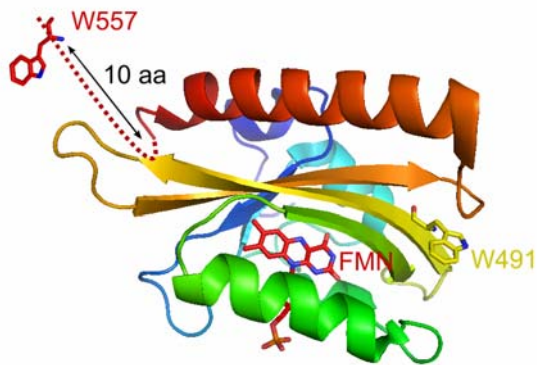


Figure 1 Crystal structure of oat phot1 LOV2-J α based on the protein data bank file 2V0W.pdb (1). The chromophore (red) and W491 (yellow) are shown as sticks. The cartoon in the upper left side indicates the position of W557 in the amino acid sequence of the LOV2 domain investigated in this study.

Introduction

Phototropins are a class of blue light photoreceptors, which control phototropism, light induced stomatal opening and chloroplast movement in response to changes in the light intensity in plants (2-6). phototropin1 from *Avena sativa* (oat) is a 996-amino acid membrane associated kinase flavoprotein. Its light sensing domains LOV1 and LOV2 are activated by blue-light absorption of their cofactors flavin mononucleotide (FMN) (7, 8). This triggers the autophosphorylation of a C-terminal kinase domain which is presumed to be essential for the downstream signal transduction (4, 9). The structurally very similar 12 kDa LOV domains are located in the N-terminal region of phototropin and are both member of the PAS domain family. While light activation of the LOV2 domain is sufficient to elicit phototropism (10), the function of the LOV1 domain is still unclear. In this study we investigated the isolated LOV2 domain from *Avena sativa* (oat). The dark state of the LOV2 domain, phot^D₄₅₀ (also called LOV^D₄₅₀) has an absorption maximum of 450 nm. Upon absorbing blue light, the FMN chromophore forms a triplet state called phot^L₆₆₀ (or LOV^L₆₆₀) with an absorption maximum of 660 nm via intersystem crossing from the excited singlet state within 5 ns (11). This transition is associated with an excited state proton transfer between the sulfhydryl group of a conserved cysteine and N5 of FMN and the formation of a Cys-C4a flavin-cysteinyl adduct (7, 12-15). The triplet state then decays with a time constant of 4 μ s to the long living intermediate phot^S₃₉₀ (or LOV^S₃₉₀) with an absorption maximum of 390 nm (13). This state is supposed to be the signaling state of LOV2 and is associated with conformational changes of the protein (15-20). Especially an amphipathic α -helix called J α following the C-terminus of the LOV2 domain dissociates from the β -sheet and unfolds upon photoactivation (16). The signaling state, also called lit state, recovers to the ground state with a time constant of \sim 40 sec.

In this study we investigated the kinetics of the light-induced conformational changes in the oat phot1 LOV2-J α domain by measuring transient changes in the quantum yield of its intrinsic tryptophan fluorescence. The construct we used contained 3 tryptophans: One is in the calmodulin binding domain attached at the N-terminus of the LOV2 domain to enable the purification of the protein. One (W491) is in the LOV2 domain itself, it is part of the "central" β -sheet on the interface between the LOV2 domain and the C-terminal amphipathic J α -helix. The distance between this tryptophan and the flavin chromophore is around 14 Å as derived from the crystal structure of oat phot1 LOV2-J α shown in Fig. 1 (1). The third tryptophan (W557) is located near the C-terminus of the construct in a domain following the J α -helix. A cartoon in Fig. 1 indicates the position of W557 in the amino acid sequence of the construct, as it was not part of the crystallized LOV2-J α domain. The tryptophans W491 and W557 undergo structural changes upon

Chapter 7

photoactivation as shown by NMR-spectroscopy (16, 17, 21). In the dark these tryptophans are in different environments, in the lit state the environments are more similar (17, 21). The tryptophan NMR peaks return to their dark values with the same kinetics as the photocycle recovery (17). The complete sequence of the LOV2-J α fusion protein investigated in this study is shown in ref. (15) and in Fig. 15A of chapter 1.

Materials and Methods

Protein production and purification. LOV2-J α samples were prepared as previously described (7). The LOV2-J α domains were expressed in *Escherichia coli*, purified by calmodulin affinity chromatography (Stratagene) and lyophilized. Prior to use the dried protein was resuspended in buffer (10mM Tris, 30mM KCl, pH 7.7). *Halorhodospira halophila* holo-PYP was produced by the use of the biosynthetic enzymes TAL and pCL and subsequently purified from *Escherichia coli* BL21 (DE3) as described (22).

Transient fluorescence spectroscopy. The transient fluorescence measurements were performed with a modification of the set-up for time-resolved absorption spectroscopy (23) described in more detail in (24) (chapter 3) and chapter 1. The tryptophan fluorescence is excited by an LED emitting at 280 nm with a full width at half maximum of 10 nm. The emission is detected by a photomultiplier (PM) and the time course of the signal is recorded from 10 μ s to seconds after exciting the sample with a 20 ns flash at 450 nm from a dye laser (Coumarin 2 dissolved in ethanol) pumped by a XeCl-excimer laser (EMG50, Lambda Physics). To protect the PM from stray light from the LED and the excitation flash, the filters WG305 and UG11 (both Schott) were placed in front of it. In this way the time course of the steady state fluorescence of the tryptophans during the photoactivation are recorded. The cuvette was placed in a thermostatted sample holder.

The transient fluorescence signal $\Delta F/F_0 = (F(t) - F_0)/F_0 = (I(t) - I_0)/I_0$ is defined as the difference of the fluorescence intensity before (F_0) and after ($F(t)$) the laser flash which triggers the photoactivation at $t=0$, normalized by F_0 . It is calculated from the PM current ($I(t)$, I_0).

Fluorescence resonance energy transfer (FRET). The rate of radiationless energy transfer k_T is given by

$$k_T = 8.71 \times 10^{23} \frac{J \kappa^2}{n^4 R_{DA}^6} \frac{\Phi_D}{\tau_D} \text{ sec}^{-1} \quad (1)$$

J is the spectral overlap integral between the emission spectrum of the donor and the absorption spectrum of the acceptor, in units of cm^3M^{-1} . κ^2 is the angular factor of the interaction between the transition dipole moments of donor and acceptor and varies between 0 and 4. n is the index of refraction. R_{DA} is the distance between the transition dipole moments of donor and acceptor in \AA . τ_D is the fluorescence lifetime of the donor in the absence of the acceptor in sec. Φ_D is the fluorescence quantum yield of the donor in the absence of the acceptor. The Förster distance R_0 is the distance at which k_T equals $\frac{1}{\tau_D}$.

Using the same units as above R_0 in \AA is given by

$$R_0 = 9.78 \times 10^3 \left[\frac{J \kappa^2 \Phi_D}{n^4} \right]^{1/6} \quad (2)$$

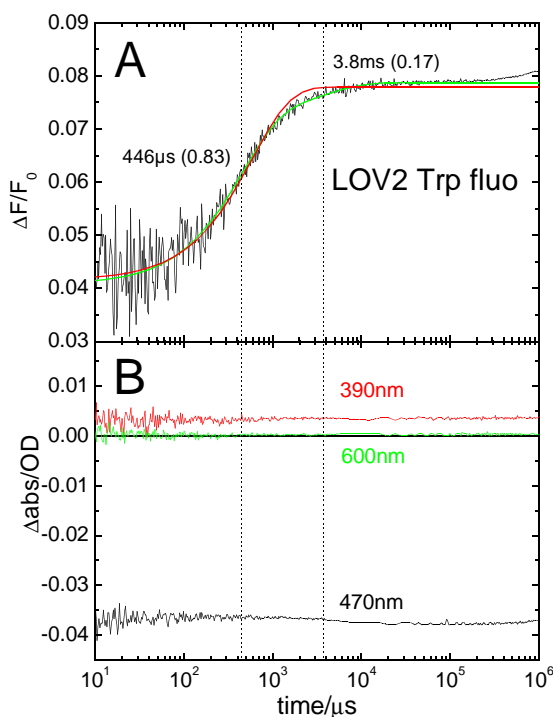


Figure 2. **A** Transient tryptophan fluorescence of the LOV2-J α domain (black). The signal is an average of 30 scans with waiting times of 2 minutes between the laser flashes. The fit curves of a one- (red) and a two-exponential (green) fit of the transient tryptophan fluorescence are superimposed on the data. The time constants corresponding to the 2-exponential fit are indicated as vertical dotted lines. **B** Transient absorption signal for the wavelengths 390, 470 and 600 nm of the same sample as in A (1 scan). Conditions: 10 mM Tris, 30 mM KCl, pH 7.7, 20 °C

Results and Discussion

Figure 2 A shows the transient tryptophan fluorescence of the isolated LOV2-J α domain of oat phototropin 1. The signal starts at 10 μ s with a positive value of about 0.04 and then increases to an end value of about 0.08. For times beyond 200 ms the signal rises further, probably due to photoactivation of LOV2 by the intense excitation light at 280 nm. The time trace was fitted up to 200 ms by a sum of two exponentials with time constants of 450 μ s and 3.8 ms (green line in Fig. 2A). The signal is dominated by the 450 μ s component, which contributes a fraction of 0.83 to the overall amplitude. A one exponential fit was unsatisfactory (red line in Fig. 2A). The positive starting value of 0.04 corresponds to a light induced increase in the tryptophan fluorescence quantum yield, which is faster than the time resolution of our measurement.

This initial positive amplitude can be explained by changes in the rate of fluorescence resonance energy transfer (FRET) between the tryptophans and the flavin chromophore. From the LOV2 tryptophan emission and the chromophore absorption spectra shown in Figure 3 we calculated the tryptophan-FMN Förster radius according to Eq. 2 for the protein in the ground state phot^D₄₅₀ ($\epsilon=13,800$ cm⁻¹M⁻¹) assuming a mean κ^2 value of 2/3. The result of 13 Å is only slightly smaller than the W491-FMN distance of ~14 Å. Therefore we suggest there is efficient energy transfer at least between this tryptophan and the flavin chromophore. The overlap integral J between the tryptophan emission and the chromophore absorption in the photointermediate phot^S₃₉₀ is 37 % smaller than in the dark state phot^D₄₅₀ (see Figure 3). As the energy transfer rate is proportional to the overlap integral (see Eq. 1) we expect a higher tryptophan fluorescence quantum yield for phot^S₃₉₀ than for the ground state. This is in line with the experiment. We assumed that κ^2 does not change (see below).

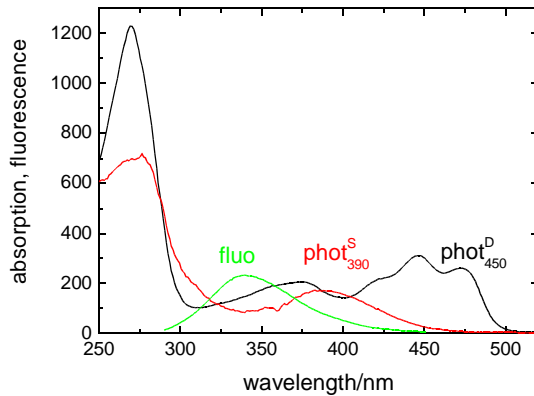


Figure 3 Spectral overlap between the tryptophan emission spectrum of the oat LOV2-J α domain and the absorption spectra of the ground state phot^D₄₅₀ and the photointermediate phot^S₃₉₀. Conditions: 10 mM Tris, 30 mM KCl pH 7.7.

The observed transient increase in fluorescence quantum yield with the time constants of 450 μ s and 3.8 ms can not be explained in this way however. In Figure 2B the transient absorption of the LOV2 construct at 390, 470 and 660 nm is shown. As the slowest transition in the photocycle of LOV2 before the recovery of the protein has a time constant of 4 μ s (formation of phot^S₃₉₀) there are no changes in the absorption spectrum of the chromophore with time constants corresponding to the transitions in the tryptophan fluorescence quantum yield. Therefore no changes in the overlap integral between tryptophan and flavin occur in the time window from 10 μ s to 1 sec, but there may be changes in the orientation or distance of the transition dipole moments of donor and acceptor due to light-induced conformational changes which also affect the FRET efficiency. We recently showed for the photoreceptor Photoactive Yellow Protein that changes in the κ^2 -factor of the FRET donor-acceptor pair W119-chromophore due to reorientations of the transition dipole moment of the chromophore changed the donor fluorescence lifetime by several orders of magnitude (24, 25). In LOV2 no big differences in the orientation of the flavin transition dipole moment between phot^D₄₅₀ and phot^S₃₉₀ are expected, as photoactivation does not result in big rearrangements of the chromophore as is the case for PYP (14, 26, 27), but there might be a light-induced movement of the tryptophan residues relative to the chromophore. Another possibility is that changes in the environment of the tryptophans affect the rate for radiationless internal conversion (k_{IC}) or quenching (k_Q). It is well known that the quantum yield and the emission wavelength of tryptophan fluorescence is for example sensitive to the polarity of its environment (28).

To check this possibility we measured the effect of illumination on the steady state tryptophan fluorescence spectra of LOV2-J α as shown in Figure 4. In the dark LOV2 is in the ground state phot^D₄₄₇ whereas background illumination by an LED emitting at 470 nm leads to a photostationary equilibrium, which is composed of 85% phot^S₃₉₀ and 15% phot^D₄₅₀. These values were derived from an analysis of the absorption spectra of the illuminated sample (data not shown). The spectra in Figure 4 show that there is an increase in fluorescence quantum yield of ~15 % upon illumination of LOV2 as calculated by numerical integration of the fluorescence spectrum. This is consistent with our time resolved measurement shown in Figure 2A. The transient fluorescence change is only 8% since less LOV2 was excited by the flash than by background illumination.

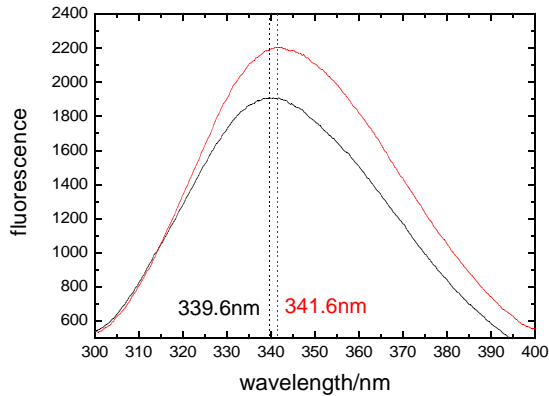


Figure 4: Tryptophan fluorescence emission spectrum of the LOV2-J α domain in the dark (black line) and under background illumination with an LED emitting at 470 nm (red line). The emission maxima of the spectra are indicated by vertical dotted lines. Conditions 10 mM Tris, 30 mM KCl, pH 7.7.

Additionally there is a slight red shift in the emission maximum from 340 nm to 342 nm. This suggests that the tryptophans enter a more polar environment when LOV2-J α is photoactivated. We note that the 340 nm emission wavelength in the dark already indicates a quite polar environment. In general the tryptophan fluorescence quantum yield decreases when the amino acid is exposed to water due to fluorescence quenching by the nearby water molecules, but for the LOV2-J α domain we see the opposite effect. This contradiction might be explained by a nearby amino acid which efficiently quenches the tryptophan fluorescence in the dark state and moves away from it in the course of the structural rearrangements caused by the photoactivation of the protein. H519 which is in close contact to W491 could cause such an effect, because histidines are well known as tryptophan fluorescence quenchers (29). Note that in an NMR-study of a oat phot1 LOV2-J α domain of the same length as in our investigation but without the calmodulin binding site a light induced exposure of W491 in the lit state was proposed (16). This is in line with our results.

But the more interesting aspect of this study is not *that* there is a change in the tryptophan fluorescence of the LOV2 construct upon photoactivation, but *when* these changes occur.

As mentioned in the introduction the UV-VIS absorption photocycle of the LOV2-J α domain contains only two photointermediates phot^L₆₆₀ and phot^S₃₉₀ which decay with time constants of 4 μ s and 40 sec. The transitions of the transient tryptophan fluorescence which have time constants of 450 μ s and 3.8 ms therefore belong to photocycle intermediates which can not be distinguished by their UV-VIS absorption spectrum. As a consequence the photocycle scheme of the oat phot1 LOV2-J α domain has to be expanded by two additional intermediates we called phot^{S2}₃₉₀ and phot^{S3}₃₉₀ as shown in Figure 5. Note that the second transition contributes only to 17 % of the overall amplitude of the transient fluorescence signal. Therefore we tagged the intermediate phot^{S3}₃₉₀ with a question mark, because additional experiments need to be performed to confirm its presence in the LOV2 photocycle and to characterise the structural differences between phot^{S2}₃₉₀ and phot^{S3}₃₉₀.

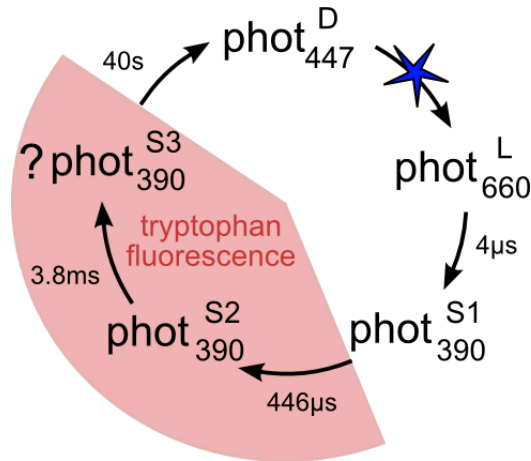


Figure 5: Photocycle of the LOV2-J α domain with apparent time constants. The intermediates and transitions in the red part of the cycle are necessary to explain the transient tryptophan fluorescence data and are not observable in the UV-VIS absorption.

So far the knowledge about the kinetics of the light-induced conformational change in oat phot1 LOV2-J α is limited to a time resolved optical rotary dispersion (ORD) spectroscopy study which detected a small transient decrease in the far-UV signal (~ 230 nm) appearing with a time constant of $90 \pm 36 \mu\text{s}$ at 24°C (18). The authors attributed this transition to a light-induced decrease in secondary structure, which was detected in earlier studies under steady-state conditions by circular dichroism spectroscopy. In comparison a single exponential fit of the transient tryptophan fluorescence signal at 25°C results in a time constant of $355 \mu\text{s}$ (see Fig. 6). As the amplitude of the ORD-transition barely exceeded the noise level of the data and therefore the derived time constant is not very precise, it is conceivable that both signals sense the same transitions and the transient increase in tryptophan fluorescence is coupled to a decrease in the secondary structure of the LOV2-J α domain.

In another study on a LOV2-linker construct from *Arabidopsis* phot1 probed by transient lens (TrL) spectroscopy the authors detected two transitions in their signal with time constants of $300 \mu\text{s}$ and 1 ms caused by changes in the index of refraction of the sample, which were attributed to conformational changes of the protein (20). The linker domain is a 110 amino acid extension to the C-terminus of the LOV2 domain. Although we investigated a LOV2 domain of a different length and from a different organism it is noteworthy that the time constants of the transient tryptophan fluorescence signal measured at 20°C and the TrL signal in the *Arabidopsis* phot1 LOV2-linker construct match very well suggesting similar photoactivation kinetics in both systems.

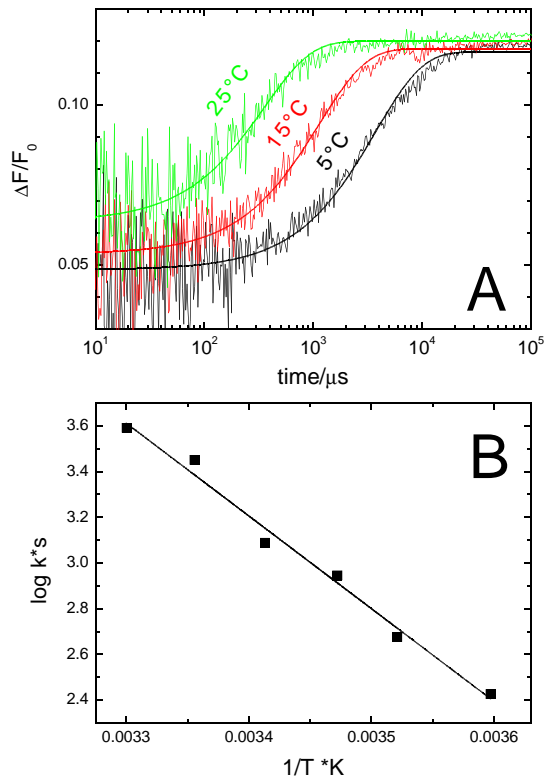


Figure 6: **A** Temperature dependence of the transient tryptophan fluorescence of the LOV2-J α domain. The signals at 5 (black), 15 (red) and 25 °C (green) are an average of 10 scans with waiting times of 2 minutes between the laser flashes and are scaled to the same end value at 100ms. Curves for a single exponential fit of the transient tryptophan fluorescence are superimposed on the data. **B** Arrhenius-plot of the mean kinetics of the transient fluorescence. The rate constants were derived by fitting the average of 10 transient fluorescence scans measured at each temperature with a single exponential. The activation energy of 18.2 kcal/mol was calculated from the slope of the linear fit of the logarithmic rate constants.

To calculate the activation energy for the light-induced conformational change in the oat phot1 LOV2-J α domain we also determined the temperature dependency of the mean transient tryptophan fluorescence kinetics. The transient fluorescence signals for 6 temperatures between 5 and 30 °C were measured and fitted with a single exponential; the corresponding curves for the temperatures 5, 15 and 25 °C are shown in Figure 6A. An Arrhenius-plot of the mean rate constants is shown in Figure 6B. The plot is to a good approximation linear with an activation energy of 18.2 kcal/mol, calculated from the slope of the fit curve.

We then compared this value with the activation energy of the conformational change in a related photoreceptor system Photoactive Yellow Protein (PYP) from *H. halophila*. This is a 125 amino acids long photoreceptor which binds p-coumaric acid as a chromophore. Light-induced isomerization initiates a self-contained photocycle with several thermal relaxations, which ends in the recovery of the dark state in less than one second (30). Like LOV2, PYP is also a PAS-domain protein, but with a ~30 amino acid long N-terminal extension. This part called N-terminal cap resembles in many ways the J α -helix in the LOV2-J α domain. Like J α it packs against the central β -sheet of the PAS-domain and consists of two short α -helices which are thought to unfold upon photoactivation (31). The step in the photocycle of PYP associated with the light-induced conformational change is the transition from I₂ to I₂' as was shown by several time resolved biophysical techniques (32-35). At room temperature for neutral pH this transition occurs ~1 ms and can be monitored very well by transient tryptophan fluorescence spectroscopy as we have shown in chapter 3 for the alkaline pH range, because the tryptophan fluorescence lifetimes of I₂ and I₂' differ by a factor of ~20 (24, 25) (chapter 1 and 2). As in LOV2 the change in fluorescence lifetime is presumably caused by global changes in the protein structure during the I₂/I₂' transition (25) (chapter 2). To determine the temperature dependency of the I₂/I₂' transition we measured the transient tryptophan fluorescence signals of PYP at pH 7.9 for 5 temperatures between 5 and 25 °C. The corresponding signals for the

temperatures 5, 15 and 25 °C are shown in Figure 7A. Curves of a 3-exponential fit (resembling the transitions from I_1 to I_2 , from I_2 to I_2' and the recovery of the protein) are superimposed on the data. An Arrhenius-plot of the rate constants for the I_2/I_2' transition is shown in Figure 7B. The plot is to a good approximation linear with an activation energy of 18.5 kcal/mol. Although there is a factor of ~ 2 between the rates of the conformational change in PYP and LOV2-J α under the investigated conditions, the activation energies of the reaction, which in both cases include a partial unfolding of the protein, are nearly identical, underlining the similarities between both systems. Nevertheless this result is surprising as the ligand and the photochemistry of PYP and LOV2-J α are quite different. While illumination of LOV2 leads to a transient covalent bond between the flavin and a conserved cysteine residue the absorption of light by PYP causes a *trans-cis* isomerization of the already covalently bound chromophore p-coumaric acid. X-ray crystallography studies of illuminated protein crystals showed that in PYP the isomerized chromophore swings out of the binding pocket, while in LOV2 besides the covalent bond formation only minor rearrangements in the chromophore binding pocket occur (14, 27).

We therefore suggest that the kinetics of the formation of the signaling state in PYP and LOV2-J α are determined by the common PAS-domain fold of the two proteins (and the interaction between the PAS-domain and N-terminal cap resp. J α) and not by the specific interaction between the different chromophores and the protein. As a consequence this implies that the kinetics of the signal transduction from the PAS-domain to the neighbouring effector domain (N-terminal cap in PYP, J α -helix in LOV2-J α) might be similar in all PAS-domain proteins. Of course the last conclusion is somehow speculative and additional experimental work has to be done to verify it.

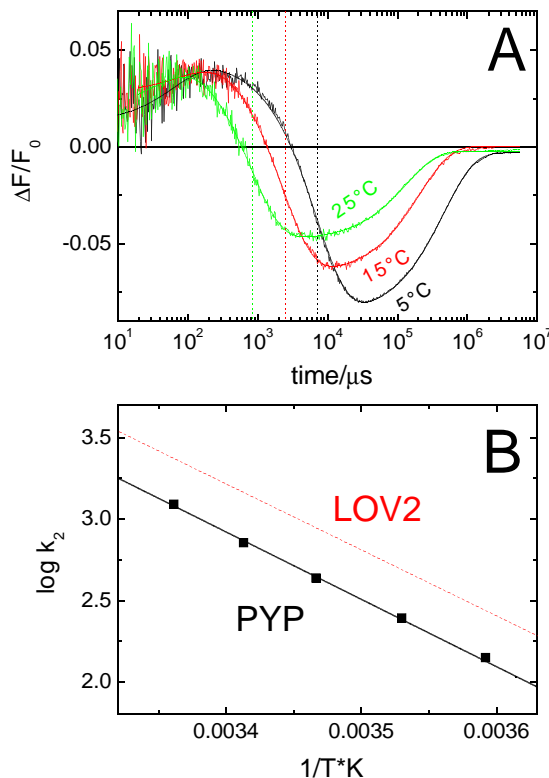


Figure 7: **A** Temperature dependence of the transient tryptophan fluorescence of photoactive yellow protein. The signals at 5.4 (black), 15.5 (red) and 24.5 °C (green) are an average of 20 shots. Curves for a 3-exponential fit of the transient fluorescence signals are superimposed on the data. The time constants of the I_2/I_2' transition which is associated with a global structural change of the protein are indicated by vertical dotted lines. Conditions: pH 7.9, 30 mM KCl, 10 mM Tris. **B** Arrhenius-plot of k_2 corresponding to the I_2/I_2' transition associated with global conformational changes in PYP. The activation energy of 18.5 kcal/mol was calculated from the slope of the linear fit of the logarithmic rate constants. The dashed red line is the fit curve of the corresponding LOV2 data in Figure 6A.

Conclusions

In this study the photocycle of the oat phot1 LOV2 domain including the J α helix was investigated by transient tryptophan fluorescence spectroscopy. Two new transitions with time constants of 450 μ s and 3.8 ms which are invisible in the UV-VIS chromophore absorption were identified and attributed to conformational changes of the protein. The activation energy of the mean transient fluorescence kinetics was determined to be 18.2 kcal/mol. The results were compared with the kinetics of the conformational change in the photocycle of the photoreceptor PYP with an activation energy of 18.5 kcal/mol also determined by transient tryptophan fluorescence spectroscopy. The similar kinetics of the conformational change of both photoreceptor systems were attributed to their shared PAS-domain fold.

References

1. Halavaty, A. S., and K. Moffat. 2007. N- and C-terminal flanking regions modulate light-induced signal transduction in the LOV2 domain of the blue light sensor phototropin 1 from *Avena sativa*. *Biochemistry* 46:14001-14009.
2. Huala, E., P. W. Oeller, E. Liscum, I. S. Han, E. Larsen, and W. R. Briggs. 1997. *Arabidopsis* NPH1: A protein kinase with a putative redox-sensing domain. *Science* 278:2120-2123.
3. Jarillo, J. A., H. Gabrys, J. Capel, J. M. Alonso, J. R. Ecker, and A. R. Cashmore. 2001. Phototropin-related NPL1 controls chloroplast relocation induced by blue light. *Nature* 410:952-954.
4. Christie, J. M., P. Reymond, G. K. Powell, P. Bernasconi, A. A. Raibekas, E. Liscum, and W. R. Briggs. 1998. *Arabidopsis* NPH1: A flavoprotein with the properties of a photoreceptor for phototropism. *Science* 282:1698-1701.
5. Kagawa, T., T. Sakai, N. Suetsugu, K. Oikawa, S. Ishiguro, T. Kato, S. Tabata, K. Okada, and M. Wada. 2001. *Arabidopsis* NPL1: A phototropin homolog controlling the chloroplast high-light avoidance response. *Science* 291:2138-2141.
6. Kinoshita, T., M. Doi, N. Suetsugu, T. Kagawa, M. Wada, and K. Shimazaki. 2001. phot1 and phot2 mediate blue light regulation of stomatal opening. *Nature* 414:656-660.
7. Salomon, M., J. M. Christie, E. Knieb, U. Lempert, and W. R. Briggs. 2000. Photochemical and mutational analysis of the FMN-binding domains of the plant blue light receptor, phototropin. *Biochemistry* 39:9401-9410.
8. Christie, J. M., and W. R. Briggs. 2005. Blue Light Sensing and Signaling by the Phototropins. In *Handbook of Photosensory Receptors*. W. R. Briggs, and J. L. Spudich, editors. Wiley-VCH, Weinheim. 277-303.
9. Salomon, M., E. Knieb, T. von Zeppelin, and W. Rudiger. 2003. Mapping of low- and high-fluence autophosphorylation sites in phototropin 1. *Biochemistry* 42:4217-4225.
10. Christie, J. M., T. E. Swartz, R. A. Bogomolni, and W. R. Briggs. 2002. Phototropin LOV domains exhibit distinct roles in regulating photoreceptor function. *Plant Journal* 32:205-219.
11. Kennis, J. T. M., S. Crosson, M. Gauden, I. H. M. van Stokkum, K. Moffat, and R. van Grondelle. 2003. Primary reactions of the LOV2 domain of phototropin, a plant blue-light photoreceptor. *Biochemistry* 42:3385-3392.
12. Salomon, M., W. Eisenreich, H. Durr, E. Schleicher, E. Knieb, V. Massey, W. Rudiger, F. Muller, A. Bacher, and G. Richter. 2001. An optomechanical transducer in the blue light receptor phototropin from *Avena sativa*. *Proceedings of the National Academy of Sciences of the United States of America* 98:12357-12361.
13. Swartz, T. E., S. B. Corchnoy, J. M. Christie, J. W. Lewis, I. Szundi, W. R. Briggs, and R. A. Bogomolni. 2001. The photocycle of a flavin-binding domain of the blue light photoreceptor phototropin. *Journal of Biological Chemistry* 276:36493-36500.
14. Crosson, S., and K. Moffat. 2002. Photoexcited structure of a plant photoreceptor domain reveals a light-driven molecular switch. *Plant Cell* 14:1067-1075.
15. Corchnoy, S. B., T. E. Swartz, J. W. Lewis, I. Szundi, W. R. Briggs, and R. A.

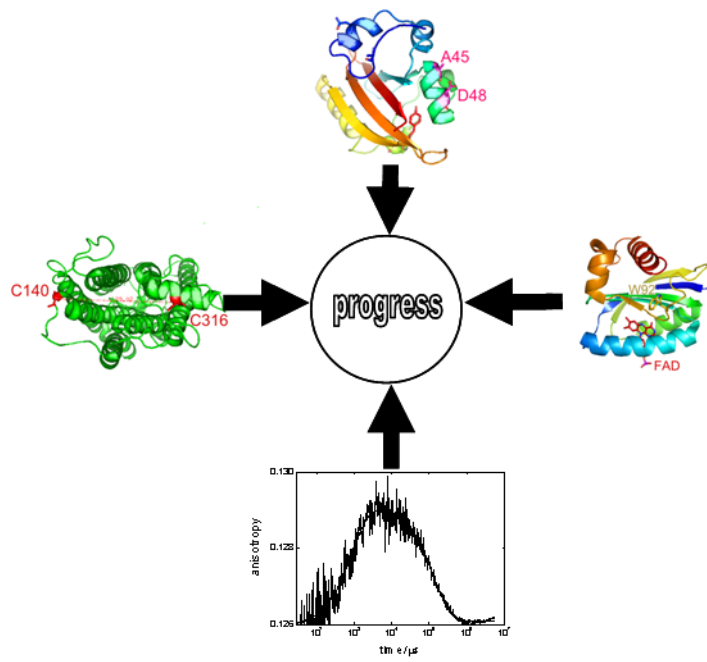
Chapter 7

- Bogomolni. 2003. Intramolecular proton transfers and structural changes during the photocycle of the LOV2 domain of phototropin 1. *Journal of Biological Chemistry* 278:724-731.
16. Harper, S. M., L. C. Neil, and K. H. Gardner. 2003. Structural basis of a phototropin light switch. *Science* 301:1541-1544.
 17. Harper, S. M., L. C. Neil, I. J. Day, P. J. Hore, and K. H. Gardner. 2004. Conformational changes in a photosensory LOV domain monitored by time-resolved NMR spectroscopy. *Journal of the American Chemical Society* 126:3390-3391.
 18. Chen, E. F., T. E. Swartz, R. A. Bogomolni, and D. S. Kliger. 2007. A LOV story: The signaling state of the Phot1 LOV2 photocycle involves chromophore-triggered protein structure relaxation, as probed by far-UV time-resolved optical rotatory dispersion spectroscopy. *Biochemistry* 46:4619-4624.
 19. Nakasako, M., T. Iwata, D. Matsuoka, and S. Tokutomi. 2004. Light-induced structural changes of LOV domain-containing polypeptides from Arabidopsis phototropin 1 and 2 studied by small-angle X-ray scattering. *Biochemistry* 43:14881-14890.
 20. Nakasone, Y., T. Eitoku, D. Matsuoka, S. Tokutomi, and M. Terazima. 2007. Dynamics of conformational changes of Arabidopsis phototropin 1 LOV2 with the linker domain. *Journal of Molecular Biology* 367:432-442.
 21. Harper, S. M., J. M. Christie, and K. H. Gardner. 2004. Disruption of the LOV-J alpha helix interaction activates phototropin kinase activity. *Biochemistry* 43:16184-16192.
 22. Kyndt, J. A., F. Vanrobbaeys, J. C. Fitch, B. V. Devreese, T. E. Meyer, M. A. Cusanovich, and J. J. Van Beeumen. 2003. Heterologous production of Halorhodospira halophila holo-photoactive yellow protein through tandem expression of the postulated biosynthetic genes. *Biochemistry* 42:965-970.
 23. Borucki, B., H. Otto, and M. P. Heyn. 1999. Reorientation of the retinylidene chromophore in the K, L, and M intermediates of bacteriorhodopsin from time-resolved linear dichroism: Resolving kinetically and spectrally overlapping intermediates of chromoproteins. *Journal of Physical Chemistry B* 103:6371-6383.
 24. Hoersch, D., H. Otto, M. A. Cusanovich, and M. P. Heyn. 2008. Distinguishing chromophore structures of photocycle intermediates of the photoreceptor PYP by transient fluorescence and energy transfer. *Journal of Physical Chemistry B* 112:9118-9125.
 25. Otto, H., D. Hoersch, T. E. Meyer, M. A. Cusanovich, and M. P. Heyn. 2005. Time-resolved single tryptophan fluorescence in photoactive yellow protein monitors changes in the chromophore structure during the photocycle via energy transfer. *Biochemistry* 44:16804-16816.
 26. Ihee, H., S. Rajagopal, V. Srajer, R. Pahl, S. Anderson, M. Schmidt, F. Schotte, P. A. Anfinrud, M. Wulff, and K. Moffat. 2005. Visualizing reaction pathways in photoactive yellow protein from nanoseconds to seconds. *Proceedings of the National Academy of Sciences of the United States of America* 102:7145-7150.
 27. Genick, U. K., G. E. O. Borgstahl, K. Ng, Z. Ren, C. Pradervand, P. M. Burke, V. Srajer, T. Y. Teng, W. Schildkamp, D. E. McRee, K. Moffat, and E. D. Getzoff. 1997. Structure of a protein photocycle intermediate by millisecond time-resolved crystallography. *Science* 275:1471-1475.
 28. Lakowicz, J. R. 2006. Protein Fluorescence. In *Principles of Fluorescence*

Chapter 7

- Spectroscopy. Springer, New York. 530-577.
29. Chen, Y., and M. D. Barkley. 1998. Toward understanding tryptophan fluorescence in proteins. *Biochemistry* 37:9976-9982.
 30. Cusanovich, M. A., and T. E. Meyer. 2003. Photoactive yellow protein: A prototypic PAS domain sensory protein and development of a common signaling mechanism. *Biochemistry* 42:4759-4770.
 31. Harigai, M., Y. Imamoto, H. Kamikubo, Y. Yamazaki, and M. Kataoka. 2003. Role of an N-terminal loop in the secondary structural change of photoactive yellow protein. *Biochemistry* 42:13893-13900.
 32. Brudler, R., R. Rammelsberg, T. T. Woo, E. D. Getzoff, and K. Gerwert. 2001. Structure of the I-1 early intermediate of photoactive yellow protein by FTIR spectroscopy. *Nature Structural Biology* 8:265-270.
 33. Chen, E. F., T. Gensch, A. B. Gross, J. Hendriks, K. J. Hellingwerf, and D. S. Kliger. 2003. Dynamics of protein and chromophore structural changes in the photocycle of photoactive yellow protein monitored by time-resolved optical rotatory dispersion. *Biochemistry* 42:2062-2071.
 34. Hendriks, J., T. Gensch, L. Hviid, M. A. van der Horst, K. J. Hellingwerf, and J. J. van Thor. 2002. Transient exposure of hydrophobic surface in the photoactive yellow protein monitored with Nile red. *Biophysical Journal* 82:1632-1643.
 35. Borucki, B., S. Devanathan, H. Otto, M. A. Cusanovich, G. Tollin, and M. P. Heyn. 2002. Kinetics of proton uptake and dye binding by photoactive yellow protein in wild type and in the E46Q and E46A mutants. *Biochemistry* 41:10026-10037.

Chapter 8



Conclusions and Outlook

PYP

The aim of the studies described in this thesis was to investigate light-induced conformational changes in several photoreceptor systems by time resolved absorption and fluorescence spectroscopy .

This thesis focusses on investigations of PYP from *H. halophila*. This photoreceptor is the structural prototype for a PAS-domain fold. As over 2000 proteins, many of them are sensor proteins, have been identified to contain one or more PAS domains, investigations on the signaling mechanism of PYP are of general interest for the field of protein signal transduction.

As described in chapter 2 and 3 the efficient fluorescence resonance energy transfer from the single tryptophan W119 in PYP to the chromophore was used to get detailed information about the configuration of the chromophore in different photointermediates. The methods of single photon counting and transient fluorescence spectroscopy were used to determine the tryptophan fluorescence lifetime in different photointermediates. The two methods are somehow complementary as single photon counting only resolves the fluorescence decay of stationary states but is able to differentiate between mixtures of states with different fluorescence lifetimes. On the other hand transient fluorescence spectroscopy only measures the mean fluorescence quantum yield of an ensemble but resolves changes in this value during the photocycle with a time resolution of 1 μ s.

The experimentally derived fluorescence lifetimes were then compared with theoretical ones calculated from high resolution crystal structures. As shown in chapter 3 in this way one of two published structures for the intermediate I_1 could be ruled out to be present in the photocycle of PYP under the investigated conditions and the chromophore orientation of the alkaline intermediate I_1' , for which the crystal structure is not known yet, was predicted to be similar to that of the known I_2 intermediate.

Another interesting aspect of this study is that it clearly showed the essential role of the κ^2 -factor on the rate of energy transfer as predicted by the Förster theory (1). For most applications of fluorescence resonance energy transfer (FRET) the κ^2 -factor is assumed to be 2/3, which is only the correct value for a highly mobile donor-acceptor pair (2, 3). In PYP for the donor acceptor pair W119-chromophore and presumably in many other proteins this assumption is not valid. The results of chapter 2 clearly show that every intermediate has its own specific κ^2 -factor. This example showed the importance of performing additional experiments on the mobility of donor and acceptor - for example by measuring the time resolved fluorescence anisotropy decay- before doing calculations on donor-acceptor distances based on FRET data.

In chapter 4 and 5 the interaction between the PAS-domain and the N-terminal cap of PYP was investigated. The N-terminal cap is a ~30 amino acid long domain consisting of loops and two short α -helices packed against the central β -sheet of the PAS-domain and undergoes major structural changes upon photoactivation. Unraveling the mechanism which transduces the light-induced structural signal from the binding pocket of the chromophore through the β -sheet to the N-terminal cap in PYP is of general interest because it might also give insights how PAS sensor-domains communicate with their

Chapter 8

effector domains in multidomain sensor proteins.

In chapter 4 the knowledge about the tryptophan fluorescence lifetimes of different photointermediates was used to examine the salt dependency of the I_2/I_2' equilibrium. As a complementary method the time traces of the intermediate concentrations were calculated from transient absorption spectroscopy data, using their known absorption spectra. With this approach it was also possible to investigate the salt dependency of the recovery rate of the photoreceptor.

Both, the salt dependency of the I_2/I_2' equilibrium and of the recovery rate could be explained on the basis of the well known Debye-Hückel theory (4), suggesting the screening of a monovalent ion pair being responsible for the observed salt effect. Furthermore this ion pair was identified to be the K110/E12 salt bridge which connects the central β -sheet of the protein with the N-terminal cap. This was concluded from investigations of the mutants K110A and E12A in which the salt bridge is missing.

This result gives interesting insights in the signaling mechanism of PYP and PAS-domain proteins in general. It shows that the conformational changes occurring during the activation of the photoreceptor in the I_2 to I_2' transition involve the breakage of this highly conserved salt bridge and supports a model for signal transduction in PYP in which the N-terminal cap detaches from the central β -sheet upon photoactivation and leads to an exposure of an interface for a potential binding partner.

As the signaling state I_2' is partially unfolded (5, 6), the salt dependency of the recovery kinetics to the folded ground state P is also of general interest for the field of protein folding, because not much research has been performed so far on the influence of the ionic strength of the solvent on the kinetics of protein folding processes. As mentioned above we were able to explain this effect in PYP quantitatively with the theory of Debye-Hückel.

In chapter 5 we investigated the signaling mechanism of PYP further by attaching dye molecules to specific parts of the N-terminal cap and studying changes in their absorption spectrum upon photoactivation of the protein. As reporter dye iodoacetamidofluorescein (IAF) was chosen, which was attached to the cysteine side chain of the mutants A5C and N13C by site-specific labeling. The absorption spectrum of fluorescein is dependent on the polarity of the solvent (7) and the possibility to form H-bonds with its environment (8, 9). Thus the transient absorption changes of IAF measured at high buffer concentration during the photocycle monitors structural changes in the local protein environment of the dye. The main result of the measurement was that the kinetics of the structural change is coupled with different photointermediates in A5C-AF and N13C-AF.

As the structural changes near A5 appear one step earlier in the photocycle than the ones near N13, this has interesting consequences for the photoreceptor's mechanism of signaling. It suggests that the light-induced structural change propagates through the N-terminal cap first appearing near A5 and then being transduced to the region near N13. This finding is in line with a signaling mechanism model derived from time resolved X-ray crystallography on PYP crystals. There the structural signal is transmitted via helix α_3 from the chromophore binding pocket to the N-terminal cap (10, 11).

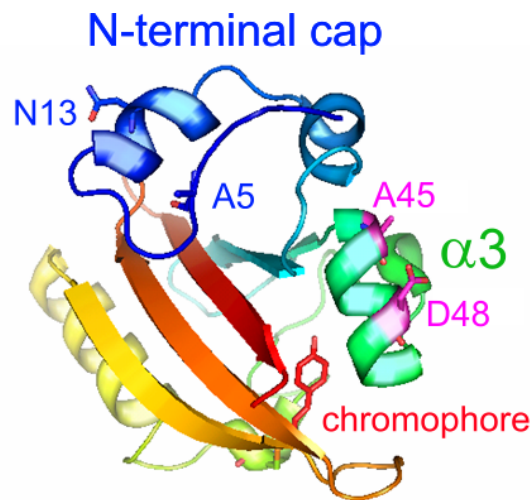


Figure 1 Backbone crystal structure of PYP based on Protein Data Bank file 1NWZ.pdb (12). The chromophore with C69 and several actual or potential labeling sites are shown as sticks.

In future experiments several new labeling sites might elucidate the pathway of the light-induced structural signal further. Especially binding sites on $\alpha 3$ should be useful to get a better understanding of the signaling mechanism of PYP. Possible targets for mutagenesis are for example the solvent exposed side chains A45 and D48. Their position in the crystal structure of PYP is shown in Figure 1.

Another point to improve is the right choice of the reporter molecule. First the absorption spectrum of the dye should be sensitive to the properties of its environment. Second its absorption spectrum should not overlap with the photoreceptor chromophore absorption. In the case of PYP this means that reporter dyes with absorption maxima of 500 nm or above are preferable. Third the size of the reporter molecule limits the spatial resolution of the experiment; therefore it should be as small as possible. Point 2 and 3 are somehow conflicting as in general the wavelength of the absorption maximum of a dye scales with the length of its conjugated π -electron system. Nevertheless recently a new thiol-reactive dye, aminophenoxazone maleimide (APM) was developed with excellent properties to probe conformational changes of proteins (13). Its absorption spectrum depends strongly on the polarity of the environment with $\lambda_{\max}=598$ nm in water and $\lambda_{\max}=523$ nm in dioxane. The chemical structure of APM and IAF are shown in Figure 2. It shows that although the absorption maximum of APM in water is red-shifted by ~ 100 nm in comparison to IAF the size of the molecule is even smaller than the former. Therefore we conclude that APM would be a superior alternative to IAF for probing light-induced conformational changes in PYP or other photoreceptor systems by transient absorption spectroscopy in future experiments.

The next topic of this thesis was to apply the technique of transient fluorescence spectroscopy to other photoreceptors. In PYP the kinetics of the transient tryptophan fluorescence is closely coupled to the photocycle kinetics of the transient chromophore absorption. The main reason for this is that the fluorescence lifetime of W119 is dictated by efficient resonance energy transfer to the chromophore (see chapter 2). As W119 is tightly packed in the central β -sheet of the protein, changes in the rate of energy transfer are caused by reorientations of the chromophore transition dipole moment and changes in its absorption spectrum which affect the κ^2 -factor and the overlap integral. This might be different in other photoreceptors.

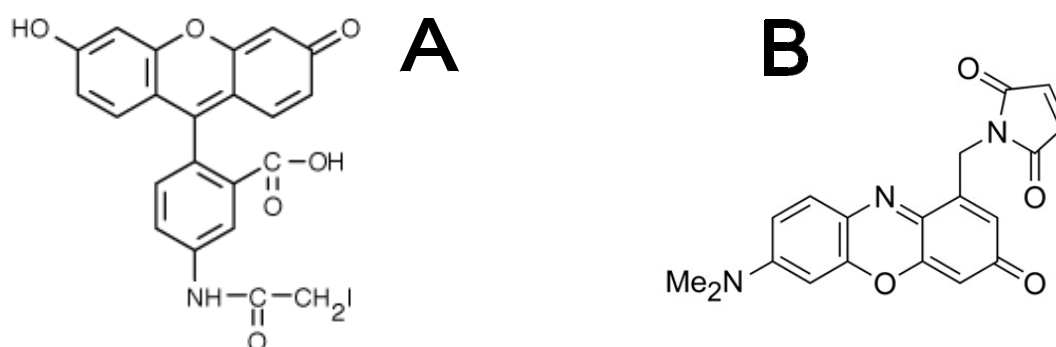


Figure 2 Chemical structure of the thiol reactive dyes iodoacetamidofluorescein (5-IAF, A) taken from the Molecular Probes online catalogue and aminophenoxazone maleimide (APM, B) taken from (13).

Rhodopsin

Rhodopsin is the photoreceptor of dim light vision in the vertebrate eye. Furthermore it is a model system for the family of G-protein coupled receptors, which regulate a wide range of physiological processes and are targets of many therapeutically relevant drugs in humans. Although lots of research has been performed on this photoreceptor system during the last decades, the knowledge about the kinetics of the photoactivation process and in particular on the kinetics of the several molecular steps leading to the formation of the signaling state is limited. In our approach we used transient fluorescence spectroscopy to resolve the kinetics of the light-induced conformational change in rhodopsin as described in chapter 6.

First we performed transient tryptophan fluorescence experiments on rhodopsin in ROS membranes. They showed that there is a decrease in the tryptophan fluorescence in parallel to the formation of the signaling state Meta_{II} . This could be explained by a more efficient energy transfer from the tryptophans to the retinylidene chromophore caused by the increased spectral overlap in Meta_{II} . Although there is a light-induced rearrangement of W265 in the retinal binding pocket (15, 16), this could not be resolved by transient fluorescence spectroscopy, because the W265 fluorescence is completely quenched by ultra efficient energy transfer to the retinal and does not contribute to the overall rhodopsin tryptophan fluorescence. This was shown by calculations on the energy transfer efficiency of the 5 tryptophans in rhodopsin, based on its known crystal structure.

In future, experiments on rhodopsin mutants with a reduced number of tryptophans might give new information on the kinetics of the light-activation process, because the overall tryptophan fluorescence in wild type might be dominated by tryptophans which do not undergo major structural changes.

Another way to resolve the kinetics of the light induced conformational changes of photoreceptors is to attach a reporter dye to the protein. In this study C316 on the cytoplasmic side of rhodopsin which is suggested to be part of the binding interface for transducin was selectively labeled with the dye Alexa594 maleimide, whose fluorescence is known to increase by 20 % upon photoactivation (17). In contrast to the transient tryptophan fluorescence, the kinetics of the transient Alexa594 fluorescence is different to the kinetics of the Schiff base deprotonation, which was determined from the transient

absorption signal at 360 nm. Furthermore the kinetics of the transient Alexa594 fluorescence is different from the kinetics of the transient proton uptake measured with the pH indicator dye BCP. Additionally Schiff base deprotonation, structural change and proton uptake have different activation energies calculated from the temperature dependency of their rate constants. Therefore the sequence of molecular events of rhodopsin activation in ROS membranes was concluded to be Schiff base deprotonation, structural change and proton uptake.

These results give new insights in the signaling mechanism of the photoreceptor, as previous time resolved ESR-studies on rhodopsin in DM micelles showed the same kinetics for the structural change and the proton uptake (18). In contrast to that study our results showed that this is clearly not the case for rhodopsin in native disc membranes.

In bovine rhodopsin there are two cysteines on the cytoplasmic surface, C140 and C316, which are both accessible for site-directed labeling (19). For future investigations it might be of interest to do transient fluorescence experiments on rhodopsin selectively labeled at C140 with a fluorescence dye to compare the kinetics of the structural changes near C140 and C316. Note that C140, which is 29 Å away from C316 in the crystal structure of rhodopsin (see Figure 3), is located at the cytoplasmic end of helix 3 in the direct neighborhood of the functionally important ERY motif (20, 21). A next step would be the simultaneous labeling of C140 and C316 with different fluorescence dyes, which act as donor-acceptor pair for fluorescence resonance energy transfer experiments. Changes in the energy transfer rate upon photoactivation of rhodopsin might give additional insights in the molecular events and kinetics of the photoactivation process.

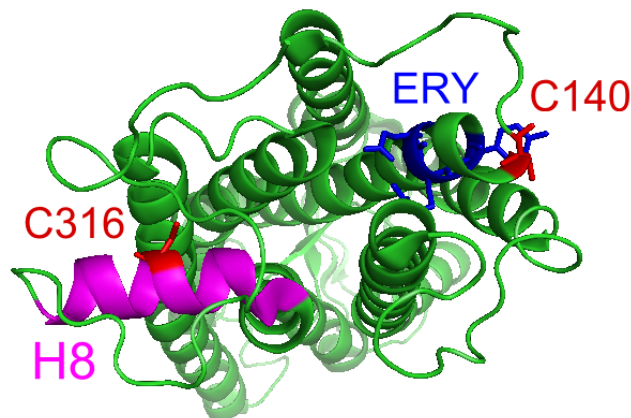


Figure 3 Backbone crystal structure of bovine rhodopsin based on Protein Data Bank file 1U19.pdb (14). Top view on the cytoplasmic side of the receptor. The potential labeling sites C140 and C316 are shown as sticks and coloured red. Also shown are the functionally important ERY motif (blue sticks) and helix 8 (magenta).

Another even more interesting field for future experiments is the use of transient fluorescence spectroscopy to resolve the rhodopsin-transducin interaction. If the kinetics of transducin binding and activation is not limited by diffusion but by conformational changes of the photoactivated rhodopsin, this approach should give new insights in the molecular mechanism of the signal transduction process. Indeed *in vivo* measurements of the rod cell hyperpolarization with reduced rhodopsin density in the rod discs suggested that the diffusion of transducin to photoactivated rhodopsin is the rate limiting step in the phototransduction cascade (22), but for *in vitro* measurements under the right conditions

this limitation can be overcome however (23). It is furthermore known that the transducin tryptophan fluorescence increases upon the nucleotide exchange from GDP to GTP. This is used in assays which probe the transducin activation by measuring the tryptophan fluorescence of transducin/rhodopsin mixtures (24, 25). Transient tryptophan fluorescence measurements on transducin/rhodopsin mixtures should be able to resolve the kinetics of transducin activation in response to a light stimulus and might help to answer the question which molecular events of rhodopsin photoactivation are necessary for transducin activation: Schiff base deprotonation, structural change or proton uptake. This is possible because we have shown in chapter 6 that these three events have quite different kinetics in ROS membranes at physiological temperatures.

LOV2

In chapter 7 the LOV2-J α domain from oat phototropin1 was investigated by transient fluorescence spectroscopy. LOV1 and LOV2 are the light sensing flavin binding domains of the photoreceptor phototropin, which *inter alia* mediates phototropism in plants (see chapter 1). Light-activation of LOV2 leads to an autophosphorylation of a histidine kinase effector domain in phototropin. As LOV domains are part of the PAS-domain family, LOV2-J α is an example of a PAS-domain being part of a multidomain sensor protein. Therefore the search for similarities in the mechanism of photoactivation in LOV2 and PYP could give information of the general mechanism of PAS-domain signaling.

Our approach was to use the sensitivity of the native tryptophan fluorescence in LOV2-J α to environmental changes to resolve the kinetics of light-induced conformational changes in the photoreceptor domain. The transient tryptophan fluorescence measured in a time window from 10 μ s to seconds increased biexponentially with time constants of 450 μ s and 3.8 ms at 20 °C. These transitions are invisible in the UV-VIS absorption photocycle of LOV2-J α . Therefore the transient fluorescence signal suggests the presence of at least two more spectrally silent intermediates, which are associated with structural changes of the protein.

Steady state NMR spectroscopy experiments already showed that there is a light-induced structural change for W491 and W557 in the LOV2-J α domain, which were attributed to the unfolding of the helix J α upon formation of the lit state (26, 27). We were now able to resolve the conformational change of the protein in time by probing the transient changes of the tryptophan fluorescence quantum yield. This interpretation is supported by a time resolved ORD study on the same protein indicating a light-induced decrease in secondary structure content with a time constant in the same order of magnitude (90 ± 36 μ s) as the transition in the transient tryptophan fluorescence signal but which suffered from a poor signal to noise ratio (28).

From the temperature dependency of the transient fluorescence signal the mean activation energy of this structural change was calculated to be 18.2 kJ/mol. We compared this result with the kinetics of the conformational change in PYP, probed by the temperature dependency of the I₂/I₂' transition using the transient fluorescence of its single tryptophan W119 (see chapter 2 and 3). The kinetics of the transition in the two systems differs by a factor of ~2 and the activation energy of the conformational change in PYP with 18.5 kcal/mol is very similar to the corresponding value of 18.2 kcal/mol in LOV2-J α . This similarity suggests that the kinetics of the structural change in both photoreceptor systems PYP and LOV2-J α might be related to their common PAS-domain fold.

Chapter 8

Furthermore the results on LOV2-J α show that transient tryptophan fluorescence spectroscopy can give new kinetic information about the photoreceptor activation, as it probes regions of the protein outside the chromophore binding pocket. In this way the response of the protein to the light-induced local structural perturbation in the binding pocket of the chromophore can be investigated, which is not possible by the standard technique of transient spectroscopy of the chromophore absorption in the UV-VIS.

For future experiments on LOV2-J α two approaches might be of interest: There are three tryptophans in the protein construct investigated in this thesis, decreasing the spatial resolution of the measurement. Reducing their number to one tryptophan per protein by mutagenesis might allow to show, whether one specific tryptophan causes the transient fluorescence signal of LOV2-J α . In this way it should be possible to locate the regions where the light-induced structural changes occur. If more than one tryptophan is responsible for the transient fluorescence signal it would be of interest if there are any kinetic differences in the response of the individual tryptophans to light-activation. This is not unreasonable keeping in mind the results of chapter 5 which suggested a transient propagation of the structural change through the N-terminal cap of PYP. Another way to get information about the kinetics of light-induced conformational changes in specific parts of LOV2-J α would be the introduction of additional cysteines in the amino acid sequence of the protein. This would enable site-specific labeling of LOV2-J α with thiol reactive dyes and the investigation of conformational changes in the label environment by transient absorption or transient fluorescence spectroscopy similar to the experiments with PYP described in chapter 5.

BLUF

Another photoreceptor system which is of interest for future transient fluorescence measurements is the BLUF-domain. BLUF is an acronym for “sensor of **blue-light using FAD**” (30, 31). In many respects these domains are similar to LOV domains, as they also bind flavin as a chromophore and respond to blue light activation with a self-contained photocycle. BLUF domains were first found in the photoreceptor AppA from *Rhodobacter sphaeroides* (32) which controls blue-light regulation of photosystem synthesis (33). The longest living intermediate of the AppA BLUF domain photocycle is formed within picoseconds, is 10 nm red-shifted with respect to the dark state and recovers to the ground state with a time constant of ~30 min (34). The amino acid sequence of the AppA BLUF domain contains 2 tryptophans W64 and W104, with W104 supposed to play an important role in the photoactivation of the domain (35, 36). In particular W104 is proposed to swing out of the FAD binding pocket upon formation of the signaling state. This was concluded from a structural heterogeneity in protein crystals of the AppA BLUF domain and the single BLUF domain protein Slr1694 from *Synechocystis* (29, 37). In Figure 4 two Slr1694 structures from the same crystal are depicted with different orientations for the single tryptophan W94. As the tryptophan fluorescence decreases upon illumination it was suggested that the structure with a surface exposed W94 (Figure 4A) resembles the lit state of the protein (29).

Figure 5A shows the crystal structure of the AppA BLUF domain and Figure 5B the one of the single BLUF domain protein BlrB also from *Rhodobacter sphaeroides*. BlrB is a 136 amino acid long photoreceptor, whose amino acid sequence contains only one tryptophan W92, at the corresponding position of W104 in AppA BLUF, for which NMR-spectroscopy experiments showed a significant structural change upon illumination (38). For W104 in AppA and W92 in BlrB the proposed light induced movement should result in changes in their fluorescence properties similar to Slr1694, but steady state fluorescence

spectroscopy on both proteins showed no significant reversible differences in tryptophan fluorescence quantum yield (37) of the dark and lit state. This might be caused by two different compensating fluorescence changes, which occur at different steps of the photocycle. Therefore transient tryptophan fluorescence measurements of Slr1694 as well as of the AppA BLUF domain and BlrB could be of interest to get information on the kinetics of the light induced conformational changes in these proteins and in BLUF domains in general. On the other hand time resolved anisotropy measurements on the single tryptophans of Slr1694 and BlrB in the dark and lit state could resolve changes in the mobility of the amino acid, which may have no effect on the fluorescence quantum yield.

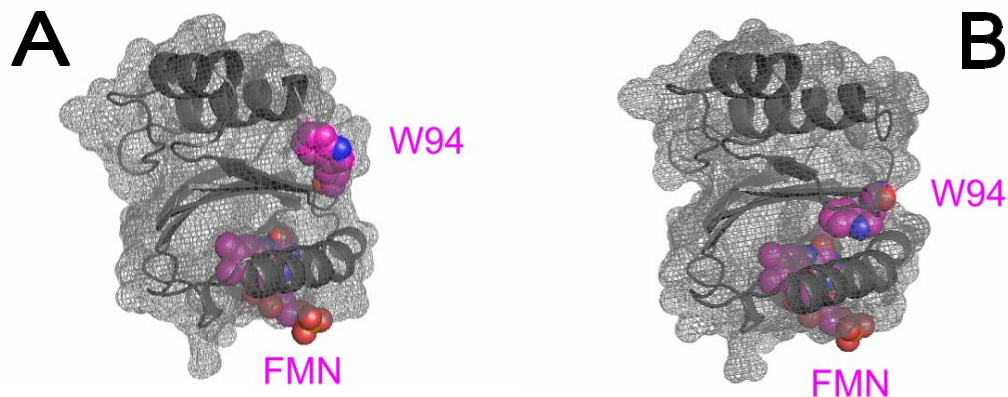


Figure 4 Backbone crystal structure and surface of the BLUF domain protein Slr1694 from *Synechocystis* with the single tryptophan W94 buried in the protein (**B**) or solvent exposed (**A**) based on Protein Data Bank file 2HFN.pdb (29). The chromophore FMN and the tryptophan W94 are shown as spheres.

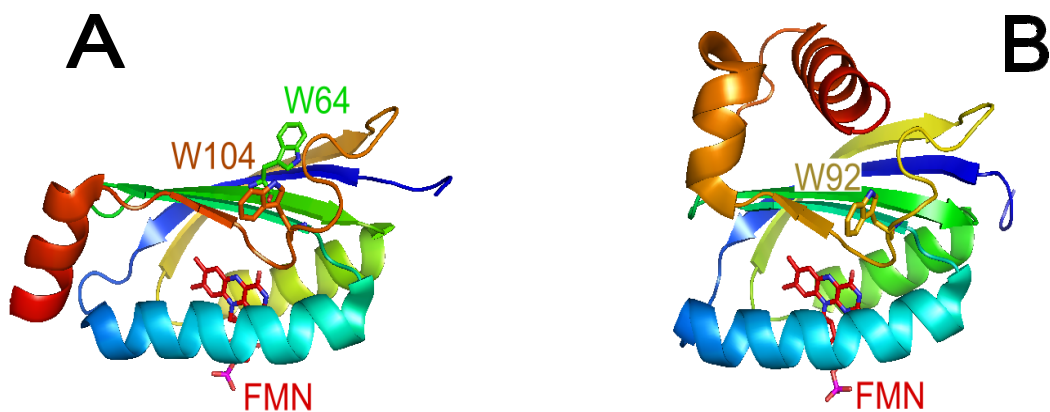


Figure 5 **A** Backbone crystal structure of the BLUF domain of the photoreceptor AppA from *Rhodospirillum rubrum* based on Protein Data Bank file 2IYG.pdb (37). **B** Backbone crystal structure of the BLUF domain protein BlrB from *Rhodospirillum rubrum* based on Protein Data Bank file 2BYC.pdb (39). The chromophore FMN (red) and the tryptophans W64 (green) and W104 (orange) from AppA BLUF and W92 (yellow) from BlrB are shown as sticks.

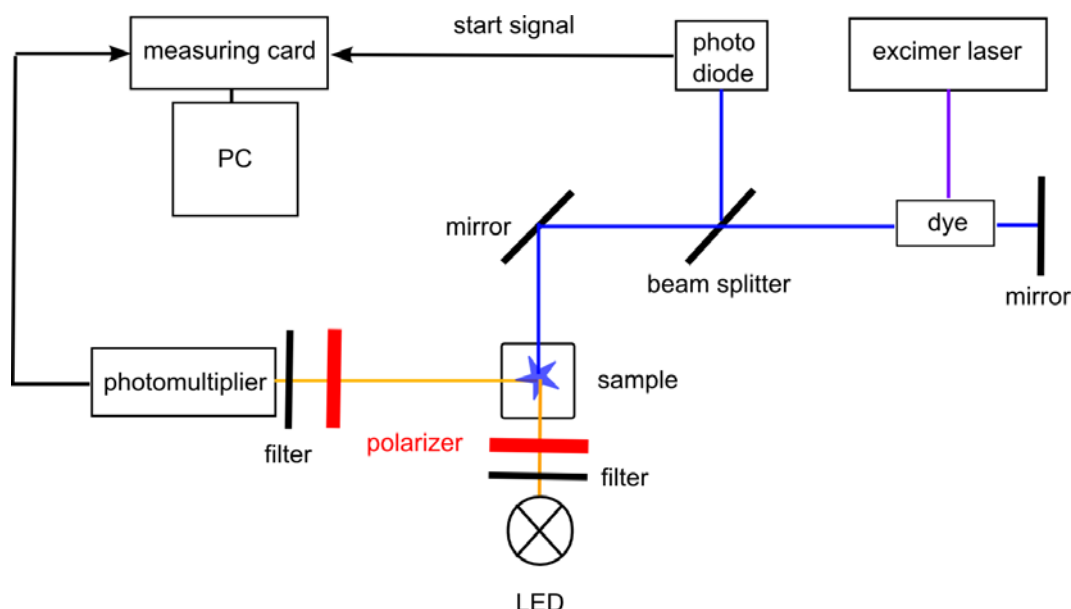


Figure 6 Set-up for measurements of the transient fluorescence anisotropy.

Transient Fluorescence Anisotropy

A methodical improvement of interest for future experiments is the measurement of the transient fluorescence anisotropy. Here the use of polarized excitation and fluorescence detection can give information about the mobility of a fluorophore. The anisotropy was already defined in Eq. 1 in chapter 1. There the measurement of the time resolved fluorescence anisotropy decay using single photon counting was discussed. In contrast to this technique, the transient fluorescence anisotropy probes the steady state anisotropy during the photocycle of a photoreceptor. For this we use a modification of the set-up for transient fluorescence spectroscopy which is shown in Figure 6.

The fluorescence of the sample is excited with vertically polarized light. This is achieved by positioning a linear polarizer between the excitation light source and the sample holder. The fluorescence light also passes a linear polarizer which is placed in front of the photomultiplier tube (PM). The transient anisotropy $r(t)$ is calculated from the photomultiplier currents $I_{\parallel}(t)$ and $I_{\perp}(t)$ measured in two independent experiments with detection polarization plane parallel and perpendicular to the excitation polarization plane via

$$r(t) = \frac{I_{\parallel}(t) - I_{\perp}(t)}{I_{\parallel}(t) + 2I_{\perp}(t)}$$

We did a preliminary experiment on the transient fluorescence anisotropy of the PYP mutant N13C labeled with the thiol reactive dye tetramethylrhodamine-iodoacetamide (TMRIA). As excitation light source we used a high power LED emitting at 530 nm. Stray light from the LED and the flash at 460 nm exciting the PYP photocycle was cut off with the long pass filter OG 570 which was placed in front of the PM. Figure 7 shows the transient TMRIA-fluorescence (A) and the transient TMRIA-fluorescence anisotropy (B) of the labeled sample. Both the fluorescence quantum yield and the fluorescence anisotropy of the attached label changed transiently during the PYP photocycle. The

Chapter 8

signals are to a good approximation mirror images. Note that this is the expected behavior even if the mobility of the fluorophore does not change, as the steady state fluorescence anisotropy is not only influenced by the rotational diffusion of the fluorophore but also by the fluorescence lifetime. This is expressed in the Perrin equation (40) for the case of a spherical rotor

$$\frac{r_0}{r} = 1 + \frac{\tau}{\tau_c}$$

with r the steady state anisotropy, r_0 the initial anisotropy in the absence of rotational diffusion, τ the fluorescence lifetime and τ_c the rotational correlation time (see chapter 1).

Therefore the light-induced changes in the TMRIA anisotropy may be caused entirely by the changes of the fluorescence lifetime of the dye and are no proof for changes in its mobility.

Nevertheless transient fluorescence anisotropy could be a good method to investigate other photoreceptor systems where illumination leads to conformational changes, which have a big influence on the rotational diffusion of the protein such as for example dimerization or adhesion to a membrane.

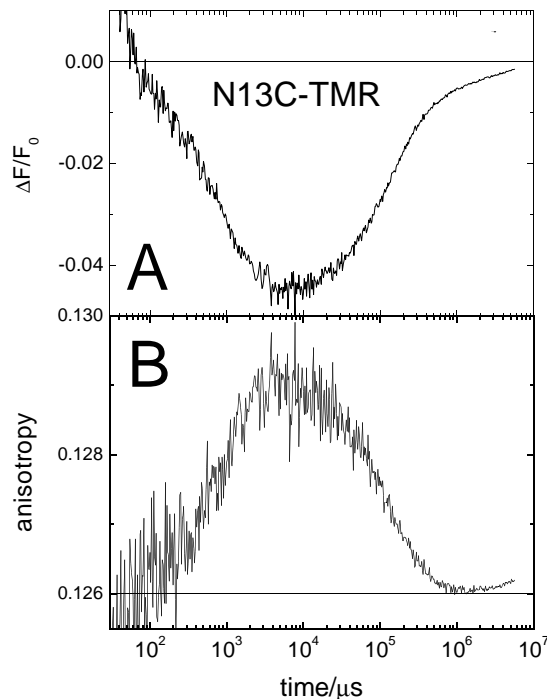


Figure 7 Transient label fluorescence (A) and transient label fluorescence anisotropy (B) for the PYP mutant N13C labeled with the thiol reactive dye tetramethylrhodamine-iodoacetamide (TMRIA). Conditions: 10 mM Tris, pH 8, 20°C.

Summary

To sum up, in this thesis light-induced conformational changes in photoreceptors were investigated by time resolved spectroscopy. The focus was on structural changes of the protein in response to the light-induced changes in the chromophore configuration.

The investigated systems were the PAS-domain proteins or protein domains PYP and LOV2 and the G-protein coupled receptor rhodopsin.

For PYP we obtained new information on the detailed chromophore structures in the intermediates I_1 and I_1' from a comparison of their tryptophan fluorescence lifetimes with published crystal structures (chapter 3). Furthermore we investigated the interaction between the PAS-domain and the N-terminal cap of PYP: We elucidated the important role of a conserved salt-bridge connecting the PAS-domain and the N-terminal cap in the activation of the photoreceptor by investigating the salt-dependency of its photocycle (chapter 4), and we probed the kinetic response of different parts of the N-terminal cap to photoactivation, which suggested a pathway of structural change in this part of the protein (chapter 5).

For rhodopsin we resolved the kinetics of the light-induced conformational change with high time resolution in native ROS membranes using fluorescence techniques and showed that it is different to the kinetics of Schiff-base deprotonation and proton uptake (chapter 6).

For LOV2-J α we showed that the kinetics of the conformational change is not coupled to the photocycle kinetics of the chromophore absorption by monitoring the transient fluorescence of native tryptophans in the domain and found that the kinetics of the structural change in LOV2-J α and PYP are remarkably similar, suggesting it might be related to the shared PAS domain fold of both systems (chapter 7).

A new method applied in this thesis was transient fluorescence spectroscopy either of native tryptophan residues of the investigated photoreceptors or attached fluorescence labels (chapter 3, 6 and 7). This method gave new information on the kinetics of photoreceptor activation not available by transient absorption spectroscopy of the chromophore. As transient fluorescence spectroscopy on the native tryptophans in a protein is facilitated by the development of LEDs emitting in the UV-region and can be done without further modification of the protein, this method could become a standard method for probing the kinetics of conformational changes in photoreceptors.

An interesting photoreceptor system for future experiments with this method are the BLUF domains in which a conserved tryptophan is thought to undergo major structural changes upon photoactivation.

A promising methodical advancement might be the transient fluorescence anisotropy spectroscopy, which is able to resolve the kinetics of light-induced reactions affecting the rotational diffusion of fluorescent groups in a photoreceptor.

References

1. Förster, T. 1948. Zwischenmolekulare Energiewanderung und Fluoreszenz. *Annalen der Physik* 2:55-75.
2. Eisinger, J., and R. E. Dale. 1974. Interpretation of intramolecular energy transfer experiments. *Journal of Molecular Biology* 84:643-647.
3. Dale, R. E., J. Eisinger, and W. E. Blumberg. 1979. The orientational freedom of molecular probes- The orientation factor in intramolecular energy transfer. *Biophysical Journal* 26:161-193.
4. Atkins, P. W. 1998. *Physical Chemistry*. Oxford University Press, Oxford.
5. Lee, B. C., P. A. Croonquist, and W. D. Hoff. 2001. Mimic of photocycle by a protein folding reaction in photoactive yellow protein. *Journal of Biological Chemistry* 276:44481-44487.
6. VanBrederode, M. E., W. D. Hoff, I. H. M. VanStokkum, M. L. Groot, and K. J. Hellingwerf. 1996. Protein folding thermodynamics applied to the photocycle of the photoactive yellow protein. *Biophysical Journal* 71:365-380.
7. Kibblewhite, J., C. J. Drummond, F. Grieser, and P. J. Thistlethwaite. 1989. Lipoidal eosin and fluorescein derivatives as probes of the electrostatic characteristics of self-assembled surfactant water interfaces. *Journal of Physical Chemistry* 93:7464-7473.
8. Martin, M. M. 1975. Hydrogen-bond effects on radiationless electronic-transitions in xanthene dyes. *Chemical Physics Letters* 35:105-111.
9. Klonis, N., A. H. A. Clayton, E. W. Voss, and W. H. Sawyer. 1998. Spectral properties of fluorescein in solvent-water mixtures: Applications as a probe of hydrogen bonding environments in biological systems. *Photochemistry and Photobiology* 67:500-510.
10. Rajagopal, S., S. Anderson, V. Srajer, M. Schmidt, R. Pahl, and K. Moffat. 2005. A structural pathway for signaling in the E46Q mutant of photoactive yellow protein. *Structure* 13:55-63.
11. Ihee, H., S. Rajagopal, V. Srajer, R. Pahl, S. Anderson, M. Schmidt, F. Schotte, P. A. Anfinrud, M. Wulff, and K. Moffat. 2005. Visualizing reaction pathways in photoactive yellow protein from nanoseconds to seconds. *Proceedings of the National Academy of Sciences of the United States of America* 102:7145-7150.
12. Getzoff, E. D., K. N. Gutwin, and U. K. Genick. 2003. Anticipatory active-site motions and chromophore distortion prime photoreceptor PYP for light activation. *Nature Structural Biology* 10:663-668.
13. Cohen, B. E., A. Pralle, X. J. Yao, G. Swaminath, C. S. Gandhi, Y. N. Jan, B. K. Kobilka, E. Y. Isacoff, and L. Y. Jan. 2005. A fluorescent probe designed for studying protein conformational change. *Proceedings of the National Academy of Sciences of the United States of America* 102:965-970.
14. Okada, T., M. Sugihara, A. N. Bondar, M. Elstner, P. Entel, and V. Buss. 2004. The retinal conformation and its environment in rhodopsin in light of a new 2.2 angstrom crystal structure. *Journal of Molecular Biology* 342:571-583.

Chapter 8

15. Crocker, E., M. Eilers, S. Ahuja, V. Hornak, A. Hirshfeld, M. Sheves, and S. O. Smith. 2006. Location of Trp265 in metarhodopsin II: Implications for the activation mechanism of the visual receptor rhodopsin. *Journal of Molecular Biology* 357:163-172.
16. Lin, S. W., and T. P. Sakmar. 1996. Specific tryptophan UV-absorbance changes are probes of the transition of rhodopsin to its active state. *Biochemistry* 35:11149-11159.
17. Imamoto, Y., M. Kataoka, F. Tokunaga, and K. Palczewski. 2000. Light-induced conformational changes of rhodopsin probed by fluorescent Alexa594 immobilized on the cytoplasmic surface. *Biochemistry* 39:15225-15233.
18. Knierim, B., K. P. Hofmann, O. P. Ernst, and W. L. Hubbell. 2007. Sequence of late molecular events in the activation of rhodopsin. *Proceedings of the National Academy of Sciences of the United States of America* 104:20290-20295.
19. Mielke, T., U. Alexiev, M. Gläsel, H. Otto, and M. P. Heyn. 2002. Light-induced changes in the structure and accessibility of the cytoplasmic loops of rhodopsin in the activated M-II state. *Biochemistry* 41:7875-7884.
20. Arnis, S., K. Fahmy, K. P. Hofmann, and T. P. Sakmar. 1994. A conserved carboxylic acid group mediates light-dependent proton uptake and signaling by rhodopsin. *Journal of Biological Chemistry* 269:23879-23881.
21. Vogel, R., M. Mahalingam, S. Luedke, T. Huber, F. Siebert, and T. P. Sakmar. 2008. Functional role of the "Ionic Lock" - An interhelical hydrogen-bond network in family a heptahelical receptors. *Journal of Molecular Biology* 380:648-655.
22. Calvert, P. D., V. I. Govardovskii, N. Krasnoperova, R. E. Anderson, J. Lem, and C. L. Makino. 2001. Membrane protein diffusion sets the speed of rod phototransduction. *Nature* 411:90-94.
23. Heck, M., and K. P. Hofmann. 2001. Maximal rate and nucleotide dependence of rhodopsin-catalyzed transducin activation - Initial rate analysis based on a double displacement mechanism. *Journal of Biological Chemistry* 276:10000-10009.
24. Ernst, O. P., C. Bieri, H. Vogel, and K. P. Hofmann. 2000. Intrinsic biophysical monitors of transducin activation: Fluorescence, UV-visible spectroscopy, light scattering, and evanescent field techniques. *Vertebrate Phototransduction and the Visual Cycle, Part A* 315:471-489.
25. Herrmann, R., M. Heck, P. Henklein, C. Kleuss, K. P. Hofmann, and O. P. Ernst. 2004. Sequence of interactions in receptor-G protein coupling. *Journal of Biological Chemistry* 279:24283-24290.
26. Harper, S. M., L. C. Neil, and K. H. Gardner. 2003. Structural basis of a phototropin light switch. *Science* 301:1541-1544.
27. Harper, S. M., J. M. Christie, and K. H. Gardner. 2004. Disruption of the LOV-J alpha helix interaction activates phototropin kinase activity. *Biochemistry* 43:16184-16192.
28. Chen, E. F., T. E. Swartz, R. A. Bogomolni, and D. S. Kliger. 2007. A LOV story: The signaling state of the Phot1 LOV2 photocycle involves chromophore-triggered protein structure relaxation, as probed by far-UV time-resolved optical rotatory dispersion spectroscopy. *Biochemistry* 46:4619-4624.

Chapter 8

29. Yuan, H., S. Anderson, S. Masuda, V. Dragnea, K. Moffat, and C. Bauer. 2006. Crystal structures of the Synechocystis photoreceptor Slr1694 reveal distinct structural states related to signaling. *Biochemistry* 45:12687-12694.
30. Gomelsky, M., and G. Klug. 2002. BLUF: a novel FAD-binding domain involved in sensory transduction in microorganisms. *Trends in Biochemical Sciences* 27:497-500.
31. Masuda, S., and C. E. Bauer. 2005. The Antirepressor AppA uses the Novel Flavin-Binding BLUF Domain as a Blue-Light-Absorbing Photoreceptor to Control Photosystem Synthesis. In *Handbook of Photosensory Receptors*. R. Briggs, and J. L. Spudich, editors. Wiley-VCH, Weinheim. 433-445.
32. Gomelsky, M., and S. Kaplan. 1995. appA, a novel gene encoding a trans-acting factor involved in the regulation of photosynthesis gene expression in *Rhodobacter sphaeroides* 2.4.1. *Journal of Bacteriology* 177:4609-4618.
33. Masuda, S., and C. E. Bauer. 2002. AppA is a blue light photoreceptor that antirepresses photosynthesis gene expression in *Rhodobacter sphaeroides*. *Cell* 110:613-623.
34. Toh, K. C., I. H. M. van Stokkum, J. Hendriks, M. T. A. Alexandre, J. C. Arents, M. A. Perez, R. van Grondelle, K. J. Hellingwerf, and J. T. M. Kennis. 2008. On the signaling mechanism and the absence of photoreversibility in the AppA BLUF domain. *Biophysical Journal* 95:312-321.
35. Masuda, S., K. Hasegawa, and T. A. Ono. 2005. Tryptophan at position 104 is involved in transforming light signal into changes of beta-sheet structure for the signaling state in the BLUF domain of AppA. *Plant and Cell Physiology* 46:1894-1901.
36. Gauden, M., J. S. Grinstead, W. Laan, H. M. van Stokkum, M. Avila-Perez, K. C. Toh, R. Boelens, R. Kaptein, R. van Grondelle, K. J. Hellingwerf, and J. T. M. Kennis. 2007. On the role of aromatic side chains in the photoactivation of BLUF domains. *Biochemistry* 46:7405-7415.
37. Jung, A., J. Reinstein, T. Domratcheva, R. L. Shoeman, and I. Schlichting. 2006. Crystal structures of the AppA BLUF domain photoreceptor provide insights into blue light-mediated signal transduction. *Journal of Molecular Biology* 362:717-732.
38. Wull, Q., W. H. Ko, and K. H. Gardner. 2008. Structural requirements for key residues and auxiliary portions of a BLUF domain. *Biochemistry* 47:10271-10280.
39. Jung, A., T. Domratcheva, M. Tarutina, Q. Wu, W. H. Ko, R. L. Shoeman, M. Gomelsky, K. H. Gardner, and L. Schlichting. 2005. Structure of a bacterial BLUF photoreceptor: Insights into blue light-mediated signal transduction. *Proceedings of the National Academy of Sciences of the United States of America* 102:12350-12355.
40. Lakowicz, J. R. 2006. *Principles of Fluorescence Spectroscopy*. Springer, New York. 353-382.

Acknowledgments

I would like to express my sincere gratitude to my supervisors Prof. Dr. Maarten P. Heyn and Dr Harald Otto for their support, regular guidance and encouragement during the course of my Ph. D. work.

I am grateful to the people at AG Heyn which also were involved in the scientific projects presented in this thesis: Dr. Chandra Joshi, Dr. Berthold Borucki for their contributing measurements, scientific advise and inspiring discussions and Ingrid Wallat for preparing the rhodopsin samples and advise concerning biochemical questions.

My special thanks go to Prof. Dr. Holger Dau for accepting to be a co-referee of my doctorate thesis and his interest in my work.

All PYP samples were prepared in the lab of Prof. Dr. Michael A. Cusanovich at the University of Arizona. The LOV2 samples were prepared in the lab of Prof. Dr. Roberto Bogomolni at the University of California. I am indebted to the staff of both collaborating groups, for their contributions to the scientific publications and a steady supply of high grade protein samples. Therefore my special thanks go to Prof. Dr. Terry E. Meyer, Elsa Chen and Farzin Bolourchian.

I am thankful to Marion Badow for her help in administrative matters and to Dr. Sven Seibeck and Daniel Sachse for helpful discussions.

Last but not least I would like to acknowledge the German Science Foundation (DFG) for paying all the bills and my salary via the grant He1382/14-2.

List of Publications

Publications in Scientific Journals

Otto H, Hoersch D, Meyer TE, Cusanovich MA, Heyn MP: **Time-resolved single tryptophan fluorescence in photoactive yellow protein monitors changes in the chromophore structure during the photocycle via energy transfer.** *Biochemistry* 2005, **44**(51):16804-16816.

Hoersch D, Otto H, Joshi CP, Borucki B, Cusanovich MA, Heyn MP: **Role of a conserved salt bridge between the PAS core and the N-terminal domain in the activation of the photoreceptor photoactive yellow protein.** *Biophysical Journal* 2007, **93**(5):1687-1699.

Hoersch D, Otto H, Cusanovich MA, Heyn MP: **Distinguishing chromophore structures of photocycle intermediates of the photoreceptor PYP by transient fluorescence and energy transfer.** *Journal of Physical Chemistry B* 2008, **112**(30):9118-9125.

Hoersch D, Otto H, Wallat I, Heyn MP: **Monitoring the conformational changes of photoactivated rhodopsin from microseconds to seconds by transient fluorescence spectroscopy.** *Biochemistry* 2008, **47**(44):11518-11527.

Hoersch D, Otto H, Cusanovich MA, Heyn MP: **Time-resolved spectroscopy of dye-labeled PYP suggests a pathway of light-induced structural changes in the N-terminal cap.** *Physical Chemistry Chemical Physics* 2009, DOI: 10.1039/b821345c.

Contributions to Scientific Conferences

Harald Otto, Daniel Hoersch, Terry E. Meyer, Michael A. Cusanovich, Maarten P. Heyn. **Chromophore isomerisation changes during the photocycle of photoactive yellow protein as monitored by energy transfer from tryptophan 119.** *Annual Meeting of the American Biophysical Society*, Salt Lake City 2006, Poster.

Daniel Hörsch, Harald Otto, Chandra P. Joshi, Berthold Borucki, Michael A. Cusanovich, Maarten P. Heyn. **Effect of ionic strength on the rate of formation and stability of an interdomain salt-bridge involved in the activation and recovery of the photoreceptor Photoactive Yellow Protein.** *Annual Meeting of the American Biophysical Society*, Baltimore 2007, Poster.

Harald Otto, Daniel Hörsch, Michael A. Cusanovich, Maarten P. Heyn. **Energy transfer from Trp 119 resolves the orientation of the cinnamoyl chromophore in the alkaline photointermediate I_1' of Photoactive Yellow Protein.** *Annual Meeting of the American Biophysical Society*, Baltimore 2007, Poster.

Daniel Hoersch, Harald Otto, Michael A. Cusanovich and Maarten P. Heyn. **Photoreaction Kinetics of the photoreceptors rhodopsin and photoactive yellow protein as monitored by their transient tryptophan fluorescence.** *13th International Conference on Retinal Proteins*, Barcelona 2008, Poster.

Daniel Hoersch, Harald Otto and Maarten P. Heyn. **Transient fluorescence spectroscopy as a tool for monitoring conformational changes of activated photoreceptors from μ s to seconds.** *Jahrestagung der Deutschen Biophysikalischen Gesellschaft*, Berlin 2008, Poster.

Zusammenfassung

Photorezeptoren sind wichtige Modellsysteme für die Untersuchung von Protein-Signaltransduktion und Protein-Kinetik im Allgemeinen. Da sie durch Licht aktiviert werden, ist es möglich die Kinetik des Aktivierungsprozesses mittels optischer Methoden mit hoher Zeitauflösung zu untersuchen. Der methodische Schwerpunkt dieser Arbeit liegt auf der zeitaufgelösten Fluoreszenzspektroskopie als Mittel zur Untersuchung von lichtinduzierten, mit der Aktivierung unterschiedlicher Photorezeptoren assoziierten Konformationsänderungen. Darüber hinaus wird die Methode der transienten Fluoreszenzspektroskopie als wertvolles Mittel zur Untersuchung der Kinetik des Aktivierungsprozesses eingeführt. Transiente Absorptionsspektroskopie wird als komplementäre Methode verwendet. Die vorliegende Arbeit hat ihren Schwerpunkt in Messungen an Photoactive Yellow Protein (PYP), dem Struktur-Prototyp der weitverbreiteten Familie der PAS-Domänen. Außerdem wurden die Photorezeptoren Rhodopsin und die LOV2-Domäne des Phototropin1 untersucht, um die allgemeine Anwendbarkeit der eingeführten Methoden zu demonstrieren.

In Kapitel 1 wird eine allgemeine Einführung in die untersuchten biologischen Systeme Photoactive Yellow Protein, Rhodopsin und LOV2 gegeben. Zusätzlich werden die angewendeten Methoden vorgestellt.

Kapitel 2 (Otto et al. (2005) *Biochemistry* 44, 16804-16816) handelt von zeitaufgelösten Fluoreszenz-Intensitäts und -Depolarisationsmessungen am einzigen Tryptophan W119 des PYP aus dem Organismus *Halorhodospira halophila*, dessen Fluoreszenz durch Energietransfer zum 4-hydroxycinnamoyl Chromophor des Proteins gequenched wird. Die unterschiedlichen Fluoreszenzlebensdauern der einzelnen Photointermediate konnten durch dramatische Änderungen des κ^2 -Faktors, verursacht durch Änderungen der Orientierung des Übergangdipolmoments des Chromophors, erklärt werden. Die κ^2 -Faktoren wurden aus hochauflösenden Kristallstrukturen berechnet. Die Ergebnisse dieses Kapitels waren Teil meiner Diplomarbeit und werden hier nochmals aufgeführt, da sie für das Verständnis eines großen Teils der in den nachfolgenden Kapitel beschriebenen Arbeiten notwendig sind.

Kapitel 3 (Hoersch et al. (2008) *J. Phys. Chem. B* 112, 9118-9125) führt die Methode der transienten Fluoreszenzspektroskopie als Mittel zur Untersuchung des Photozyklus des PYP im alkalischen pH-Bereich ein. Dadurch konnte die Fluoreszenzlebensdauer des kurzlebigen Intermediats I_1 bestimmt werden. In nächsten Schritt wurde diese mit theoretischen Lebensdauern verglichen, die unter Zuhilfenahme zweier unterschiedlicher I_1 -Kristallstrukturen berechnet wurden. Da nur eine der berechneten Lebensdauern im Einklang mit den experimentell bestimmten Wert ist, konnte eine der Kristallstrukturen als nicht in Lösung bei alkalischem pH vorkommend ausgeschlossen werden. Außerdem

Zusammenfassung

wurde die Tryptophan-Fluoreszenzlebensdauer des alkalischen Intermediats I_1' aus Messungen des Tryptophan-Fluoreszenzzerfalls in einem photostationären Gleichgewicht unter Hintergrundbeleuchtung bestimmt. Die Chromophorkonformation dieses Intermediats, dessen Kristallstruktur noch nicht bekannt ist, wurde als I_2 ähnlich vorausgesagt.

Kapitel 4 (Hoersch et al. (2007) *Biophysical Journal* 93, 1687-1699) beschäftigt sich mit der Rolle einer konservierten Salzbrücke zwischen dem PAS-core und dem N-terminal cap in der Aktivierung von PYP. Dazu wurde der Effekt der Ionenstärke auf das Gleichgewicht zwischen den Intermediat I_2 und dem Signalzustand I_2' und auf die Rückkehrtrate untersucht. Die Salzabhängigkeit der Gleichgewichtskonstante und der Rückkehrtrate konnte mit der Abschirmung eines monovalenten Ionenpaars erklärt werden. Außerdem verschwindet der Salzeffekt in der Mutante K110A unterhalb von 600 mM KCl. Daraus wurde geschlossen, dass die Salzbrücke K110/E12 zwischen dem β -Faltblatt des PAS-core und dem N-terminal cap den Photorezeptor in seinem inaktiven Zustand stabilisiert und in Folge der lichtinduzierten Bildung des Signalzustands aufbricht.

In Kapitel 5 (Hoersch et al. (2009) *Physical Chemistry Chemical Physics*, DOI: 10.1039/b821345c) wird die Kinetik der Strukturänderung in der N-terminalen Domäne von PYP durch transiente Absorptionsspektroskopie an den farbstoffgelabelten Mutanten A5C und N13C untersucht. Die transiente Rotverschiebung der Absorptionsbande des gebundenen Farbstoffs Iodoacetamidofluorescein (IAF) legt Konformationsänderungen in der Umgebung der Labelstellen nahe. Da das transiente Farbstoffsignal in A5C-AF mit dem Intermediat I_2 und in N13C-AF mit I_2' korreliert, wurde gefolgert, dass sich das lichtinduzierte Struktursignal von der Chromophorbindungs tasche über A5 nach N13 hin ausbreitet, wo es größere Änderungen in der Proteinkonformation hervorruft.

In Kapitel 6 (Hoersch et al. (2008) *Biochemistry* 47, 11518-11527) wird die Methode der transienten Fluoreszenzspektroskopie auf Rhodopsin angewendet. Die transiente Tryptophan-Fluoreszenz dieses Photorezeptors nimmt mit der gleichen Kinetik ab wie der transiente Anstieg der Absorption bei 360 nm. Dies konnte durch eine Steigerung des Energietransfers zum Retinal-Chromophor, verursacht durch eine Vergrößerung des spektralen Überlapps im Signalzustand M_{II} , erklärt werden. Außerdem wurde die Kinetik des Anstiegs der Alexa594-Fluoreszenz in selektiv an Cystein 316 gelabelten ROS-Membranen gemessen. Diese wurde mit den Kinetiken der M_{II} -Bildung und der Protonenaufnahme aus dem Lösungsmittel verglichen. Da die Fluoreszenz-Kinetik hinter der Kinetik der Schiff-Base Deprotonierung zurückbleibt aber der der Protonenaufnahme vorangeht, scheint die Reihenfolge Schiff-Base Deprotonierung, Strukturänderung, Protonenaufnahme die richtige Beschreibung der molekularen Ereignisse der Rhodopsin-Aktivierung zu sein. Bislang wurde diese Reihenfolge nur im weniger relevanten Rhodopsin/Mizellen System mit anderen Ergebnissen festgestellt.

Kapitel 7 handelt von der transienten Tryptophan-Fluoreszenz der LOV2-J α Domäne des Phototropin1 des Hafers. Das transiente Tryptophan-Fluoreszenzsignal steigt bei 20 °C biexponentiell mit den Zeitkonstanten von 450 μ s und 3,8 ms an. Da diese Übergänge in den transienten Absorptionsdaten in UV-VIS Wellenlängenbereich nicht sichtbar sind muss das ursprüngliche LOV2-Photozyklusmodell um 2 zusätzliche Intermediate erweitert werden. Diese haben das gleiche Absorptionsspektrum aber unterschiedliche Tryptophan Fluoreszenzquantenausbeuten und sind mit Konformationsänderungen des Proteins assoziiert. Außerdem wurde die Aktivierungsenergie der mittleren Kinetik des transienten Fluoreszenzsignals von 18,2 kcal/mol gemessen. Der Wert wurde mit der Aktivierungsenergie von 18,5 kcal/mol für den I_2/I_2' -Übergang im Photorezeptor PYP verglichen, der ebenfalls mittels transienter Tryptophanfluoreszenz gemessen wurde. Die ähnliche Kinetik der Konformationsänderungen in beiden Photorezeptorsystemen könnte

Zusammenfassung

mit ihrer gemeinsamen PAS-Domänenstruktur in Zusammenhang stehen.

In Kapitel 8 werden die Ergebnisse und Schlussfolgerungen der in dieser Arbeit dargestellten Experimente zusammengefasst und zukünftige Experimente vorgeschlagen.